The Messenger

No. 135 – March 2009

Headquarters building extension
The ALMA Correlator
Wolf-Rayet stars with VLTI
Galaxy mass assembly at z ~ 2

ESO

An Extension for ESO Headquarters

Robert Fischer[1]
Jeremy Walsh[1]

[1] ESO

The ESO Headquarters was completed in 1980, but is now too small to house all the ESO staff and currently only about 50% reside in the original building. A decision was taken to seek an extension to the Headquarters building in close proximity to the current one and a competition was launched for architectural designs. Three designs were shortlisted and the process of selection for the final design is described. Construction will begin in 2010 and is due for completion in 2012.

When ESO moved from temporary offices at CERN, Geneva, in 1980 there were a total of 40 staff members. The Headquarters building was designed by the architects Hermann Fehling and Daniel Gogel, who also designed the neighbouring Max-Planck Institute for Astrophysics. It had 120 offices, an auditorium, workshops, laboratories and storage rooms. The generous curves and lack of 90-degree corners are two of its defining characteristics. The original building had four floors and some basement area. By the end of the 1980s, however, with the gradual increase in numbers of ESO staff as the number of telescopes at the La Silla Observatory increased and with the development of the Very Large Telescope (VLT) project, the addition of a fifth floor was necessary. When the VLT became operational in 1998 and as more ESO member-state countries joined, more staff were recruited; the need for more offices had to be satisfied by a prefabricated office block ("portakabin") in the car park. As more VLT Unit Telescopes came online, new instruments were commissioned and the ALMA project entered its planning phases, staff numbers increased again and a second temporary building had to be erected. In addition, offices were rented from the Max-Planck Institute for Plasma Physics in a building located about four minutes walk away from the Headquarters. In 2007 more offices were rented from the Max-Planck Institute to house the ALMA staff, whose numbers were increasing rapidly during the construction phase. By the end of 2008 the ESO "campus" consisted of the Headquarters building, two temporary buildings and two locations of rented offices with a staff complement of 444, only 230 of whom were actually located in the original Headquarters building.

The difficulties of working closely on joint projects with offices spread over an extended area were not just perceived. In 2007 a decision was made to try to improve the scientific atmosphere by bringing all faculty astronomers, fellows, students and science visitors together in the main building. Logistically this proved possible only for a short while and new

Figure 1. Montage of the 20 entries for the Architectural Competition for an extension to the ESO Headquarters.



Figure 2. The three prize-winning architectural concepts for the Headquarters extension building in their revised form. **Left:** Koch and Partner, Germany; **Centre:** RISCO, Portugal; **Right:** Auer + Weber, Germany.

scientific staff, e.g., for ALMA, are increasingly located in offices in the ALMA building. The situation is exacerbated by the small number of meeting rooms and the limited size of the auditorium, which can only seat about 100. The instrument assembly hall and laboratories are also too small for the level of development and the typical size of second generation VLT instruments. An important issue was the need for further expansion after the European Extremely Large Telescope (E-ELT) design study was approved in 2007 and a substantial increase in scientific and engineering staff is required to develop Phase B (see Spyromilio et al., 2008). In order to improve communication and the proximity of the science, operations, engineering, software and administration groups working towards common goals, to raise the team focus and to provide ESO with a hallmark building that embodies its profile, an increase of office, conference and workshop space by an extension to the present Headquarters building was proposed. Provision of an extension to the existing building was confirmed by the ESO Council.

Architectural designs

The specifications for an extension to the ESO Headquarters building were defined with careful consideration of future expansion and enhancement of the current facilities and a Call for Tender for architectural concepts was drawn up. This was sent to 24 architectural offices in the ESO member states on 11 July 2007 with a deadline for entries of 24 September. An international jury consisting of eminent architects, representatives of the town of Garching and ESO was constituted to judge the designs. Twenty responses to the Competition were received and all are shown in Figure 1. The jury assessed the designs, and awarded two first prizes (€25 000 each), a third and a fourth prize (€15 000 and 10 000 respectively) in October 2007. One additional very innovative design, which did not however meet the local building regulations, was recognised with a "purchase" prize (€5000).

The top three prize-winning concepts, shown in Figure 2, did not fulfill all the requirements and further technical clarification was required, such as the link to the current Headquarters building and the realisation of the instrument assembly hall/laboratory complex (whether as a separate building or integrated into the extension). The baseline proposal would only have been sufficient to provide 476 work places together with the current Headquarters building. Given the expected increase to 520 by the time of completion, an expansion of 1100 m^2 was considered necessary. The new office and conference extension would then provide a total floor area of 9500 m^2 and the technical building 2900 m^2. For comparison the existing building has a floor area of 10 200 m^2 and the storage hall a surface area of 770 m^2. Thus the extension almost doubles the existing area of the current Headquartes building. By the time the new building is completed, the current one will be more than 30 years old and is in need of major maintenance and upgrading; it was decided to include this upgrade in the revised concept. This concept was then submitted for revised tender to the three prize-winning architectural firms with a closing date of 13 June 2008 with the aim of achieving "one signature headquarters". A fixed fee of €75 000 was awarded for each submission.

Initially it was planned to build the extension to the south of the current building (see the aerial photograph on p. 26 of *The Messenger* 130) and the original competition had specified this position. This land is owned by a consortium of local farmers. However negotiations could not be concluded by the time of the revised tender and it was decided to site the building to the southeast on land owned by the Max Planck Society. The rent for this land will be paid by the German Federal Ministry of Education and Research, just as is done for the land on which the current building is sited.

Final selection

In the final round of the selection process, the three prize-winning architects could revise their original concepts to take into account the decision to have two buildings as part of the extension — separate office and workshop/integration buildings. The three concepts were assessed between June and October 2008. On 28 October the ESO Contract Award Committee agreed that the design by Auer + Weber best met all the high level requirements by providing, in particular, the very important parameter of one signature ESO Headquarters building. This recommendation of the committee was approved by the ESO Council on 2–3 December. The same architect's office was also responsible for the award-winning design of the Paranal Residencia.

The new extension

The first concept submitted by Auer + Weber was already marked out by its

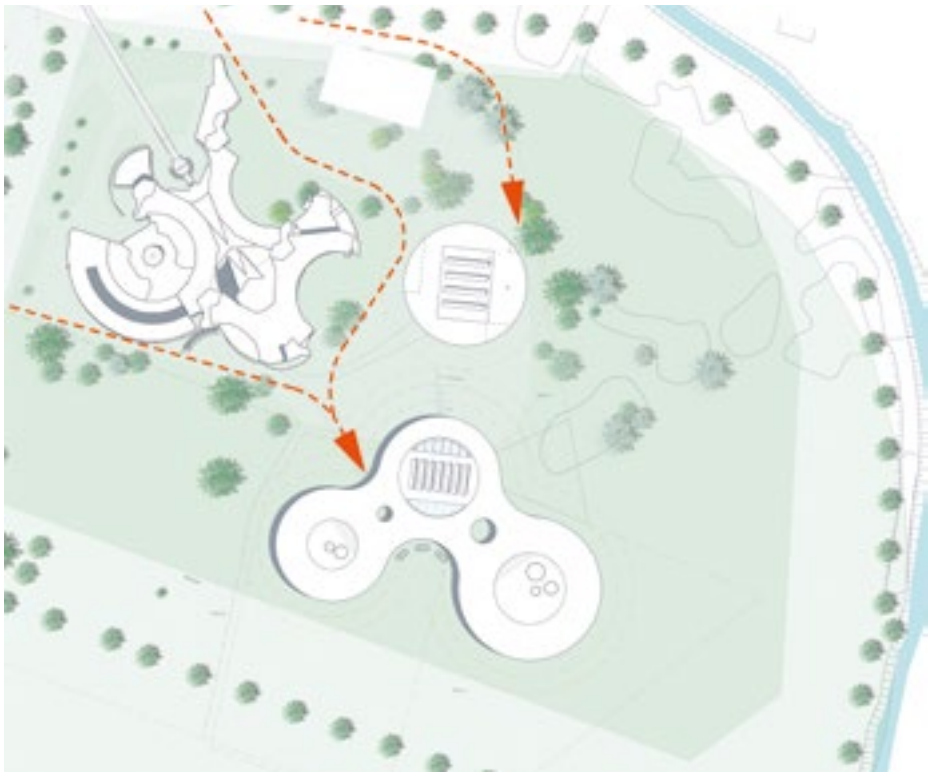

Figure 3. Ground plan of the Auer + Weber design for the ESO Headquarters. The single circular building to the north is the technical building.

harmony with the existing building; the revised concept further emphasises the impression of community between the two parts. There is, in close reference to the original design by Fehling and Gogel, extensive use of circles and this is taken further in the dimensions of several aspects, such as internal light wells that are identical to those of the ESO telescope mirrors (2.2, 3.6 and 8.2 metres). The two buildings will be connected by an enclosed bridge whose length is on the natural axis of the current building (see Figure 3). Figure 4 shows an artist's impression of the new building from the southwest. The workshop and integration laboratory is a circular building and, although separate, will be accessible by a tunnel from the existing building. A large cleanroom will be housed within the workshop building.

As part of the process of approval for the building plans, a presentation to the local authorities took place at ESO Garching in December 2008. The ESO Director General Tim de Zeeuw outlined the reasons for seeking a new building and the proposed architectural solution was presented by Professor Fritz Auer from the office of Auer + Weber. The planned extension received the full support of the town of Garching and the District Office of Munich.

The final aspects of the design are currently being agreed and construction work is expected to begin in early 2010, with the new extension ready for occupancy in 2012. With the ESO flag flying above its signature Headquarters, the staff will be in pole position to manage the current activities — La Silla Paranal Observatory, ALMA, construction of the E-ELT — and to forge the next large astronomy project.

References

Spyromilio, J. et al., The Messenger, 133, 2

Figure 4. Side view of the Auer + Weber design for the ESO Headquarters extension from the southwest.

The highest (5000 m) and fastest (17 peta-operations/second) computer ever used at an astronomical site — the ALMA Correlator. Here the first quadrant is shown in place at the ALMA Operations Site (AOS) Technical Building.

Credit: ESO/A. Wicenec

The ALMA Correlator: Performance and Science Impact in the Millimetre/Submillimetre

Alain Baudry[1 2]

[1] University of Bordeaux, LAB, France
[2] European ALMA Project Office, ESO

The basic properties of digital correlation are introduced and the main blocks that form the correlator system designed for the ALMA main array are described. Some technical challenges and the performance of this system are presented, together with examples of observational modes, total bandwidths and spectral resolutions. The high flexibility of the ALMA correlator is emphasised and its ability to bring new data in molecular line or continuum astrophysics projects is discussed.

ALMA signal processing and correlation

The Atacama Large Millimeter/submillimeter Array (ALMA), under construction at the 5000-metre high altiplano of northern Chile, will explore the Universe in the millimetre/submillimetre wave range up to 1 THz (300 micrometres). With an impressive collecting area of 50 + 16 large antennas moveable over an area from about 150 m to more than 15 km in diameter, ALMA offers an unprecedented angular resolution and imaging capability (see Haupt & Rykaczewski, 2007). The 50+ (up to 64) 12-metre antennas form the ALMA main array; four 12-metre and twelve 7-metre antennas form the ALMA Compact Array (ACA). The radio waves, once they have been captured with the ALMA antennas, are converted into low frequency signals (while preserving the phase information of the incoming waves), digitised in specific modules and finally combined in a large digital machine, named the correlator. The digital correlator is the system combining the outputs of all antennas, as selected in the array, to detect the astronomical source power by measuring the cross-correlation coefficients of all antenna pairs in addition to the auto-correlation coefficients of each antenna. From these coefficients, and by further processing of the data, images of the astronomical sources are obtained. In mathematical terms the source image is directly related to the Fourier transform in the spatial frequency domain of the cross-correlation functions (or the interferometer complex visibilities). Moreover, time offsets or time lags are easily implemented in digital systems and thus the spectral information contained in the observed sources is also available from a digital correlator; the correlation lag functions and the astronomical spectra are related by a time/frequency Fourier transform.

There are two main correlator architectures: (a) the XF architecture where the X-part (cross- or auto-correlation part) is performed first and the Fourier transform (F-part) is applied at a later stage to analyse the source spectral properties; (b) the FX architecture where the Fourier transform is performed first. In terms of signal processing the XF or FX approaches are equivalent. ALMA has adopted two different types of correlator. One FX correlator constructed by a Japanese team processes the signals collected by 16 antennas of the ACA. The second correlator, constructed by an NRAO/European "integrated team", processes up to 64 ALMA antennas. It is a highly flexible "Digital hybrid XF" design in which the 2 GHz input baseband is digitally split into several sub-bands to enhance the spectral resolution, a concept first proposed in the European Second Generation Correlator (2GC) study. The Digital Hybrid XF correlator now merges the main ideas from the initial NRAO parallel array XF architecture with the frequency division scheme of the 2GC study. More generally, it is important to stress that digital filtering/processing offers great advantages with respect to analogue signal processing: reproducibility of performance, stability with respect to temperature drifts, easier calibration and higher flexibilty.

Specifications and architecture

The hardware sub-systems, in which the digital filtering and correlation functions have been implemented for the ALMA main array and the associated firmware, form what is referred to as the ALMA baseline correlator system (see specifications in Table 1).

The ALMA correlator designers have faced two major challenges, driven by the main science goals in the millimetre and submillimetre: (a) process a broad signal bandwidth of 16 GHz (8 GHz per polarisation) from each of 64 antennas (each antenna provides 96 Gbits/s); (b) extract from the input band various spectral windows and provide flexible spectral resolutions. Figure 1, adapted from Escoffier et al. (2005), presents the baseline correlator system schematically. This includes "correlator station electronics" boards processing the digitised data streams from each antenna in the array and "correlator baseline electronics" boards providing the interferometric cross-products from up to 2016 independent antenna pair combinations (for 64 antennas).

We briefly describe below some of the main parts of the ALMA correlator and refer to the main blocks in Figure 1:

Filtering: After digitisation and time demultiplexing of the antenna signals for each baseband, frequency division is accomplished in the Tunable Filter Bank (TFB) boards placed in the station electronics racks. These boards divide the 2 GHz baseband into 32 frequency-mobile sub-bands of 62.5 MHz. Each sub-band is independently processed, assigned to one of the 32 correlator

Item	Specification
Antennas	Up to 64 (up to 2016 interferometric baselines)
Baseband inputs per antenna	8 x 2 GHz
Input sample format	3-bit, 8-level at 4 Gsample/s
Output correlation sample format	2-bit, 4-level or 4-bit, 16-level
Processing rate	125 MHz
Spectral points per baseband (Frequency Division Mode)	Up to 8192 per correlator quadrant
Spectral points per baseband (Time Division Mode)	64, 128 or 256 per correlator quadrant
Polarisation products	1, 2 or 4

Table 1. Main top level specifications of the ALMA baseline correlator

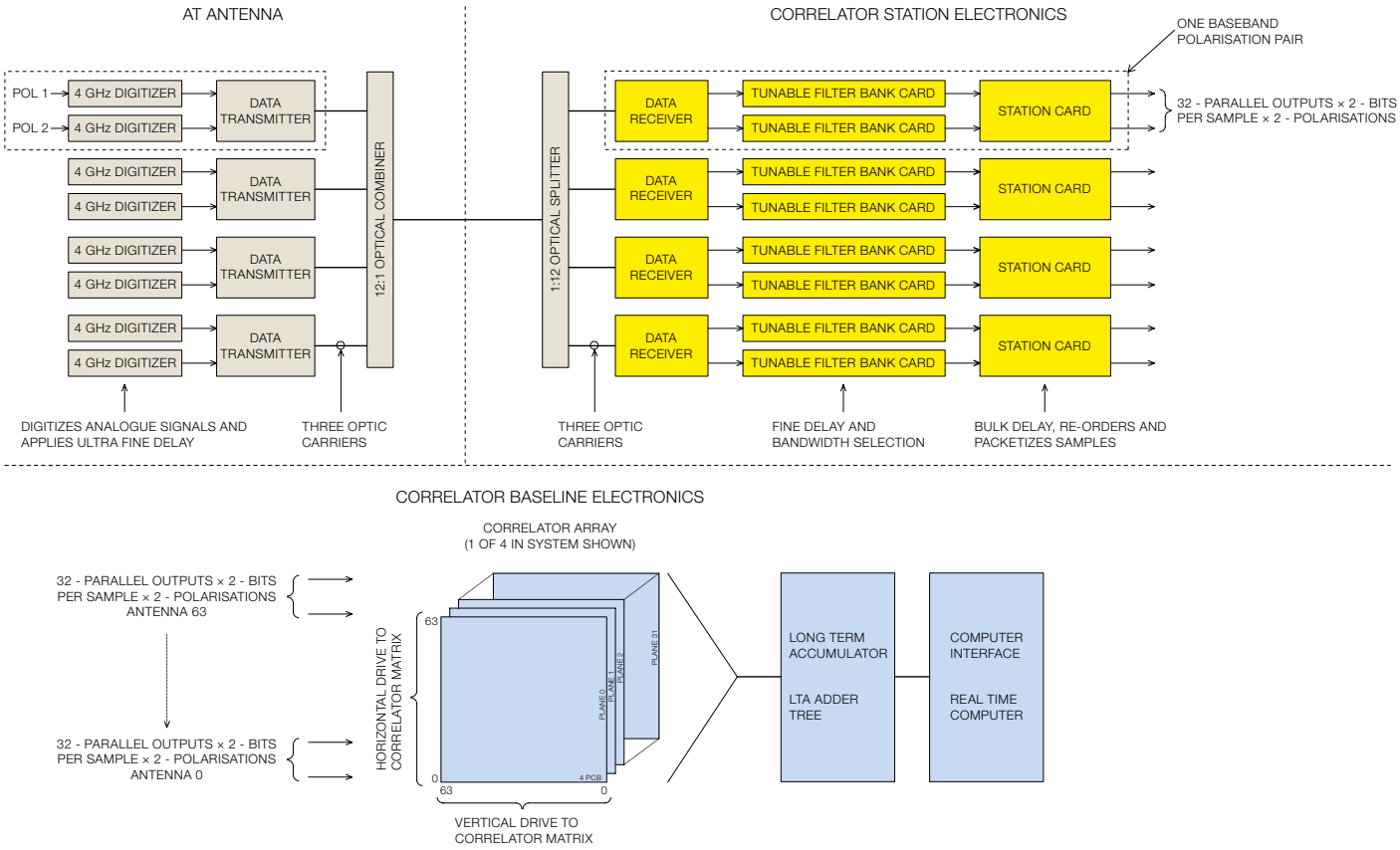

Figure 1. Block diagram of the ALMA 64-antenna correlator showing the main components of the correlator antenna and correlator baseline electronics (adapted from Escoffier et al., 2005). The digitiser and data transmitter boards at the antennas are also shown. The digitised data flow is carried to the correlator system by optical fibres.

"planes" (see below) and the resulting spectra are later stitched together to form a final spectrum with 32 times more spectral channels across the original baseband. Distributing the correlator plane resources to fewer than 32 digital filters narrows the input bandwidth and increases the spectral resolution. The 62.5 MHz sub-band is extracted from 2 GHz in a three-stage digital filter structure implemented in a programmable logic device (or Field Programmable Gate Array, FPGA). The last stage determines the final filter sub-band characteristics and enables the bandwidth to be further narrowed to 31.25 MHz by downloading a specific set of pre-calculated digital weights.

Correlation: All independent cross-products for all 64 antennas are derived from the 32 correlator planes of the baseline electronics boards (see Correlator Array in Figure 1, lower). A correlator plane is a 64 x 64 matrix formed by four printed circuit boards, each with several assembled specific integrated circuits (the correlator chips) in which the signal is multiplied by its time- (or lag-) shifted version to derive the correlation coefficients. Each basic 256-lag circuit in a single correlator chip is driven by the two polarisation signals sent from each receiver band and there is the further ability to address fewer lag blocks in the chip to support double polarisation modes or a full Stokes parameter analysis of the incoming waves.

Two other system aspects are critical: signal digitisation and data transmission from station electronics to correlator board electronics. Prior to digital correlation, the analogue baseband signals are converted to digital samples in a digitiser module specifically designed for ALMA. These modules, plugged into the antenna digital racks, are not part of the correlator system, but their reliability and efficiency are essential in the signal processing chain. The data encoding is made on 3 bits and corresponds to a theoretical 96% correlation efficiency. Because the ALMA correlator cannot process the data at the 4 GHz sampling rate (for 2 GHz input baseband), the digitiser also includes a time-demultiplexed stage consistent with the 250/125 MHz clock rates. The correlator system is a synchronous machine with a very large number of filter and correlator boards (1024) in many racks that makes data transmission a difficult problem. The processing clock rate in all racks is at 125 MHz, but the station rack to correlator rack communication system involves 16 384 cables working at 250 MHz. The output phases of these cables are remotely controlled and adjusted at the link frequency for error-free data transmission.

The correlator system is basically organised by quadrants, each quadrant processing one baseband pair, to accommodate four baseband pairs for two polarisations per antenna. This architecture makes it possible to enhance

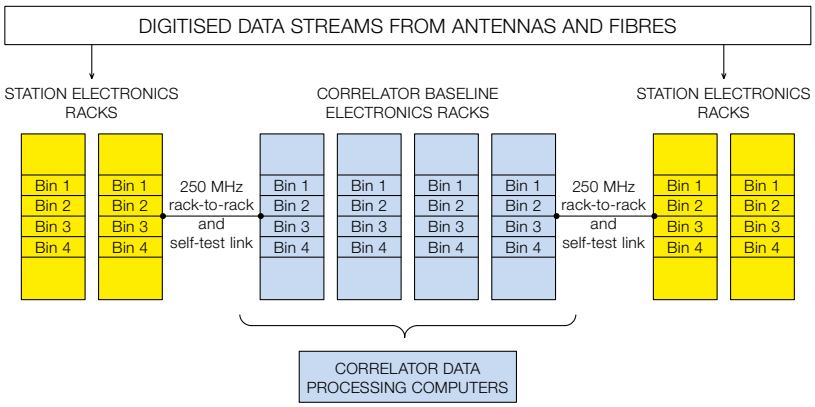

Figure 2. Schematic layout of one quadrant of the correlator system. Station and correlator baseline printed circuit boards are distributed in bins and racks and the correlator outputs are passed to the long-term accumulation boards and the real-time correlator data processing computers.

the total bandwidth, if that were to be required, by adding another quadrant. Figure 2 shows the schematic layout of a single correlator quadrant. There are 32 racks in total (8 racks per quadrant) with, in addition, power supply racks and the Correlator Data Processor and Correlator Control computer racks. All racks and computers are installed in the correlator room of the 5000-metre altitude Array Operations Site (AOS) technical building (see photograph on p. 5).

Technical challenges and performance

Novel hardware or firmware developments have been made to meet the ALMA baseline correlator specifications. Two examples are given for illustration: the digital filter subsystem conceived by the European team; and the correlator chip designed by NRAO. Several original aspects of the TFB design concern the ability to move sub-bands and implementation of the firmware required to meet the challenging filter specifications (e.g., high stop band rejection, low baseband ripple and low power dissipation). All filter functions must be implemented without exhausting the resources available in high performance FPGAs purchased from industry. We have selected a large FPGA with recent 90-nanometre technology to implement two 62.5 MHz sub-band filters in one FPGA. A matrix of 4 x 4 FPGAs is required for frequency division of each baseband and these 16 devices are assembled on a multi-layer TFB board together with other components (fine interferometric delay tracking is implemented in other small FPGAs). Several difficulties were met and solved during the industrial production phase of the TFB cards. These included questions as diverse as the Ni–Au finishing of the cards for long term protection or definition of the optimum temperature profile for reliable assembly of components free of lead (to meet the EC directive on Restriction Of Hazardous Substances). Special test equipment and test procedures were developed to validate the digital filter functionality and check the industrial production quality. This testing was required because of the complexity of the printed circuit board, the large number of ball grid array connections to each board for each large FPGA and the large number of TFB boards to be produced (512 for 8 basebands per antenna x 64 antennas, see Figure 3).

The ALMA correlator chip is a specific, highly integrated microcircuit providing an unsurpassed number of multipliers in a single custom-made chip. There are 4096 multipliers (also named “lags”) per chip providing 2-bit x 2-bit multiplication, 20 bits of integration and secondary storage for readout of the correlation coefficients. The 32 768 chips required for full operation of the four quadrants have been industrially produced. Use of these chips in the correlator environment of the integration centre and of the ALMA high site has proved to be extremely reliable. The correlator chip resources can also be combined to provide 4-bit x 4-bit multiplication so that the quantisation efficiency is enhanced, thus improving ALMA’s interferometric sensitivity overall.

The correlator system is a very large specific computing machine. With 4096 multipliers per chip performing 2-bit correlation at a 125 MHz clock rate and for 64 chips per correlator board, the number of operations performed per second in the full system is 1.7×10^{16}. The computing power in a single TFB board is already impressive. With several hundreds of multi-bit (typically 8 to 16) adder and multiplier stages implemented in one digital filter, around 10^{12} operations per second are performed in a board. The correlator output streams must reach a reasonable rate for final processing and archiving. From the basic accumulation mode of the ALMA correlator chip, the Long Term Accummulator (LTA in Figure 1) transfers 16, or integer multiples of 16, milliseconds of integrated data to

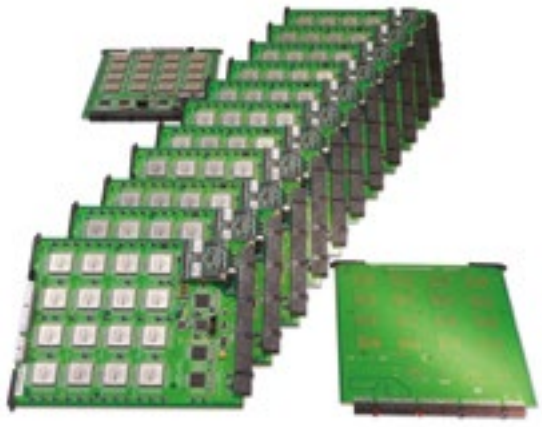

Figure 3. A small series of boards required for digital filtering before correlation. 512 boards have been produced and functionally tested for the full four-quadrant system.

the “real-time computer system” to process the correlation coefficients further. The maximum correlator output capacity reaches 1 GByte/s (in 16 data streams) or 256 MByte/s per correlator quadrant (in four data streams). Lowering the output rate is equivalent to sacrificing interferometric baselines.

Because the ALMA baseline correlator is such a large machine, power dissipation is a difficult task at the high altitude AOS, where the air density is roughly half that at sea level. There was an initial concern with the TFB boards because they implement several functions (and thus dissipate much power) and are plugged in racks where the air circulation is slowed down for practical reasons. With 75 W dissipated power per TFB board, the first engineering goal of 100 W was well met. The latest firmware optimisation and the develoment of a newer filter design have further reduced the dissipation below 60 W. This new performance lowers the temperatures inside the FPGAs, leading to a longer lifetime of these components. Based on the power dissipation measured at the high site with the first quadrant, we anticipate a total power dissipation of 150 kW for the four-quadrant system including the real-time data processor and control computers.

First operational results and installation at AOS

In parallel with the construction of the large 64-antenna correlator, two scaled-down models of the large machine have been made. One for the ALMA Test Facility (ATF) consisting of two prototype antennas at the NRAO VLA site (Very Large Array, New Mexico) and one for the 3000-metre high ALMA Operations Support Facility (OSF) site. The first scaled-down model was moved to the ATF site in 2007 and used through to the end of 2008. First successful end-to-end interferometric operation was demonstrated on the sky in January 2008 in the direction of the Orion Nebula (see Laing, 2008) where many spectral lines were observed at the expected frequencies. The second two-antenna correlator was installed at the OSF in 2008. It is used to test the production antennas and the associated equipment before they are moved to the AOS.

Figure 4. Front panel image of two bins in a Station Electronics rack showing TFB cards, station cards and other system cards (see Correlator Station Electronics in Figure 1). The pairs of holes seen in front of each TFB card allows cool air from the correlator room to be blown into the rack.

The first quadrant of the 64-antenna correlator has been shipped to Chile, installed in the AOS technical building and was successfully commissioned in the summer of 2008 (Figure 4). The air circulation from the floor up to the top of the station racks and temperature throughout the bins and racks are remotely controlled. The 64-antenna correlator room is next to the antenna “patch panel” room, which enables the fibre outputs of each antenna pad to be physically connected to the correlator inputs. The patch panel supports connections to about 200 antenna pads for all moveable 50 + 16 antennas and allows the ACA antenna data to be processed in the ALMA baseline correlator. When all 50 antennas of the main array are combined in the 64-antenna correlator with 14 of the 16 ACA antennas we then reach the ultimate ALMA sensitivity. For compact sources the sensitivity may be improved by about 8% with respect to the main array alone and all calibration sessions are performed more quickly. The ACA 16-antenna correlator has also been installed on the high site. Processing the same data (up to 16 antennas) in two different correlators is of great value for an advanced comparison of these two large machines, whose specifications are similar (except that the ACA correlator processes 16 instead of 64 antennas). In the Japanese FX-type correlator, spectral averaging is performed after the F-part and the correlation is directly performed in 4 bits, but these details should remain invisible to the astronomers; only the effective spectral resolution should differ slightly.

Correlator modes for astronomical science

The ALMA baseline correlator supports a broad variety of observing modes, which may be classified into two main categories, the Time and Frequency Division Modes (TDM and FDM). In the TDM operation mode there are 32 parallel correlator planes, each processing, at 125 MHz, one-millisecond signal time slices from the digitised input baseband, and the correlator behaves as a pure XF system. In the FDM operation mode each of the 32 sub-bands in the 2 GHz input baseband is processed in one of the 32 correlator planes, or fewer sub-bands are processed by all planes to enhance the spectral resolution. The TFB filter boards are designed to support both

Total Bandwidth	Resolution (Nyquist, kHz)	Resolution (Double Nyquist, kHz)
2 GHz	244	488
1	122	244
500 MHz	61	122
250	30.5	61
125	15.3	30.5
62.5	7.6	15.3
31.25§		3.8§

Table 2. Bandwidth and resolution for 2-bit correlation with one 2 GHz baseband processed per correlator quadrant in frequency division operation mode (FDM).

§ Available with specific digital weights downloaded in last stage of the digital filter.

TDM and FDM, the data being directly sent to the final requantisation stage of each TFB board in the TDM operation mode. Examples of the spectral resolution achieved in FDM observing modes, for the case of only one baseband processed per quadrant, are given in Table 2 for different input bandwidths. Nyquist sampling is the basic working model of the correlator, but double Nyquist sampling is also available to improve the correlation efficiency (7% better) at the expense of lower correlator resources and so lower spectral resolution. The maximum resolution achievable, 3.8 kHz, enables extremely detailed spectral studies to be carried out.

If two basebands are processed per quadrant, the resolutions shown in Table 2 are twice as poor. There is another degradation by a factor of two with the additional polarisation cross-products required for a full Stokes parameter analysis. In order to improve the correlation efficiency, 4-bit correlation is also supported, but the frequency resolution is now four times poorer than that shown in Table 2. Double Nyquist sampling is also available with 4-bit correlation; it does not improve the already high efficiency much, but decreasing the spectral resolution speeds up the data dump rate. About 70 different observing modes are available with only a few TDM modes. TDM is to be preferred for fast dump rates (16 ms minimum) and moderate resolution (31.25, 15.6 or 7.8 kHz) across 2 GHz.

The 64-antenna correlator has the ability to move spectral sub-bands within the input baseband and to split one correlator quadrant into independent sub-units so that several options are supported: (a) high resolution in a given spectral region from 2 GHz to 62.5 MHz (or 31.25 MHz) with 62.5 MHz sub-bands tunable anywhere within 2 GHz; (b) multiple disjoint spectral regions fitting within 2 GHz but with the same spectral resolution, sensitivity and polarisation options; (c) multi-spectral resolution over different bandwidths to zoom on specific spectral features. All quadrants are independent and these different modes could also be implemented simultaneously with overlapping quadrants.

Spectral line and continuum astrophysics

The ALMA baseline correlator, with its flexible resolution and ability to analyse multi-spectral windows, is extremely well adapted to any type of spectral work. Two parameters are of interest, the total bandwidth and the spectral resolution:

Total bandwidth: Table 3 shows the typical total velocity coverage required for line analysis in a number of Galactic and extragalactic molecular sources, or in planets, and the corresponding total bandwidths at two widely separated frequencies (around 90 GHz where molecular transitions from HCO^+ or HCN are observed, and around 602 GHz where methanol is present). These frequencies fall in the ALMA receiver Bands 3 and 9, respectively. They have been arbitrarily selected to illustrate our discussion on required bandwidth. The total velocity coverage corresponds to the expected velocity extent at the base of the line profile with some additional spectral noise channels on each side of the line feature(s) of interest to provide a reference intensity level.

The maximum bandwidths that the baseline correlator can process match rather well with the total bandwidths in Table 3. These maximum bandwidths are: 2 or 1 GHz, 500, 250, 125, 62.5 or 31.25 MHz, with one quadrant; 4 GHz with two quadrants; or 8 GHz with four quadrants.

Spectral resolution: The various resolutions available with the baseline correlator are suited to a large variety of astrophysical environments. Table 2 gives examples, but there are more selectable modes with the 4-bit correlation and polarisation cross-products options. We give a few examples. About 1 MHz resolution is convenient to provide many details in the CO J = 2–1 line of many nearby galaxies or in energetic galactic outflows. This can be achieved, for

Source	Typical Total Velocity Coverage (km/s)	Total Bandwidth 90 GHz, 602 GHz
Galactic Sources		
Energetic Outflow in Young Stellar Objects	600	180 MHz, 1.2 GHz
Spectral Line Survey	300	90 MHz, 600 MHz
Orion, Galactic Centre	80–160	24–48 MHz, 161–321 MHz
Compact H II regions	40	12 MHz, 80 MHz
Molecular Cloud Spectra	10–40	3–12 MHz, 20–80 MHz
Dark Clouds	5	1.5 MHz, 10 MHz
Extragalactic Sources		
Nearby Galaxies (≤ 200 Mpc)	≤ 2000	≤ 0.6 GHz, ≤ 4 GHz
Highly Redshifted Sources		As large as possible
Planets		
Pressure Broadened Lines	1000–3000	0.3–0.9 GHz, 2–6 GHz

Table 3. Examples of total velocity coverage required for line observations of Galactic and extragalactic sources.

example, with 1 GHz total bandwidth in the Nyquist sampling TFD mode and with the high sensitivity 4-bit option; the resolution for the CO J = 2–1 line is then 1.3 km/s. At the higher frequencies of CO, one may either bin the spectral channels or use the coarser resolution of the TDM mode (7.8–31 MHz). On the other hand, there are a number of interesting astrophysical cases where velocity resolutions as high as 0.02–0.05 km/s are required: study of protostellar discs, dark molecular clouds, wind velocities in planets or thermal line widths in comets. In ALMA Band 3 for instance, around 6 kHz resolution is needed to reach 0.02 km/s and the observing modes providing 3.8 or 7.6 kHz are thus well suited. Analysis of Zeeman splitting or cosmic maser lines also requires high resolutions.

The ALMA baseband correlator will be configured for a number of broadband continuum projects in Galactic or extragalactic sources. The TDM mode is ideal for processing 2 GHz bandwidths with low spectral resolution in single, double or full polarisation observing modes. In all modes, combining independent quadrants broadens the total bandwidth if that were necessary. Moderately broad bandwidth will be sufficient in projects such as the thermal dust temperature study of Galactic young stellar objects and polarisation imaging of dust in young objects or molecular clouds in order to investigate the role of the magnetic field. FDM modes with 0.5–1 GHz bandwiths may often be appropriate depending on the selected receiver band. There is always the option to perform continuum and spectral line observations simultaneously with overlapping quadrants. For example 2 GHz continuum with low spectral resolution in TDM mode can be combined with higher FDM frequency resolution mode in 2 GHz or lower bandwidth.

An outstanding tool for molecular complexity

The ALMA correlator will offer new opportunities to help understand the complexity observed in the molecular Universe. Complexity refers to aspects as different as the identification or discovery of new molecules in the interstellar medium or in circumstellar envelopes, the relationship to astrobiology and the roots of prebiotic chemistry in the interstellar gas, the range of different environments in our Galaxy and distant galaxies, etc. Extremely rich spectra and complex molecules, prebiotic or not, have been observed with several existing millimetre-wave telescopes in a broad range of objects (very young stellar objects, pre-stellar cores, nearby or starburst galaxies, etc.). In the Orion Nebula or in the Galactic Centre, crowded line spectra and “forests” of lines have been observed, so that identification of the molecular carrier of a given line becomes difficult. An example of the crowded spectra obtained with the IRAM interferometer is given for Orion-KL, a massive star-forming region, around 223 GHz (see upper panel of Figure 5, adapted from Favre et al., 2008). An even more extreme case is that of Sgr B2(N) where Belloche et al. (2008) detected about 100 lines every 1 GHz around 100 GHz. From 88 transitions free of any spectral contamination, and from line maps in a subset of these lines, Belloche et al. have identified the complex amino acetonitrile molecule — a potential precursor of glycine. Crowded line spectra are expected in several ALMA submillimetric bands and spectroscopic databases or new techniques to predict spectral confusion may become essential. Despite these difficulties we believe that the ALMA correlator will greatly contribute to molecular astronomy in the mm/submm domains because of the following advantages: (a) in a broad bandwidth many lines are detectable at once and this allows the observer to identify the regions in crowded line spectra with less confusion; (b) multi-spectral resolution and very high spectral resolution help to resolve line blends; (c) multi-spectral windows offer the ability to compare properties of various molecules in the same source; (d) resolution can be traded for sensitivity options or polarisation modes. Of course, in complex molecular sources, and with adequate sensitivity, interferometric maps showing different spatial distributions may also help in the spectral confusion problem (see lower panel in Figure 5 showing good spatial separation of moderately blended lines).

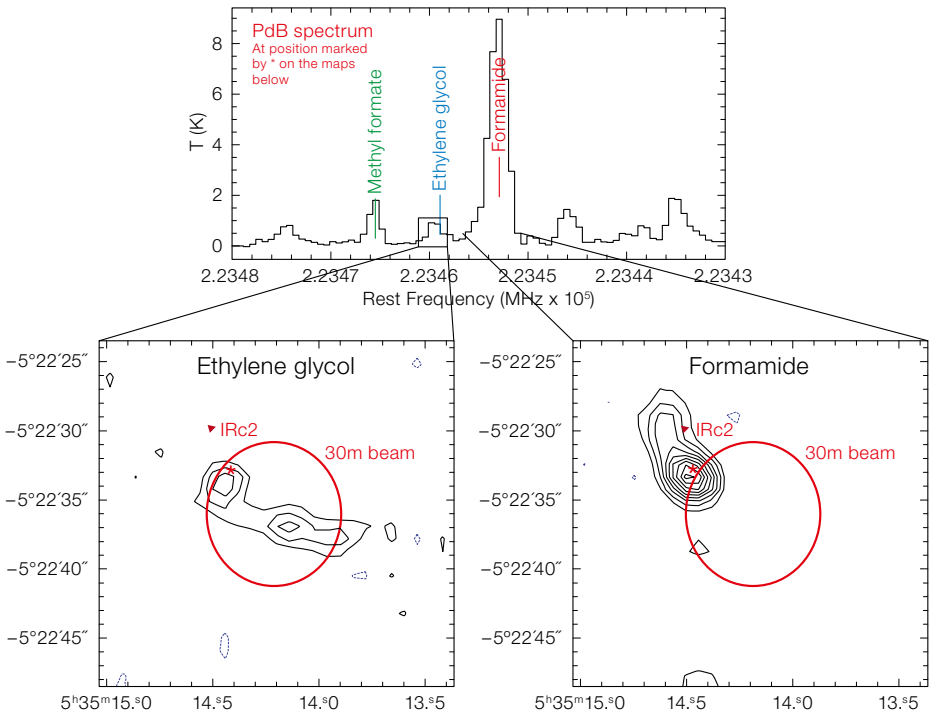

Figure 5. Upper panel: Cross-correlation spectrum of the Orion Nebula showing spectral features of complex molecules observed with the IRAM interferometer around 223 GHz. **Lower panel:** Spatial distribution of the ethylene glycol and formamide molecules obtained with the IRAM interferometer; the red circle corresponds to the spatial extent of the 30-metre telescope beam.

Future possibilities — near and longer term

The first quadrant of the baseline correlator system installed in the AOS technical building (see p. 5) supports up to 16 antennas. It is available for interferometric commissioning tasks and it meets the conditions for early science requiring 16 antennas and a basic set of spectral line modes. The first call for ALMA proposals is expected around 2011. One may anticipate that several FDM and TDM operational modes including double or full polarisation modes with different total bandwidths will be scheduled for early science. The second correlator quadrant will be installed in 2009 and the third and fourth quadrants, required to support up to 64 antennas, could be assembled by the end of 2010.

Other correlator configuration modes will become available in the future. Sub-arraying, namely the ability to process independent subsets of antennas operated in different modes, is an important ALMA feature. Initial implementation of two sub-arrays is a high priority. For instance, one group of antennas will map a source, while just one other antenna will perform single dish observations, or one sub-array will track a source while the second one will perform antenna commissioning tasks. Each correlator quadrant may support more than two sub-arrays.

The summed output signals from two or more antennas in the array will also be available in the correlator to form a big single antenna which can be combined with other antennas located on other continents to provide extremely high spatial resolution. This observing mode, named Very Long Baseline Interferometry (VLBI), will require some additional equipment at the AOS, but will certainly be used in the future. Pulsar observations may be supported as well, provided that pulsar period models can be implemented and that the ALMA receiver bands are of interest in pulsar astrophysics.

Finally, thanks to the ACA patch panel and the 16-antenna correlator being installed next to the 64-antenna baseline correlator, the following can be achieved: (a) the overall ALMA sensitivity can be enhanced by combining all data from a maximum of 64 antennas; (b) calibration of the twelve smaller 7-metre antennas can be efficiently accomplished when they are cross-correlated with all other 12-metre antennas; (c) comparison and cross-calibration of the ACA and baseline correlator performance becomes easier. ALMA science will benefit from these future possibilities.

Acknowledgements

The ALMA 64-antenna correlator has been constructed by a large group of people within the ALMA Correlator Integrated Product Team with support from the American and European ALMA Executives and from the various institutes involved in the design, production and testing: in the USA, NRAO, Charlottesville where the correlator quadrants are first assembled; in Europe, LAB at Université de Bordeaux, Osservatorio di Arcetri, Florence and Astron, Dwingeloo. It is a great pleasure to acknowledge the great spirit of co-operation which always prevailed between NRAO, Charlottesville and Université de Bordeaux from the design reviews to the ultimate construction/testing phases. The ALMA correlator software group played a key role in all the integrated tests of the correlator system. Highly stimulating exchanges developed between the European and Japanese correlator teams at the time when the European Second Generation Correlator concept was emerging.

References

Belloche, A. et al. 2008, A&A, 492, 769
Escoffier, R., Webber, J. & Baudry, A. 2005, ALMA System document, ALMA-60.00.00.00-001-B-SPE
Favre, C. et al. 2008, The Molecular Universe International Meeting, Arcachon, 5–8 May 2008
Haupt, C. & Rykaczewski H. 2007, The Messenger, 128, 25
Laing, R. 2008, The Messenger, 132, 28

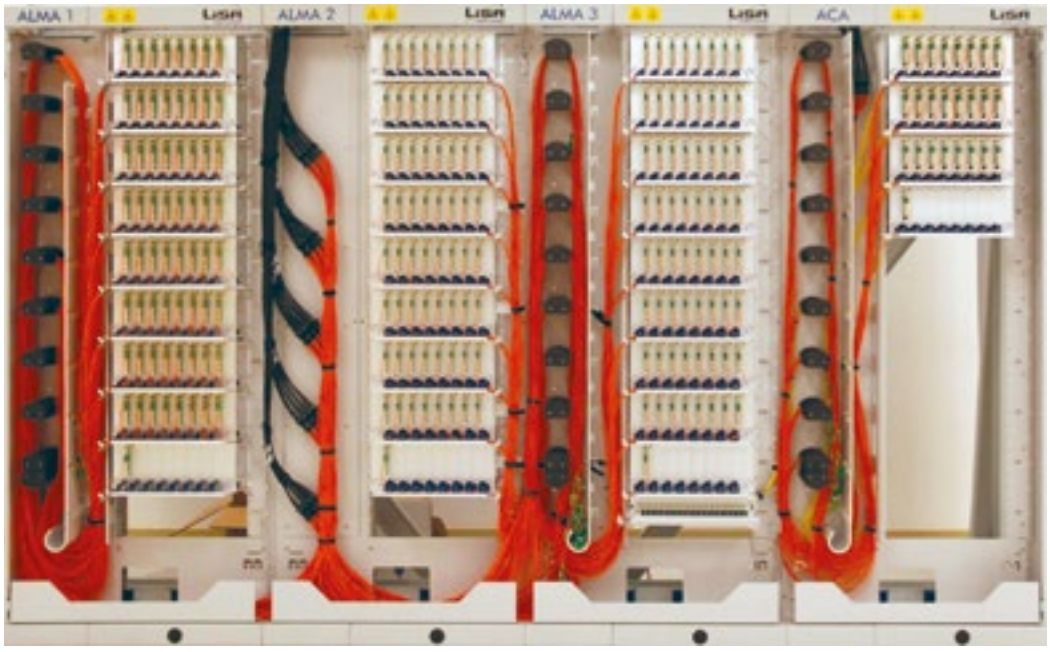

The ALMA Optical Fibre Network Patch Panel, shown left, was successfully installed in the AOS technical building at 5000 m altitude on the Chajnantor Plateau in December 2008. The Patch Panel, an ESO deliverable to ALMA, is used to send the Central Local Oscillator signal to all the ALMA antennas on Chajnantor, to receive the astronomical signals and redirect them to the Amplifier and Demultiplexer, before the real correlation takes place in the ALMA Correlator.

Improving the Multiplexing of VIMOS MOS Observations for Future Spectroscopic Surveys

Marco Scodeggio[1]
Paolo Franzetti[1]
Bianca Garilli[1]
Olivier Le Fèvre[2]
Luigi Guzzo[3]

[1] INAF IASF-Milano, Italy
[2] LAM, Marseille, France
[3] INAF Osservatorio Astronomico di Brera, Merate, Italy

The need to reduce the negative effects of fringing on VIMOS spectra has led astronomers to use observing techniques that significantly limit the multiplexing of VIMOS observations in multi-object spectroscopy mode. In this paper we propose a new observing strategy which, coupled with a new data reduction technique, has the potential to double VIMOS multiplexing while producing spectra of a quality comparable to that obtained in the major surveys performed so far.

Modern spectroscopic surveys are generally based on multi-object observations, where many tens to hundreds of objects are observed simultaneously during each telescope pointing, to speed up the completion of projects that collect the spectra of many thousands of objects. As it is often the case with astronomical instrumentation, the practical requirements to achieve this high degree of multiplexing are quite at odds with those necessary to obtain high quality spectra for each of the surveyed objects. In this paper we describe an observing strategy and a specific data reduction procedure for the ESO Very Large Telescope (VLT) VIsible Multi-Object Spectrograph (VIMOS), designed to increase the multiplexing of MOS observations, without significantly affecting the quality of the spectra thus produced. In the optimal case of a deep survey with a large set of potential targets for the spectroscopic observations, it will be possible to double the multiplexing of the MOS observations with VIMOS using this new strategy.

VIMOS fringing problems

The most important characteristic of the VIMOS spectrograph (Le Fèvre et al., 2002) is its high degree of multiplexing, conceived specifically to speed up the execution of spectroscopic surveys significantly. Unfortunately, the VIMOS CCDs installed when the instrument was commissioned are thinned E2V detectors from early 2000 technology, and they are affected by significant fringing redwards of approximately 800 nm, as shown in Figure 1. Without proper corrections the spectra obtained with VIMOS red grisms (including the LR_red, MR, HR_orange and HR_red grisms) for faint extragalactic sources are very difficult to use above this wavelength. The effects of fringing need to be counteracted to obtain spectra that can take full advantage of the wavelength coverage provided by these grisms (reaching approximately 950 nm), and in order to extend the wavelength and the redshift coverage of the redshift surveys as much as possible. This is why the data for the two main surveys carried out so far with this instrument in MOS mode, the VLT VIMOS Deep Survey (VVDS; Le Fèvre et al., 2005), and the zCOSMOS survey (Lilly, 2008), and the data for many other smaller VIMOS programmes, have all been obtained starting from observations carried out in jitter mode. The total exposure time for each instrument pointing is subdivided into separate shorter exposures, and the telescope is offset by a small amount after each exposure (typically 1 or 2 arcseconds), making sure that the objects are kept inside the MOS mask slits. As a result of the offsets, the object spectra fall on different pixels on the CCD in different exposures, and it is possible to obtain a relatively accurate and complete reconstruction of the fringing pattern by median-combining all the available exposures.

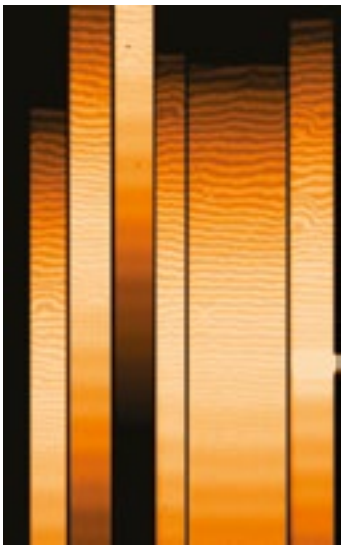

Figure 1. Fringing pattern in VIMOS MOS red data. A small portion of a flat-field exposure obtained with the LR_red grism is shown, including spectra from six different MOS slits. The red end of the spectra is towards the top.

The cost of implementing this observing technique is a reduced multiplexing for MOS observations. To make sure the target objects remain visible inside the slits after the offsets, the slits must be designed and cut longer than they would otherwise need to be (in practice, one has to specify a larger sky region inside the VIMOS mask preparation software [VMMPS]). In stare mode, with a typical faint object size of 2 arcseconds (the average apparent diameter of a high redshift galaxy in ground seeing conditions), and a minimum sky region on each side of the object of 2 arcseconds to allow for an accurate sky subtraction, slits would typically be 6 arcseconds long (i.e., 30 VIMOS CCD pixels). In jitter mode, to accommodate a pattern with five jitter positions (like those used for VVDS and zCOSMOS observations), we must add another 2 to 3 arcseconds on each side of the object, for a total slit length of 10 to 12 arcseconds (i.e., 50 to 60 VIMOS CCD pixels). This approximate doubling of the typical slit length directly translates into a reduction of 50% of the VIMOS multiplexing, which is precisely what has happened for both the VVDS and zCOSMOS projects.

Searching for alternatives

In preparation for future spectroscopic surveys, we have recently studied the possibility of adopting a different observing strategy to increase the multiplexing of VIMOS observations in MOS mode, without significantly affecting the data quality and the measurement reliability of redshifts. As a first step we started using real VIMOS MOS data, originally obtained in jitter mode with long slits as part of the VVDS and zCOSMOS surveys, to simulate a number of different

observing strategies, and to evaluate their capability of providing a reliable sky subtraction and an accurate fringing pattern removal. The main indication of this work is that a data quality comparable to that of VVDS and zCOSMOS data can be obtained with observations carried out in stare mode, with relatively small slits. The necessary fringing corrections for the red spectra can be derived from a flat-field exposure, provided that such an exposure is obtained as part of the night-time calibrations, immediately before or after the wavelength calibration lamp observation that is normally executed at the end of each set of exposures in an Observing Block.

This flat-field exposure is affected by fringing, much like the scientific exposures, except for the precise positioning of the fringing pattern on the CCD pixels which, because of flexure inside the instrument, can shift by a few pixels between any two exposures. We have seen that it is possible to compensate for these offsets by allowing a search for the best-matching fringing pattern between the flat-field and the scientific exposure over a range of a few pixels (comparable to the known extent of the image shift resulting from the flexure). This technique is schematically described in Figure 2: for each row of pixels in the image of a two-dimensional spectrum produced by a MOS slit during a science exposure, we search in the corresponding image produced by a flat-field exposure for the row that best reproduces the count variations created by the fringing pattern, extending this search over a few rows (typically five) of the flat-field image.

Technically, we normalise the flat-field row counts to have the same median counts as in the science exposure row data, and then we compute a very simple χ^2 statistic adding together, pixel by pixel, the squared values of the difference between normalised flat-field and science exposure. The flat-field row that minimises the total χ^2 value is considered the best-matching one. Once such a row has been identified, we scale the total counts in this row to match those measured in the science exposure, and we subtract the scaled flat-field row values from the science exposure row values, effectively producing both a sky subtraction and a fringing pattern removal in a single step. Any region of the CCD where a significant contribution from the spectrum of an object is present on top of the general sky background in the science

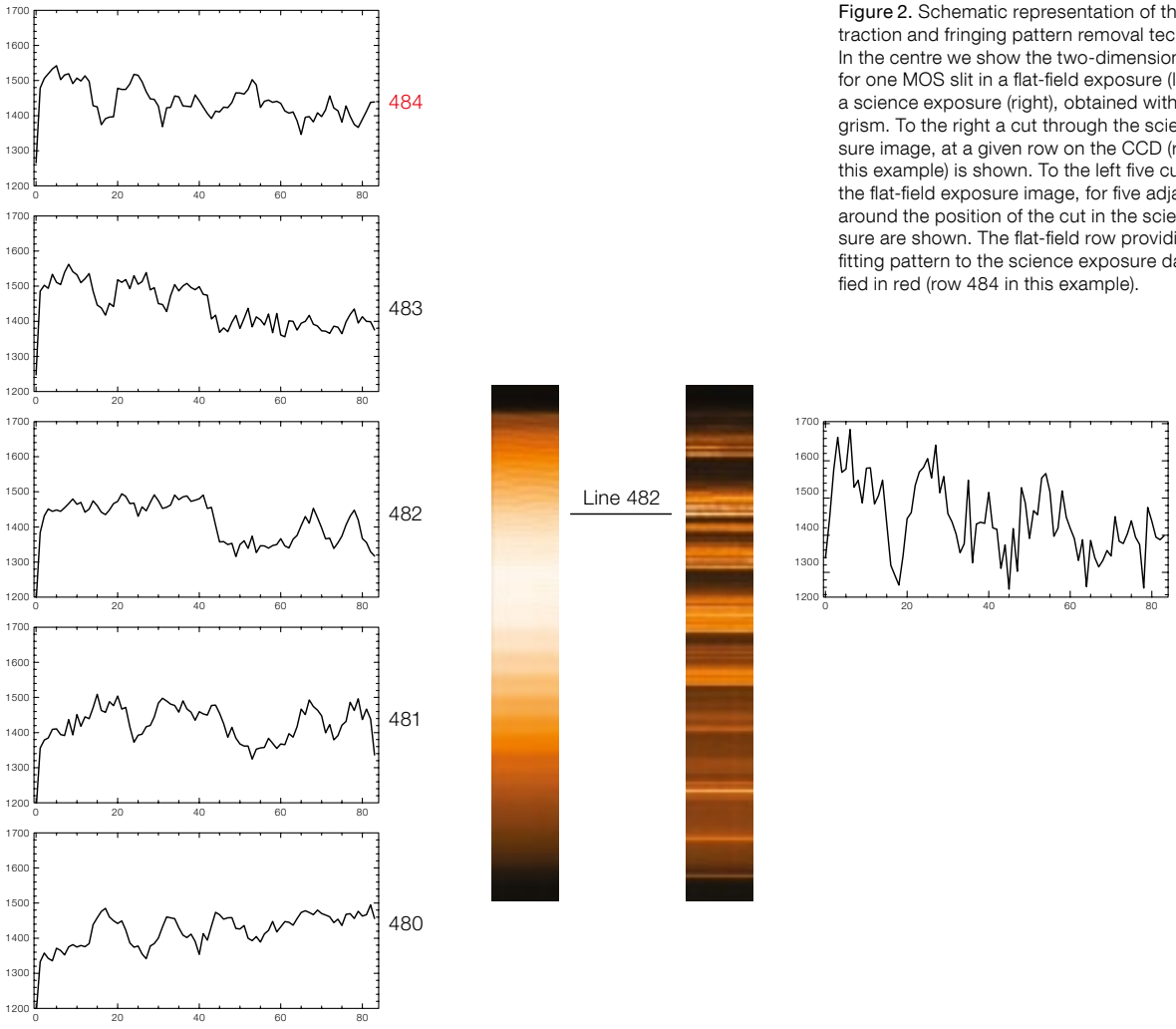

Figure 2. Schematic representation of the sky subtraction and fringing pattern removal technique. In the centre we show the two-dimensional spectrum for one MOS slit in a flat-field exposure (left) and in a science exposure (right), obtained with the LR_red grism. To the right a cut through the science exposure image, at a given row on the CCD (row 482 in this example) is shown. To the left five cuts through the flat-field exposure image, for five adjacent rows around the position of the cut in the science exposure are shown. The flat-field row providing the best fitting pattern to the science exposure data is identified in red (row 484 in this example).

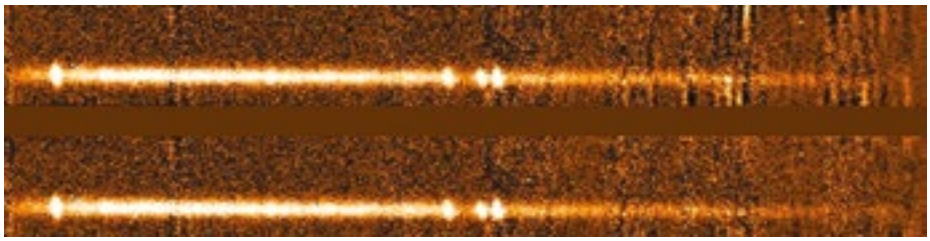

Figure 3. A comparison of results obtained using the traditional jitter sequence observation and the standard VIMOS data reduction pipeline *v.* the new stare mode observation and fringing removal technique. The same two-dimensional sky-subtracted spectrum of a galaxy observed with the LR_red grism as part of the VVDS is shown: the result of the traditional data reduction method (upper); the result of the simulated stare mode observation coupled with the newly proposed reduction technique (lower). In this example the new reduction method produces better removal of the fringing pattern than the traditional one.

exposure image is excluded from the matching pattern search and from the rescaling computation.

An example of a sky- and fringing-subtracted spectrum is shown in Figure 3, where we compare the results of the traditional jitter sequence data reduction with the results of the new technique proposed here, applied to a simulated short slit stare mode observation derived from a VVDS observation obtained with the VIMOS LR_red grism.

Validation of new method

The simulation results briefly discussed above indicate that it should be possible to obtain good quality spectra for faint astronomical targets from VIMOS spectroscopic observations in MOS mode carried out using a stare mode observing technique. The main advantage of using stare mode observations would be the possibility of using MOS slits that have, on average, half the length of the slits used in traditional jitter mode observations. Using short slits in this way would immediately translate into an approximate doubling either of the efficiency or of the total yield for a spectroscopic survey carried out with VIMOS, in comparison with the efficiency or yield obtained so far with the VVDS and zCOSMOS surveys. This result would of course be achievable only for a deep survey, where the number of potential targets is at least twice as large as the number of slits that could potentially be placed on a MOS mask. Given the very significant impact that this result could have on future spectroscopic surveys, we decided to propose a direct on-sky verification of our results.

We therefore submitted a small Director's Discretionary Time (DDT) proposal to ESO to perform one spectroscopic survey-like observation with VIMOS using short-slit masks and stare mode exposures. This was approved as programme 281.A-5044 (A), and executed on 26 September 2008. Figures 4 and 5 show the results obtained by reducing these data with both the traditional data reduction technique (Figure 4) and the newly proposed method (Figure 5). It is quite clear from a comparison of the two images that the new fringing subtraction technique is quite efficient. In order to quantify the impact of the technique better, we have systematically compared the root mean square (rms) variations in the residual background level (after sky subtraction) of the two-dimensional spectra between the red spectral region (affected by fringing) and the blue region (free of fringing). For the data shown in Figure 4, which effectively still contain the whole fringing pattern, the rms variations in the red part of the background are six to eight times as large as those in the blue part. For the data shown in Figure 5, reduced with the new fringing removal technique, the rms variations in the red part of the background are only two to four times as large as those in the blue. To visualise the impact that these residuals

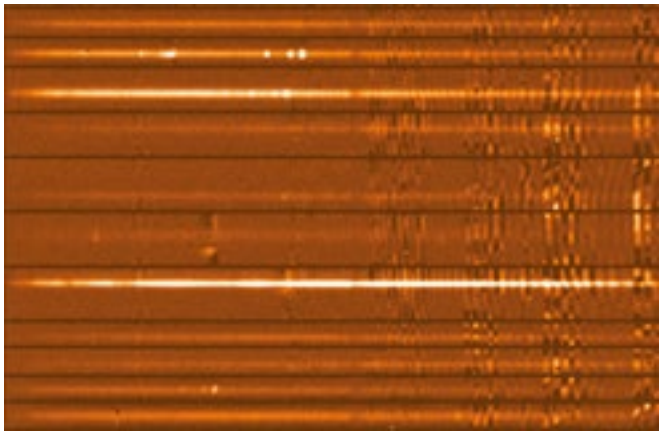

Figure 4. Two-dimensional sky-subtracted spectra for a number of slits, produced using a mask with short slits and stare mode observations as part of our DDT programme. The blue end of the spectra is to the left. The data have been reduced with the traditional method, appropriate for jitter mode observations. The fringing pattern residuals are clearly visible in the right half of the image.

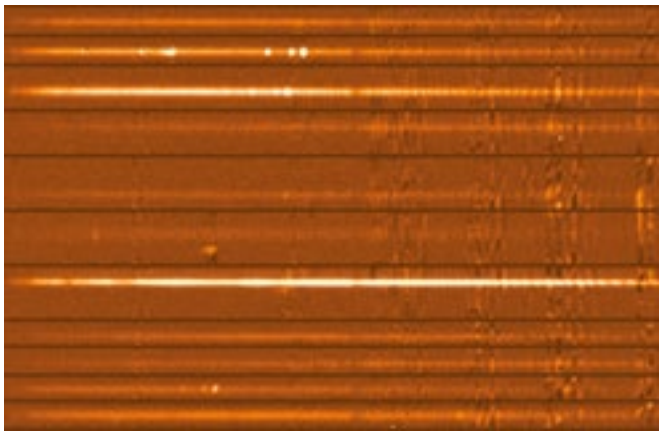

Figure 5. Same data as in Figure 4, but this time the newly proposed data reduction method has been used. The image colour cuts are identical to those in the previous figure. The significant removal of the fringing pattern, although not perfect, can be easily appreciated by comparing the two images.

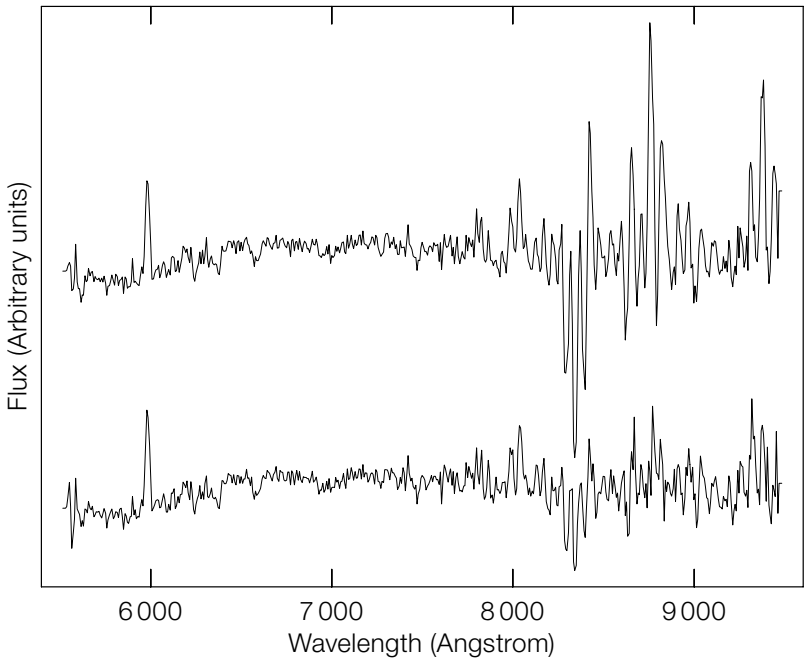

Figure 6. Comparison of one-dimensional spectra for one galaxy observed during our DDT run. The top spectrum is extracted from the data shown in Figure 4, and clearly shows the noise introduced by the strong fringing residuals. The bottom spectrum is extracted from the data shown in Figure 5, and shows a more uniform noise pattern in the blue and red half of the wavelength range.

can have on the final one-dimensional spectra extracted from these data, we show in Figure 6 a comparison of the extracted one-dimensional spectra for the same object, obtained by starting from the data shown in Figures 4 and 5. It is quite clear from this figure that the noise in the red part of the final spectra is significantly reduced by our new data reduction technique. The new data reduction technique is implemented as part of the VIMOS Interactive Pipeline Graphical Interface (VIPGI) data reduction pipeline[1] (Scodeggio et al., 2005), and will be available to the whole astronomical community with VIPGI public release 1.4.

Future prospects

The results discussed here show that it is possible to obtain spectroscopic data with a quality comparable to that of VVDS and zCOSMOS data, which in turn translates into a success rate for redshift measurement of approximately 90% for the targeted galaxies, using MOS masks with short slits coupled with stare mode observations, irrespective of the wavelength range covered by the spectra. Using MOS slits that are on average only half as long as those used for jittered observations would translate into the option to place twice as many slits on any VIMOS MOS mask. To take full advantage of this option it is necessary to have a relatively densely populated starting sample for the spectroscopic observations: our experience with VVDS and zCOSMOS indicates that MOS masks are populated with their maximum slit capacity only when the starting sample of potential targets includes at least twice as many objects per VIMOS quadrant as this maximum number of slits. This is generally the case in relatively deep extragalactic spectroscopic surveys: both the VVDS and zCOSMOS, in their Wide and Deep samples, have a density of potential targets which is two to three times as large as the potential maximum number of short slits one could accommodate on VIMOS masks.

The first project to take advantage of this new observing strategy and data reduction method is already under way: the VIPERS survey (ESO Large Programme 182.A-0886 with PI L. Guzzo). From the set of MOS masks that were designed for the first semester of observations, we can estimate that this survey should be able to observe spectroscopically 60% of the parent galaxy sample defined from the complete photometric catalogue. In contrast, with a mask design typical of jittered observations, and with the same allocation of telescope time, it would have been possible to sample only some 32% of the galaxies. This increase in efficiency has a very significant impact not only on the final survey sample, but also on the science results expected from this project.

Finally, the general capability of the ESO community to carry out very large spectroscopic surveys in an efficient manner will receive a further boost by the planned substitution of the VIMOS CCDs, which should produce spectra with much reduced fringing residuals in the red part of the spectrum with respect to the currently installed CCDs. Using the data produced by these new CCDs as input, our new reduction technique is expected to produce final one-dimensional spectra that have uniform noise levels over the whole wavelength range covered by the VIMOS grisms. This result, coupled with the higher quantum efficiency in the red part of the spectrum provided by the new CCDs, is expected to increase the overall efficiency of a VIMOS-based redshift survey for faint astronomical targets by a factor of two to three.

References

Le Fèvre, O. et al. 2002, The Messenger, 109, 21
Le Fèvre, O. et al. 2005, The Messenger, 119, 30
Lilly, S. 2008, The Messenger, 134, 35
Scodeggio, M. et al. 2005, PASP, 117, 1284

Notes

[1] http://cosmos.iasf-milano.inaf.it/pandora/vipgi.html

Report on the ESO Workshop

Six Years of FLAMES Operations

held at ESO Headquarters, Garching, Germany 1–3 December 2008

Claudio Melo[1]
Francesca Primas[1]
Luca Pasquini[1]
Ferdinando Patat[1]
Jonathan Smoker[1]

[1] ESO

A significant fraction of the community of users of the VLT multi-fibre spectrograph facility, FLAMES, gathered at ESO Headquarters in December 2008 to present scientific highlights, after six years of FLAMES operations. This proved to be a great opportunity to review the scientific impact that FLAMES has had on different fields of astrophysical research and for ESO to assess the current and future needs of FLAMES users. We report on the two and a half day meeting, during which all participants openly discussed their experience with FLAMES and shared their expertise.

The Fibre Large Array Multi Element Spectrograph — or simply FLAMES — recently completed six years of successful operations attached to the Very Large Telescope (VLT) Nasmyth A focus of Kueyen, at the La Silla Paranal Observatory.

The combination of an extended field of view with many and varied fibres (a total length of 1.6 km if stretched from end to end!) and set-ups has made FLAMES a unique facility in ground-based astronomy. Thanks to its versatility, FLAMES can be used in many different astronomical applications. Extrasolar planet-hunting, chemical abundances of stellar groups (globular, open clusters, Galactic streams, Local Group galaxies, etc.), kinematics and dark matter, planetary nebulae, the interstellar medium and stellar evolution are only some examples of the science cases that have been targeted with FLAMES.

We thought it was time to celebrate and to review the performance of FLAMES during these six years of operations. Following the successful experience inaugurated with UVES almost six years ago, the FLAMES community was invited to participate in an informal workshop held at ESO Headquarters from 1–3 December, 2008.

It was a great pleasure to see that almost all of the teams who had so far made use of FLAMES attended the workshop. The participants were asked to present their scientific results and to add one slide describing the pros and cons of using FLAMES to carry out their science. These points were collected and used in the final open discussion (see below). In addition, a few more technical talks were presented by members of the community and the FLAMES Instrument and Operations Team (IOT) presented some statistics concerning the use of FLAMES. During these six years of operations, about 9000 science frames have been taken (with an average of 100 objects per image!), the equivalent of 400 nights of VLT time in total. This corresponds to about 25% of the time available on Kueyen and is close to the fraction of UT2 time requested at proposal submission (roughly one third per UT2 instrument).

Science highlights

All participants were invited to give a talk in one of the five different sessions, namely, star formation and planets, chemical evolution of the Milky Way and streams, external galaxies, kinematics and dark matter, and stellar evolution. Each session began with an introductory review talk. All presentations are available online[1]. Many of the talks described samples of stars in the hundreds to thousands, emphasising the huge multiplex gain obtained in using FLAMES over single-slit instruments.

A few subjectively selected highlights demonstrate the range of scientific ideas and prospects presented during the workshop; the high quality of the science presentations is of course not limited to those cited in this article.

The combination of a photometric transit with the measurement of radial velocity allows the actual mass and radius of extrasolar planets to be derived. Transit candidates yielded by surveys like OGLE or CoRoT are full of impostors (i.e., different configurations can produce a light curve similar to the one observed in a genuine planetary transit). Dominique Naef and Francois Bouchy showed how FLAMES contributed to cleaning up the list of impostors for transit candidates and to deriving radial velocity curves for the very faint OGLE transit planets. Richard Jackson described a search for planets and/or binary companions in very low mass stars and brown dwarfs in which he concluded that the binarity fraction appears to be lower in these objects than for higher mass stars.

Age is one of the fundamental parameters in astrophysics. The Lithium Depletion Boundary (LDB), i.e., the position in the colour-magnitude diagram that separates low mass stars with and without detected lithium, is a function of age and is thought to be almost model-independent. Rob Jeffries showed an example of how FLAMES can be used to determine the LDB of the faint members of NGC 2547 based on the observations of the Li 670.8-nm line. His approach could be extended to a handful of clusters that would then constitute benchmarks for gauging theoretical isochrones.

The study of the Milky Way (MW) Bulge was reviewed by Alvio Renzini, who presented evidence for the very rapid formation of the Bulge. Moreover, Bulge stars seem to be chemically different from the stars in dwarf spheroidal galaxies. Although the origin of the Bulge has not been fully understood, Renzini qualified the FLAMES contribution as a “quantum jump” in this direction. Simone Zaggia presented results of FLAMES observations in the direction of the Chandra Deep Field South where they found more stars than expected beyond 20 kpc and even one star at 165 kpc. Vanessa Hill reviewed the state of our knowledge of chemical evolution in dwarf spheroidal (dSph) galaxies and the LMC. Each of the LMC, Sagittarius, Fornax, Sculptor and Carina galaxies shows a distinct chemical evolutionary track. There is

some evidence that the abundance pattern in metal-poor stars is indistinguishable everywhere, although dSph galaxies appear to lack the most metal-poor stars (Fe/H < −3) found in the MW halo.

Chris Evans and Christophe Martayan presented observations of early-type stars in the Magellanic Clouds. In the large programme (LP) described by Evans it was found that rotational mixing is not as dominant as previously thought, with both Martayan and Evans finding that low metallicity stars spin faster. However, a remaining open question is whether the birthplace of a star (in a bound cluster for example) is as important as its initial metallicity in determining the rotational parameters. Jonathan Smoker used archive data from this LP to investigate the small-scale structure of high velocity clouds towards the Magellanic system and found variations in Ca II equivalent width of a factor of 10 over a few arcminutes. In another study concerning the gas, Yiannis Tsamis and Alena Zwansig described the use of ARGUS to map planetary nebulae and protoplanetary discs in emission lines at high spatial and spectral resolution to determine the physical properties and chemical abundances of these objects.

Katrin Jordi and colleagues used FLAMES to look into the velocity dispersion of Palomar 14. They concluded that their results tend to favour more classical Newtonian mechanics rather than the MOND predictions. In an invited review, Gerry Gilmore described the use of FLAMES to observe the dynamics of dwarf spheroidals (supporting flat inner-mass profiles) and how FLAMES has been used to resolve the spatial scales of the first enrichment and reionisation. Thousands of stars have already been observed, although many targets still exist for study.

Andreas Korn put forward evidence for the need to include atmospheric diffusion to correctly explain lithium depletion in metal-poor stars. Indeed, if atmospheric diffusion is taken into account, the observed Li abundances in NGC 6397 can be reconciled with the cosmic microwave background and Big Bang nucleosynthesis predictions.

Finally, on the extragalatic front, Francois Hammer reviewed the results on the morphological and kinematical study of galaxies at $z \sim 0.6$ using the deployable Integral Field Units (IFUs). The preliminary conclusions suggest that spiral galaxies are more frequent by a factor of two at the present day than at $z \sim 0.6$ (70% versus 33%). In contrast, the rate of peculiar, compact or mergers drops from 44% at $z \sim 0.6$ to about 3% at $z = 0$, whereas the fraction of luminous infrared galaxies drops from 20% at $z \sim 0.6$ to 0.5% at $z = 0$. This work is ongoing, with the final aim being to understand the origin of the present-day spirals.

Technical talks

The morning of the last day was filled with more technically-driven talks on data reduction, analysis tools, possible (new) applications and upgrades for FLAMES.

In his talk on IFU data reduction, Christer Sandin presented his open software, used to reduce IFU and ARGUS data, and drew attention to the need to properly account for differential atmospheric refraction correctly when analysing IFU images. Giuseppina Battaglia described the sky subtraction method developed by Mike Irwin and applied by her team in the chemical study of the dSph galaxies.

The MATISSE package has been developed by the Nice Observatory team to analyse stellar spectra to be collected by the GAIA mission. A demonstration of the enormous potential of the use of MATISSE to treat FLAMES data was given by Alejandra Recio-Blanco. Fredric Royer showed a web-based tool designed to query the FLAMES GTO science-ready data obtained by the Observatoire de Paris.

Luca Pasquini showed the potential of a very interesting FLAMES IFU application to observe simultaneously the photometric and spectroscopic transit of a giant planet in front of its host star. An investigatory study is ongoing. If validated, this type of observation could help to improve mass and radius determination of extrasolar planets. It may also provide spin-orbit inclination and indications of additional (unseen) low-mass companions by studying variations of the transit time.

Closing the technical session, Francoise Roques proposed a future upgrade of FLAMES, aimed at using its large field of view to carry out fast photometry of a large area of the sky. A dedicated workshop on ESO Spectroscopic Surveys[2] will take place in March 2009 at ESO Headquarters in Garching to discuss the future of survey instruments such as FLAMES.

Open discussion

The open discussion was moderated by Luca Pasquini, who made the initial point that, in such a complex instrument, with many different modes and used in many different applications, the users are quite often the experts. Therefore, the exchange of experience, tools, etc. with ESO staff and within the community itself is desirable, and indeed necessary, to improve the data quality provided to the users by ESO.

During the workshop, it became clear that most FLAMES users do not reduce their data with the ESO pipeline software. Rather, a large fraction still uses the Geneva Baseline Data Reduction Software (BLDRS) that was the only data reduction software available at the very beginning of FLAMES operations. During the open discussion, ESO representatives reported that the ESO GIRAFFE pipeline software is now mature, robust, and produces science-ready data, especially when used interactively. Users are therefore encouraged to download the package[3] and to use it for their own data reduction. Workshop participants mentioned that the Geneva BLDRS offers some automated tools to extract further information from the GIRAFFE spectra (e.g., radial velocities, for all science and simultaneous calibration fibres). Representatives of the ESO FLAMES IOT took note of these remarks and will investigate

solutions, for example improvement of relevant algorithms or adaption of the products of the ESO pipeline to interface to relevant data analysis packages.

A number of other technical issues were brought to the attention of the ESO staff attending the Workshop, including:

– differences in equivalent widths between FLAMES/UVES and FLAMES/GIRAFFE spectra of the same objects;

– typical shifts in the cross-dispersion direction between the science and morning flats should be quantified and reported in the User Manual;

– the accuracy of sky subtraction should be quantified and reported in the User Manual;

– the need for a new set of solar spectra taken with the new CCD at all settings.

These and other points that were raised during the Workshop will be discussed within the FLAMES IOT for further follow-up. The results of these investigations will be disseminated by means of the FLAMES webpages[4] and related documents.

Acknowledgment

We would like to thank all participants for their willingness and good spirit in sharing results and experiences during the three days of the workshop. For us, the ESO staff present, it was a wonderful experience to share the room with a large fraction of the community of FLAMES users. Finally, we would like to thank the Director General Discretionary Fund programme for funding this informal workshop.

Notes

[1] http://www.eso.org/sci/facilities/paranal/instruments/flames/doc/FLAMES_6th_Anniversary/FLAMES_6th_Anniversary.html
[2] http://www.eso.org/sci/meetings/ssw2009/index.html
[3] http://www.eso.org/pipelines
[4] http://www.eso.org/sci/facilities/paranal/instruments/flames/news.html

The FLAMES facility mounted at the Nasmyth A platform of VLT UT2, Kueyen.

Colour composite image of a region of the Carina Nebula (NGC 3372) formed from exposures in six filters (U, B, V, Rc, Hα and [S II]) taken with the ESO/MPG 2.2 m telescope on La Silla and the Wide Field Imager. See 05/09 Photo Release for more details.

Studying the Magnetic Properties of Upper Main-sequence Stars with FORS1

Swetlana Hubrig[1 2]
Markus Schöller[1]
Maryline Briquet[3]
Peter De Cat[4]
Thierry Morel[5]
Donald Kurtz[6]
Vladimir Elkin[6]
Beate Stelzer[7]
Roald Schnerr[8]
Carol Grady[9]
Mikhail Pogodin[10 11]
Oliver Schütz[1]
Michel Curé[12]
Ruslan Yudin[10 11]
Gautier Mathys[1]

1 ESO
2 Astrophysikalisches Institut Potsdam, Germany
3 Instituut voor Sterrenkunde, Katholieke Universiteit Leuven, Belgium
4 Koninklijke Sterrenwacht van België, Brussel, Belgium
5 Institut d'Astrophysique et de Géophysique, Université de Liège, Belgium
6 Centre for Astrophysics, University of Central Lancashire, Preston, UK
7 INAF-Osservatorio Astronomico di Palermo, Italy
8 Institute for Solar Physics, Royal Swedish Academy of Sciences, Stockholm, Sweden
9 Eureka Scientific, Oakland, USA
10 Pulkovo Observatory, Saint-Petersburg, Russia
11 Isaac Newton Institute of Chile, Saint-Petersburg Branch, Russia
12 Departamento de Física y Astronomía, Universidad de Valparaíso, Chile

We summarise the results of our recent magnetic field studies in upper main-sequence stars, which have exploited the spectropolarimetric capability of FORS1 at the VLT extensively.

Introduction

Currently, most stellar magnetic field observations are carried out using three spectropolarimeters. In the northern hemisphere, the high resolution spectropolarimeter ESPaDOnS is installed at the 3.6-metre Canada France Hawaii Telescope (CFHT) on Mauna Kea and its twin NARVAL at the 2-metre Telescope Bernard Lyot on Pic du Midi. ESPaDOnS and NARVAL can obtain linear and circular polarisation spectra at a resolution of about 65000. In the southern hemisphere, the visual and near UV FOcal Reducer and low dispersion Spectrograph, FORS1, at UT2/Kueyen of the VLT offers a spectropolarimetric mode with a resolution of up to 4000. The two smaller telescopes, in particular the Telescope Bernard Lyot, dedicate significant amounts of observing time to magnetic studies by the French and Canadian communities, making long-term magnetic monitoring and magnetic surveys of certain types of stars possible. However only a few programmes have been devoted to the study of stellar magnetic fields with FORS1 in recent years, on account of the high demand for observing time with all instruments installed on Kueyen.

One of the biggest advantages of using FORS1 at an 8-metre telescope is the large collecting area, giving high S/N polarimetric spectra of relatively faint stars, down to magnitudes 12–13. Further, due to the use of Balmer series lines for the measurements of stellar magnetic fields in the blue spectral region, observed with grisms 600B or 1200B, fast rotators with $v \sin i$ up to 300 km/s can be studied. The technique for measuring stellar magnetic fields with FORS1 in polarimetric mode was discussed by Bagnulo et al. (2001) eight years ago, when the first measurement of the well known strongly magnetic chemically peculiar A-type star HD 94660 was discussed in detail.

The measurement of magnetic fields makes use of the presence of circular polarisation in spectral lines, allowing longitudinal magnetic field, which is the component of the magnetic field along the line of sight, averaged over the stellar disc, to be determined. Since no ESO pipeline for the FORS1 spectropolarimetric mode exists, the spectrum extraction is performed using a pipeline written by Thomas Szeifert. The software for measuring the magnetic field strength was developed by us. In the following we describe our magnetic field discoveries achieved with FORS1 in recent years.

New magnetic chemically peculiar stars

The magnetic chemically peculiar stars with spectral classes A and B (Ap and Bp stars) are presently the best-studied stars in terms of magnetic field strength and magnetic field geometry. Contrary to the case of solar-like stars, their magnetic fields are dominated by large spatial scales and remain unchanged on yearly timescales. Braithwaite & Spruit (2004) confirmed, through simulations using 3D numerical hydrodynamics, the existence of stable magneto-hydrodynamic configurations that might account for long-lived, ordered magnetic fields in these types of stars.

During 2002–2004, our first survey of a sample of more than 150 Ap and Bp stars, including rapidly oscillating Ap stars (Hubrig et al., 2006a) confirmed that low resolution spectropolarimetry of hydrogen Balmer lines obtained with FORS1 represents a powerful diagnostic tool for the detection of stellar magnetic fields. We first discovered magnetic fields in 63 Ap and Bp stars in this survey. Some of these stars were used for a re-discussion of the evolutionary state of upper main-sequence magnetic stars with accurate Hipparcos parallaxes. These new observations confirmed our previous finding that magnetic stars of mass $M < 3\ M_{\odot}$ are concentrated towards the centre of the main-sequence band, whereas stars with masses $M > 3\ M_{\odot}$ seem to be concentrated closer to the zero-age main-sequence (Hubrig et al., 2000; 2007a).

In the course of this study we discovered an extreme magnetic Ap star, HD 154708 (= CD –57°6753), which has the strongest longitudinal magnetic field ever detected in a rapidly oscillating Ap (roAp) star, with a mean magnetic field modulus $< B > = 24.5 \pm 1.0$ kG (Hubrig et al., 2005). This magnetic field is about a factor of three stronger than that of HD 166473, $< B > \approx 5.5$–9.0 kG, the roAp star with the second strongest magnetic field. In Figure 1 we present recent FORS1 measurements of the former star over three months in 2008 used to determine the rotation period of $P_{\rm rot} = 5.367 \pm 0.020$ days. HD 154708 is the first star observed with FORS1 with a sufficiently uniform phase coverage to establish its magnetic

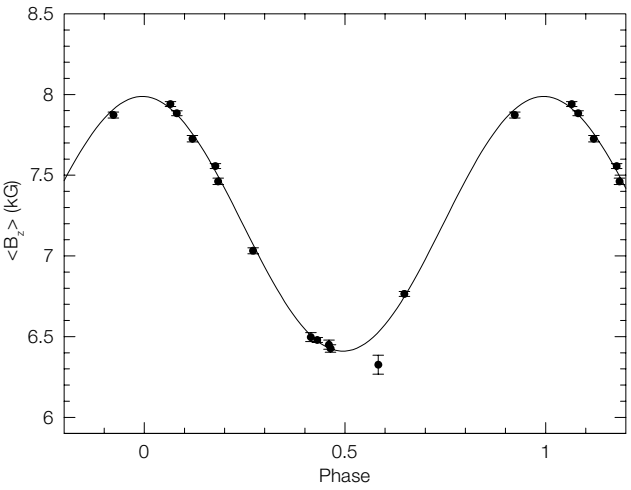

Figure 1. Phase diagram for the magnetic field measurements of the strongly magnetic star HD 154708; using hydrogen and metal lines the best frequency is 0.1863 d^{-1}, P_{rot} = 5.367 days.

period (Hubrig et al., 2009, submitted). Note that the size of the error bars is comparable to the size of the dots representing the individual measurements. The measurement with the largest sigma (< B_z > = 6.326 ± 0.059 kG) was obtained in weather conditions classified as "thick clouds", where the guide star was frequently lost and thus was repeated by the service observer a couple of nights later.

O stars, pulsating B-type stars and early-type emission line stars

Massive stars usually end their evolution with a final supernova explosion, producing neutron stars or black holes. The initial masses of these stars range from 9–100 $M_{\odot}$ or more, which correspond to spectral types earlier than about B2. The presence of magnetic fields in massive stars has been suspected for a long time. The discovery of these magnetic fields would explain a wide range of well-documented enigmatic phenomena, in particular cyclical wind variability, Hα emission variations, chemical peculiarity, narrow X-ray emission lines and non-thermal radio/X-ray emission. Direct measurements of the magnetic field strength in massive stars using spectropolarimetry to determine the Zeeman splitting of the spectral lines are difficult, since only a few spectral lines are available for these measurements and these are usually strongly broadened by rapid rotation.

For a couple of years, the O6Vpe star θ^1 Ori C remained the only massive O-type star with a detected magnetic field (Donati et al., 2002). To examine the potential of FORS1 for the measurements of magnetic fields in massive stars, in 2007 we obtained 12 observations of θ^1 Ori C distributed over the rotational period of 15.4 days and compared them with previous measurements obtained with high resolution spectropolarimeters. The FORS1 measurements were sufficiently accurate to show a smooth sinusoidal curve in spite of a phase gap between 0.60 and 0.88, but with somewhat different values of the magnetic field strength compared to previous measurements obtained with Musicos, ESPaDOnS and NARVAL (Hubrig et al., 2008). Unlike FORS1 measurements, the high resolution spectropolarimeters usually do not employ measurements on hydrogen lines and thus different values of the magnetic field strength may be expected.

Recently we acquired 38 new spectropolarimetric observations of 13 O-type stars with FORS1, which led to magnetic field detections in an additional four massive O-type stars. As the lower number hydrogen lines in massive stars generally show variable emission, the measurements of magnetic fields are usually performed in two ways: using only the absorption hydrogen Balmer lines or using the entire spectrum including all available absorption lines of hydrogen, He I, He II, C III, C IV, N II, N III and O III. As an important step, before the assessment of the longitudinal magnetic field, we exclude all spectral features not belonging to the stellar photospheres of the studied stars: telluric and interstellar features, CCD defects, emission lines and lines with strong P Cygni profiles. This was the first time that magnetic field strengths were determined for such a large sample of O-type stars, with an accuracy of a few tens of Gauss, comparable to the errors obtained with high resolution spectropolarimeters. No magnetic fields stronger than 300 G were detected in the studied sample, suggesting that large-

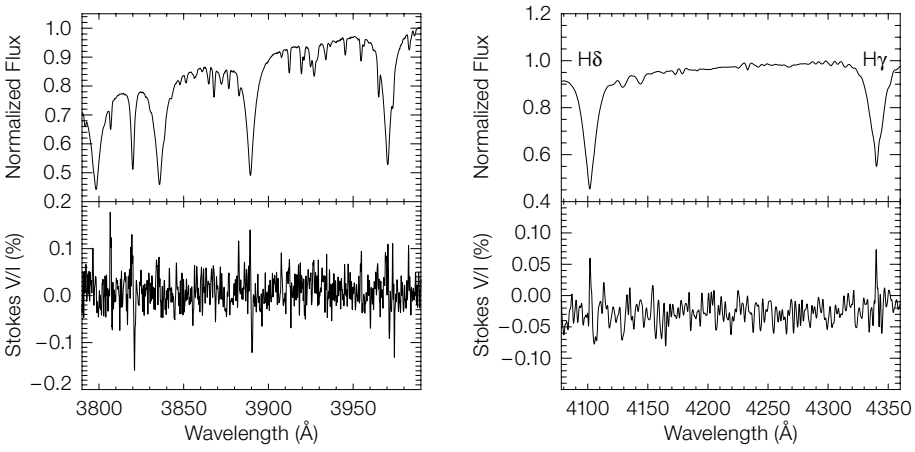

Figure 2. **Left:** Stokes *I* and *V* spectra of the β Cephei star ξ¹ CMa in the blue spectral region around high number Balmer lines. **Right:** Stokes *I* and *V* spectra of the Be star ο Aqr in the region including Hδ and Hγ lines.

scale, dipole-like magnetic fields with polar magnetic field strengths higher than 1 kG are not widespread among O-type stars.

Two other groups of massive stars, early B-type pulsating stars, such as β Cephei and slowly pulsating B (SPB) stars, and Be stars, that are defined as rapidly rotating main-sequence stars showing normal B-type spectra with superposed Balmer emission, had been a puzzle for a long time with respect to the presence of magnetic fields in their atmospheres. Only a very few stars of this type with very weak magnetic fields had been detected before we started our surveys of magnetic fields in B-type stars in 2004. Out of the 13 β Cephei stars studied to date with FORS1, four stars, δ Cet, ξ^1 CMa, 15 CMa and V1449 Aql, possess weak magnetic fields of the order of a few hundred Gauss. The star ξ^1 CMa is the record holder with the largest mean longitudinal magnetic field of the order of 300–400 G (Hubrig et al., 2006b; 2009). In Figure 2 (left) we present Stokes *I* and *V* spectra of ξ^1 CMa in the blue spectral region around the high Balmer series lines. Distinct Zeeman features, which are indicators of the presence of a magnetic field in this star, are easily detected at the wavelengths corresponding to the positions of strong spectral lines in the Stokes *I* spectrum. Figure 2 demonstrates the great advantage of using the blue-optimised EEV2 CCD of FORS1 for magnetic field measurements in the blue spectral region to cover all H Balmer lines from Hβ to the Balmer jump. Roughly half of the 34 SPB stars studied have been found to be weakly magnetic with field strengths of the order of 100–200 G.

In classical Be stars, a number of physical processes (e.g., angular momentum transfer to a circumstellar disc, channeling stellar wind matter, accumulation of material in an equatorial disc, etc.) are more easily explained if magnetic fields are invoked (e.g., Brown et al., 2004). The magnetic fields of Be stars appear to be very weak, generally of the order of 100 G and less. Furthermore, our time-resolved magnetic field measurements of a few classical Be stars indicate that some of them may display a magnetic cyclic variability on timescales of tens of minutes. In Figure 2 (right) we present Stokes *I* and *V* spectra of the typical Be star ο Aqr in the region including Hδ and Hγ lines with a measured longitudinal magnetic field $< B_z > = +104 \pm 33$ G.

Another emission line star, υ Sgr, is a magnetic variable star, probably on a few months timescale with a maximum longitudinal magnetic field $< B_z > = +38 \pm 10$ G (see Figure 3). The evolutionary status for this star is not obvious as it is a single-line spectroscopic binary system currently observed in the initial rapid phase of mass exchange between the two components (Koubský et al., 2006). The star is hydrogen-poor and the observed spectrum is extremely line-rich (see Figure 3). Future monitoring of its magnetic field over a few months with a high resolution spectropolarimeter would be of extreme interest to understand the role of the magnetic field in the evolutionary process of mass exchange in a binary system.

Our studies of massive stars revealed that the presence of a magnetic field can be expected in stars of different classification categories and at different evolutionary stages. Since magnetic fields can potentially have a strong impact on the physics and evolution of these stars, it is critical to answer the principal question of the possible origin of such magnetic fields. One important step towards answering this question would be to conduct observations of members of open clusters and associations of different ages. To date, we have studied the presence of magnetic fields only in members of the young open cluster NGC 3766 in the Carina spiral arm, known for its high content of early-B type stars, with very surprising results. Along with a strong magnetic field detected in a He-peculiar star, weak magnetic fields have been detected in a few normal B-type stars and in a few Be stars (Hubrig et al., in preparation). In Figure 4 we present the observed Stokes *I* and *V* profiles of the He-peculiar member of this cluster and of another cluster member that was classified as a potential Be star by Shobbrook (1985) with longitudinal magnetic fields of $< B_z > = +1559 \pm 38$ G and $< B_z > = -194 \pm 62$ G, respectively.

Obviously, to understand the role of magnetic fields in massive stars, future observations are urgently needed to determine the fraction of magnetic massive stars and the distribution of their typical field

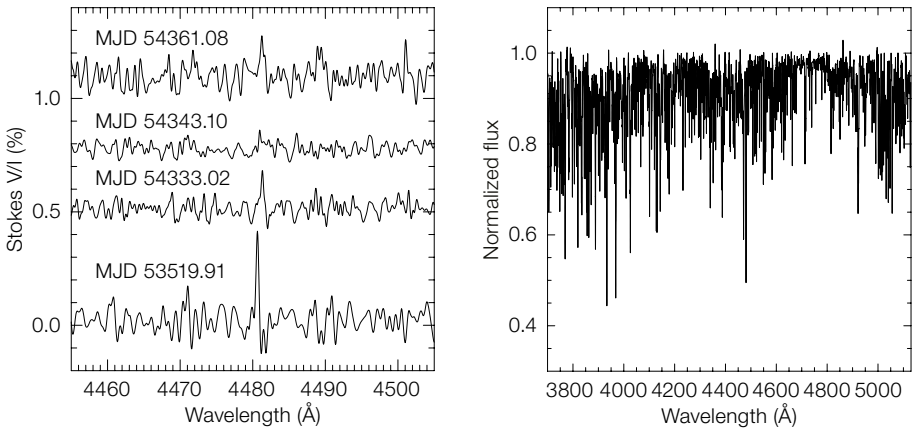

Figure 3. Left: Observed Stokes *V* spectra of the emission line star υ Sgr over two years in the vicinity of Mg II 4481. **Right:** Normalised FORS1 Stokes *I* spectrum of υ Sgr.

strengths. Further, we note that no physical properties are known that define these particular classes of stars as non-magnetic. It seems to be appropriate to admit that the inability to detect magnetic fields in massive stars in previous studies could be related to the weakness of these fields, which can, in some stars, be as little as only a few tens of Gauss (e.g., Bouret et al., 2008).

Herbig Ae/Be stars — resolving an enigma

In our recent studies of Herbig Ae/Be stars we sought to expand the sample of stars with measured magnetic fields to determine whether magnetic field properties in these stars are correlated with other observed properties such as mass-accretion rate, disc inclination, companions, silicates, PAHs, or show a correlation with age and X-ray emission as expected from the decay of a remnant dynamo (Hubrig et al., 2009, A&A submitted). During our two-night observing run in May 2008 we were able to obtain circular polarisation data for 23 Herbig Ae/Be stars and six debris disc stars. No definite detection was achieved for stars with debris discs, whereas for Herbig Ae/Be stars 12 magnetic field detections were achieved. One of the Herbig Ae stars, HD 101412, showed the largest magnetic field strength ever measured in intermediate mass pre-main-sequence stars with $< B_z > = -454 \pm 42$ G, confirming the previous FORS1 detection by Wade et al. (2007). The Stokes *I* and *V* spectra of this star are shown in Figure 5.

Strong distinct Zeeman features at the position of the Ca II H and K lines detected in four other Herbig Ae/Be stars are presented in Figure 6. As we already reported in our earlier studies (Hubrig et al., 2004, 2007b) these lines are very likely formed at the base of the stellar wind, as well as in the accretion gaseous flow and frequently display multi-component complex structures in both the Stokes *V* and the Stokes *I* spectra.

Observations of the disc properties of intermediate mass Herbig Ae stars suggest a close parallel to T Tauri stars, revealing the same size range of the discs, similar optical surface brightness and structure. It is quite possible that magnetic fields play a crucial role in controlling accretion onto, and winds from, Herbig Ae stars, similar to the magnetospheric accretion observed in T Tauri stars. Using our sample of Herbig Ae stars with masses of 3 $M_\odot$ or less, we searched for a link with other stellar parameters to put preliminary constraints on the mechanism responsible for

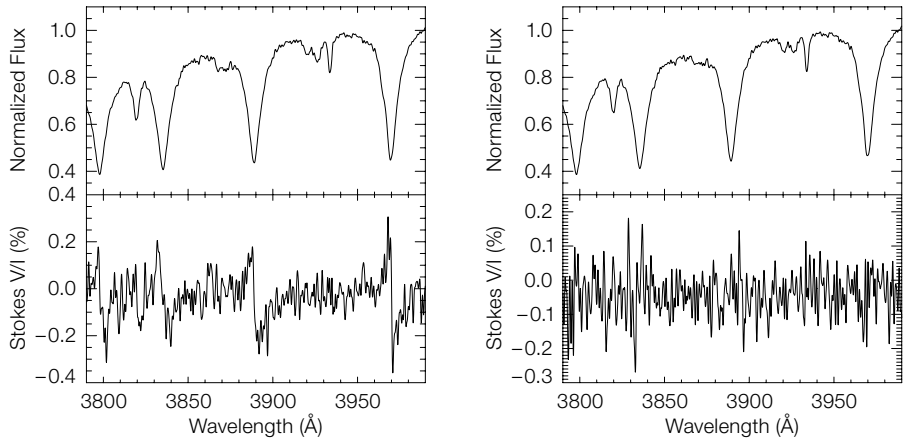

Figure 4. **Left:** Stokes *I* and *V* spectra in the blue spectral region around high number Balmer lines for an He-peculiar member of the young open cluster NGC 3766. **Right:** Stokes *I* and *V* spectra around high number Balmer lines for a candidate Be star belonging to the young open cluster NGC 3766.

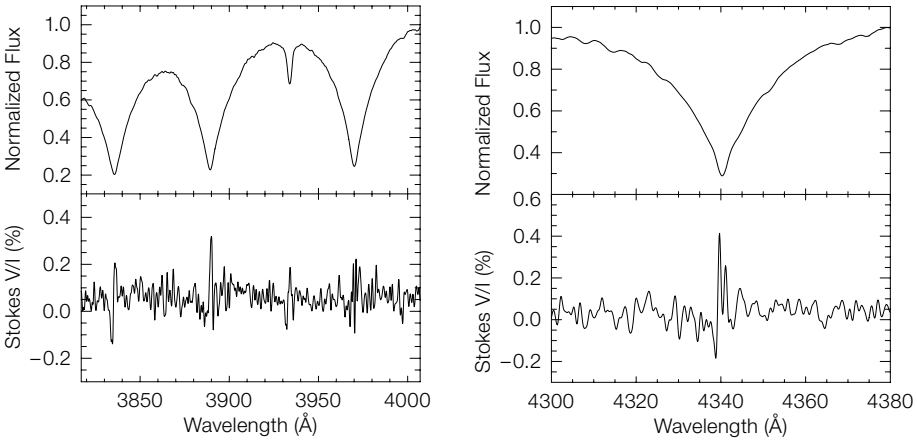

Figure 5. Stokes *I* and *V* spectra of the Herbig Ae/Be star HD 101412 with the largest detected magnetic field. **Left:** Zeeman features in H9, H8, Ca II H and K and Hε profiles. **Right:** Stokes *I* and *V* spectra in the vicinity of the Hγ line.

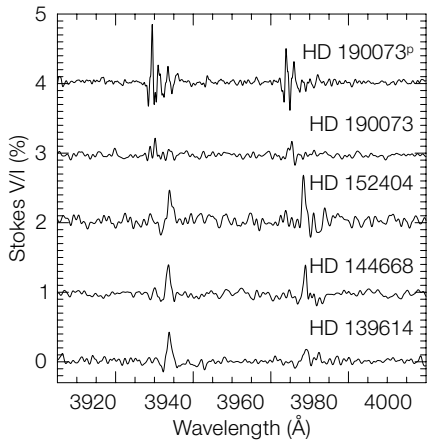

Figure 6. Stokes *V* spectra in the vicinity of the Ca II H and K lines of the Herbig Ae/Be stars HD 139614, HD 144668, HD 152404 and HD 190073. At the top is the previous observation of HD 190073, obtained in May 2005. The amplitude of the Zeeman features in the Ca II H and K lines observed in our recent measurement for this star has decreased by ~0.5% compared to the previous observations.

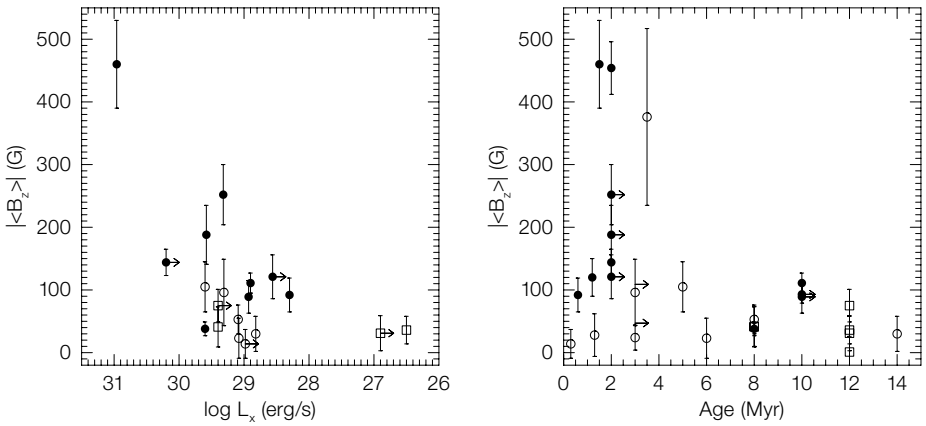

Figure 7. Left: The strength of the longitudinal magnetic field plotted against the X-ray luminosity. **Right:** The strength of the longitudinal magnetic field as a function of age. Filled circles denote Herbig Ae stars with a 3-σ magnetic field detection, while open circles denote Herbig Ae stars with a lower σ. Squares denote stars with debris discs, of which none has a 3-σ magnetic field detection.

magnetospheric activity. For the first time we established preliminary trends between magnetic field strength, mass-accretion rate, X-ray emission and age. We find that the range of observed magnetic field values is in agreement with the expectations from magnetospheric accretion models giving support for dipole-like field geometries. Both the magnetic field strength and the X-ray emission show hints of a decline with age in the range of 2–14 Myrs probed by our sample, supporting a dynamo mechanism that decays with age. In Figure 7 (left), we present the strength of the magnetic field plotted versus log L_X. It is noteworthy that we find a hint of an increase in the magnetic field strength with the level of the X-ray emission, which suggests that a dynamo mechanism may be responsible for the coronal activity in Herbig Ae stars.

There is obviously a trend showing that stronger magnetic fields tend to be found in younger Herbig Ae stars and that magnetic fields become very weak at the end of their pre-main-sequence life (see the right of Figure 7). These results are in line with the conclusions of Hubrig et al. (2000, 2007a) that magnetic fields in stars with masses less than 3 $M_\odot$ are rarely found close to the zero-age main-sequence.

Closing remarks

In summary, using FORS1 spectropolarimetric observations, considerable progress has been made over the last eight years in studies of the presence of magnetic fields in upper main-sequence stars. These results are providing several new clues, but are also posing a number of new open questions requiring future spectropolarimetric studies. Currently FORS1 in spectropolarimetric mode is the only facility regularly used for observations of circular and linear polarisation by the ESO community. Since FORS1 was decommisioned in P83, the polarimetric capability has been moved to FORS2 with the blue optimised EEV2 CCD available exclusively in visitor mode. We hope that the spectroscopic capabilities of FORS2 will be used in the future as intensively and successfully as they were used on FORS1 in the past.

References

Bagnulo, S. et al. 2001, The Messenger, 104, 32
Bouret, J.-C. et al. 2008, MNRAS, 389, 75
Braithwaite, J. & Spruit, H. C. 2004, Nature, 431, 819
Brown, J. C. et al. 2004, MNRAS, 352, 1061
Donati, J.-F. et al. 2002, MNRAS, 333, 55
Hubrig, S., North, P. & Mathys, G. 2000, ApJ, 539, 352
Hubrig, S., Schöller, M. & Yudin, R. V. 2004, A&A, 428, L1
Hubrig, S. et al. 2005, A&A, 440, L37
Hubrig, S. et al. 2006a, AN, 327, 289
Hubrig, S. et al. 2006b, MNRAS, 369, L61
Hubrig, S., North, P. & Schöller, M. 2007a, AN, 328, 475
Hubrig, S. et al. 2007b, A&A, 463, 1039
Hubrig, S. et al. 2008, A&A, 490, 793
Hubrig, S. et al. 2009, AN, in press
Koubský, P. et al. 2006, A&A, 459, 849
Shobbrook, R. R. 1985, MNRAS, 212, 591
Wade, G. A. et al. 2007, MNRAS, 376, 1145

Wolf-Rayet Stars at the Highest Angular Resolution

Florentin Millour[1]
Olivier Chesneau[2]
Thomas Driebe[1]
Alexis Matter[2]
Werner Schmutz[3]
Bruno Lopez[2]
Romain G. Petrov[2]
José H. Groh[1]
Daniel Bonneau[2]
Luc Dessart[4]
Karl-Heinz Hofmann[1]
Gerd Weigelt[1]

[1] Max-Planck-Institut für Radioastronomie, Bonn, Germany
[2] Observatoire de la Côte d'Azur, Nice, France
[3] Physikalisches-Meteorologisches Observatorium Davos, World Radiation Center, Switzerland
[4] Observatoire de Paris, France

Interferometric observations of high-mass evolved stars provide new and very valuable information of their nature. With the unique capabilities of the VLTI, direct images of their closest environment where mass loss and dust formation occur, can be obtained. The breakthrough of the VLTI in terms of angular resolution as well as spectral resolution allows competing theoretical models, based on indirect constraints, to be tested. The high angular resolution made available by the VLTI shows that there is still a lot to discover about these massive stars.

Massive stars strongly influence their surroundings due to their extreme temperature, luminosity, and mass-loss rate. In addition, they are short-lived, and their fate is to explode as core-collapse supernovae. Among the extensive zoology of massive stars, Wolf-Rayet stars probably represent the last stage of stellar evolution, just before the explosion as a supernova. So far, Wolf-Rayet stars have been mainly studied by means of spectroscopy and spectropolarimetry, based on spatially unresolved observations. Nonetheless, there is extensive evidence of binarity and geometrical complexity of the nearby wind in many Wolf-Rayet stars. In this context, high angular resolution techniques fill the gap, since they can provide spatially resolved observations of massive stars and their immediate vicinity. However, the number of Wolf-Rayet stars in the solar vicinity is very low (Van der Hucht, 2001; Crowther, 2007). Therefore, all Wolf-Rayet stars are too remote to be spatially resolved by adaptive optics. However, for a handful of objects, the geometry of the innermost circumstellar structures (discs, jets, latitude-dependent winds, or even more complex features) can be directly probed with the highest spatial resolution available, through the use of stellar interferometry.

A closer look at Wolf-Rayet stars

Wolf-Rayet (WR) stars begin their life as massive objects (usually O-type supergiant stars) with at least 20 times the mass of the Sun. Their life is brief, and they die hard, exploding as supernovae and blasting vast amounts of heavy elements into space, which are recycled in later generations of stars and planets. By the time these massive stars are near the end of their short life, during the characteristic "Wolf-Rayet" phase, they develop a fierce stellar wind — a stream of particles ejected from the stellar surface by the radiative pressure — expelling mass at a tremendous rate (up to 10^{-3} $M_{\odot}$/yr) while they are synthesising elements heavier than hydrogen in their cores. One of the characteristics of WR stars is the low hydrogen content of the atmosphere due to the stripping-off of the outer layers as a result of the strong mass loss. Before and during the WR phase, such stars eject a large amount of matter, more than 10 $M_{\odot}$, and with velocities up to 3000 km/s, which then surrounds the central star in the form of gas and dust.

Theoretically, the evolution of a WR star ends with the collapse of its core and, as a rule, the formation of a black hole or a neutron star occurs. Energetic Type Ib and Ic supernovae (SNe) are thought to be direct descendants of massive WR stars (see, for instance, Crowther, 2007). It is now recognised that long-duration gamma-ray bursts (GRBs) are linked to the collapse of massive stars. The merging of the components in a binary system, including a rapidly rotating WR, is considered to be one of the channels leading to these extraordinary events, although this is not yet firmly established. Only ~ 1% of core-collapse SNe are able to produce a highly relativistic collimated outflow and, hence, a GRB.

WR stars are characterised by an extraordinary hydrogen-deficient spectrum, dominated by broad emission lines of highly ionised elements (such as He II, C IV, N V or O VI). The dense stellar winds completely veil the underlying atmosphere so that an atmospheric analysis can only be done with dynamical, spherically extended model atmospheres, such as those developed by Schmutz et al. (1989), Hillier & Miller (1998), or Gräfener et al. (2002). In the two last decades, significant progress has been achieved in this respect, so that WR stars can be placed on the Hertzsprung-Russell Diagram (HRD) with some confidence (see e.g., Crowther, 2007).

Classification of WR stars is based upon the appearance of optical emission lines of different ions of helium, carbon, nitrogen and oxygen. The nitrogen-rich, or WN-type, is defined by a spectrum in which helium and nitrogen lines (He I–II and N III–V) dominate. In the carbon-rich, or WC-type, helium, carbon, and oxygen lines (C II–IV, He I–II and O III–VI) dominate the emission-line spectrum. Castor, Abbott & Klein (1975) demonstrated that hot-star winds could be explained by considering radiation pressure alone. In this early model, each photon is scattered once at most, and this is sufficient to drive OB-star winds, while more difficulties were encountered for WR stars. Model atmosphere studies have advanced sufficiently to enable the determination of stellar temperatures, luminosities, abundances, ionising fluxes and wind properties of WR stars. What remains uncertain are the kinematics of the wind and the wind acceleration law. Furthermore, rotation is very difficult to measure in WR stars, since photospheric features are absent. This parameter is crucial when considering GRBs.

Atmospheric models of WR stars are parameterised by the inner boundary radius R_{*}, at high Rosseland optical depth (typically above 10), but only the optically thin part of the atmosphere is seen by the observer. Therefore, the

determination of R_* depends on the assumptions made on the velocity law of the wind, considering that typical WN and WC winds have reached a significant fraction of their terminal velocity before they become optically thin in the continuum (especially in the near- and mid-IR). Typical scales for R_* are 3–6 $R_\odot$, depending on the spectral sub-type (Crowther, 2007). In the near-IR, the main opacity comes from free–free interactions, and the continuum-forming region is more extended at longer wavelengths, reaching 2–6 R_*. The core radius of WN stars is larger than of WC stars, but the wind of WC stars is denser, and the continuum forms farther away from the core radius. As a consequence, the continuum diameter is about the same, of the order of 10–20 $R_\odot$, corresponding to a diameter of about 0.1–0.2 mas for sources at 1 kpc. This implies that the continuum of both WN- and WC-type WR stars remains unresolved for the VLTI in the near-IR, even with the longest (130 m-scale) baselines. Yet, this conclusion does not hold for the line-forming regions (LFR) that can be located at typically 5–50 R_* and that can be resolved by an interferometer, provided that a minimum spectral resolution of 500 is available. Therefore, observing the LFR of WR stars with long-baseline optical interferometry offers the opportunity to probe their winds in the following ways:

– By measuring the extension of the LFR compared to the continuum. The spatial and kinematical characteristics of the wind can be better inferred and the wind velocity law (especially with access to shorter wavelength data) possibly constrained.

– By examining any deviation from sphericity of these objects. If WR stars were rapid rotators, one would expect strong wavelength-dependent deviations from spherical symmetry, as was detected for the luminous blue variable star η Car with AMBER/VLTI (Weigelt et al., 2007) for example.

– By examining the deviations and perturbations of the WR wind from purely radial motion. Such deviations may originate from dust formation very close to some of these hot stars.

The first, and still most common, method of measuring the angular extent of an astrophysical object with a stellar interferometer is to use an idealised uniform disc to model the stellar photosphere. In reality, WR stars are not "hard-edged" in the continuum, which forms directly in the wind (see Figure 1).

Probing the wind of the closest WR star: γ^2 Vel

Among all WR stars, γ^2 Vel is by far the closest, with a well-known distance today of 336 ± 8 pc (North et al., 2007), whilst all others are beyond 1 kpc. Owing to its relative proximity, γ^2 Vel is relatively bright and has been studied in great detail, mainly using spectroscopy. Through spectroscopic eyes, γ^2 Vel is shown to be a binary WR + O system (WC8 + O7.5III, P = 78.53 days), thus offering access to the fundamental parameters of the WR star, usually obtained only indirectly through the study of its dense and fast wind. The presence of X-ray emission in the system (Skinner et al., 2001) could be explained by an X-ray-emitting bow-shock between the O-star wind and the WR-star wind (the so-called wind–wind collision zone, [WWCZ]). γ^2 Vel was observed by the Narrabri intensity interferometer, operating at around 0.45 µm, as early as 1968 (Hanbury Brown et al., 1970), but since the observations lacked spectral resolution, they could not resolve the WWCZ.

Our team observed γ^2 Vel in December 2004 using the AMBER/VLTI instrument with the aim of constraining various parameters of the system, such as the brightness ratio of the two components, the spectral and spatial extent of the WWCZ, and the angular size associated with both the continuum and the lines emitted by the WR star. AMBER delivered spectrally dispersed visibilities as well as differential and closure phases and, of

Figure 1. **Left:** Simulation of the spatial extent of a WC8 star wind in the continuum at 2.10 µm (solid line) and in three different emission lines (C III 2.11 µm – dash-dotted line; C IV 2.07 µm – dotted line; C IV 2.08 µm – dashed line). The apparent size of the WR star in the emission lines can be as much as twice the continuum size. **Right:** Simulated images of the same star in the continuum region around 2.10 µm (centre) and in the C IV 2.07 µm line (right). The continuum can be described by a Gaussian intensity distribution, while the superposition of continuum and line flux leads to an intensity distribution that can be described by a limb-darkened disc.

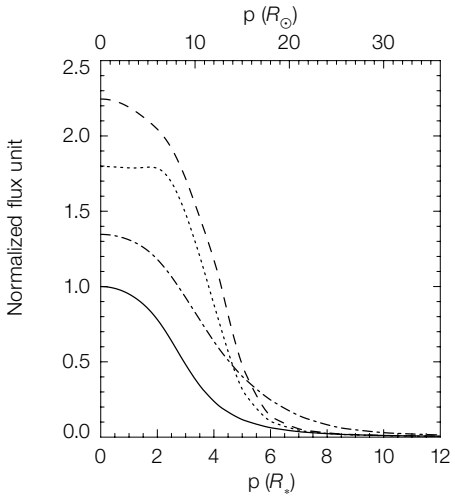

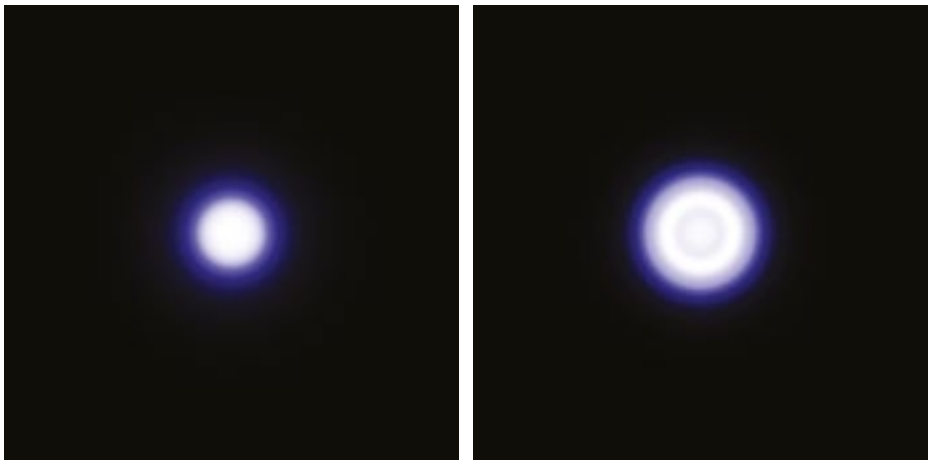

course, also a spectrum of the object. During these observations, AMBER worked with a resolution of R = 1500 in the spectral band 1.95–2.17 µm. We interpreted the AMBER data in the context of a binary system with unresolved components, neglecting, to a first approximation, the wind–wind collision zone flux contribution and the extension of the WR wind (Millour et al., 2007). Based on the accurate spectroscopic orbit and the Hipparcos distance (258^{+41}_{-31} pc), the expected separation at the time of the observations was 5.1 ± 0.9 mas. However, our observations showed that the Hipparcos distance was incorrect since we observed a separation of $3.62^{+0.11}_{-0.30}$ mas, implying a distance of 368^{+38}_{-13} pc, which is in agreement with recent spectrophotometric estimates. An independent observation by the Sydney University Stellar Interferometer (SUSI) confirmed and refined the distance estimate of γ^2 Vel at 336^{+8}_{-7} pc (North et al., 2007).

In contrast to SUSI, which uses broadband filters, AMBER allowed us to disperse the *K*-band light with a resolution of 1500. Therefore, we were able to separate the spectra of the two components; i.e., we obtained, for the first time, an independent spectrum of the WR component of γ^2 Vel in the *K*-band. This allowed us to compare the WR spectrum with line-blanketed radiative transfer models of WR stars (Dessart et al., 2000). The match between the inferred WR spectrum and the modelled spectrum is

Figure 2. γ^2 Vel as seen by AMBER in 2004 (Millour et al., 2007): the observations (lower plots) are fitted successfully by a model involving a WR star and an O star (grey lines). One can extract the spectrum of the Wolf-Rayet star alone from this model-fitting (top-right panel, blue curve) and compare it with a radiatively-driven WR wind model spectrum (red curve). The general view of the system (top-left) also involves a wind–wind collision zone.

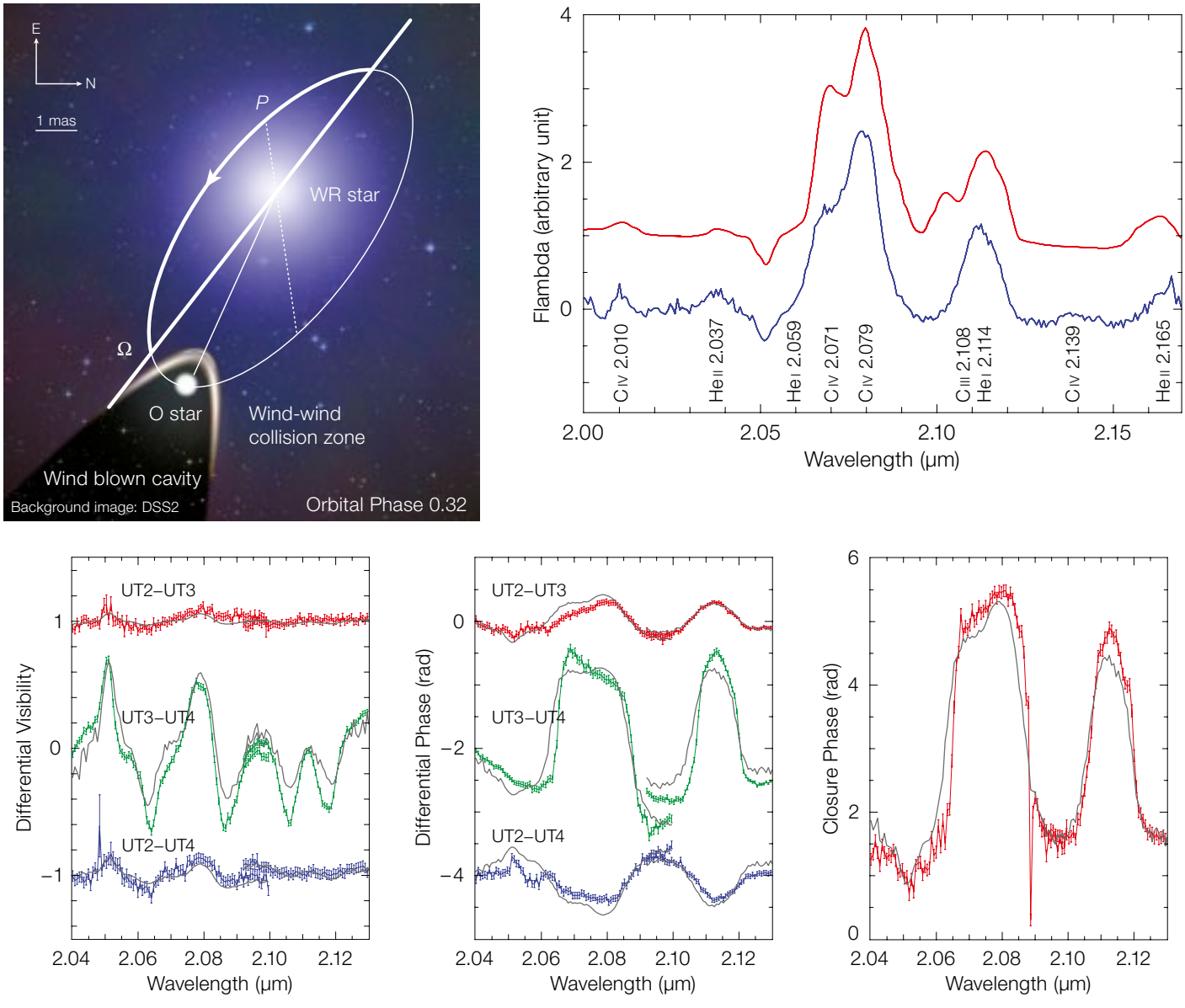

relatively good, except for some regions where the match is worse (especially in a few emission lines and in some parts of the continuum, see Figure 2). This suggests that as a second order perturbation, an additional light source in the system may affect our fit. We checked that this marginal mismatch cannot come from a flat continuum emission, and therefore, we favoured the presence of an additional compact light source in the system.

After that first study, we carried out follow-up observations of γ^2 Vel in 2006 and 2007. In addition to a refinement of the orbital solution of North et al., (2007), Millour et al. (2008) were able to locate this additional light source in the system between the two main stars. If this source is confirmed, it would be located closer to the O star than to the WR star and would contribute approximately 5% of the total flux of the system (i.e., additional free–free emission). This is in agreement with the expectations from Millour et al. (2007) and, possibly, we have detected the wind–wind collision zone (WWCZ) between the two stars.

However, other effects, such as the LFR extent, can also affect our interferometric signal. Indeed, in the past, different velocity laws were used for models of γ^2 Vel, e.g., a steep velocity law or a combined law with a steep inner region and a flat outer region. Leaving aside the technical details, this basically implies that different velocity laws predict a different extent of the LFR. Therefore, we are currently continuing our investigations on γ^2 Vel with the VLTI to disentangle better the different light contributions in this fascinating system.

The dust formation puzzle

One challenging problem related to WR stars is understanding how dust can form in the hostile environment of these hot stars. It turns out that several of the dusty WR stars harbour a so-called pinwheel nebula, as shown recently by the observations of Tuthill et al. (see, for example, their article in 2008). From an interferometric point of view, pinwheel nebulae appear in the visibilities as typical whirlpool modulations that can be detected with the current performance of the VLTI (see Figure 3). When the number of datasets is very limited, clues to the presence of a pinwheel can also come from a plateau-like shape in the visibilities towards longer baselines. Of course the detection of new pinwheel nebulae would provide a more direct evidence of the binarity of the observed stars, but a clear detection of the underlying binary in known pinwheels is also one of the goals of studying these dusty WR stars. Up to now, we have successfully observed a few dusty

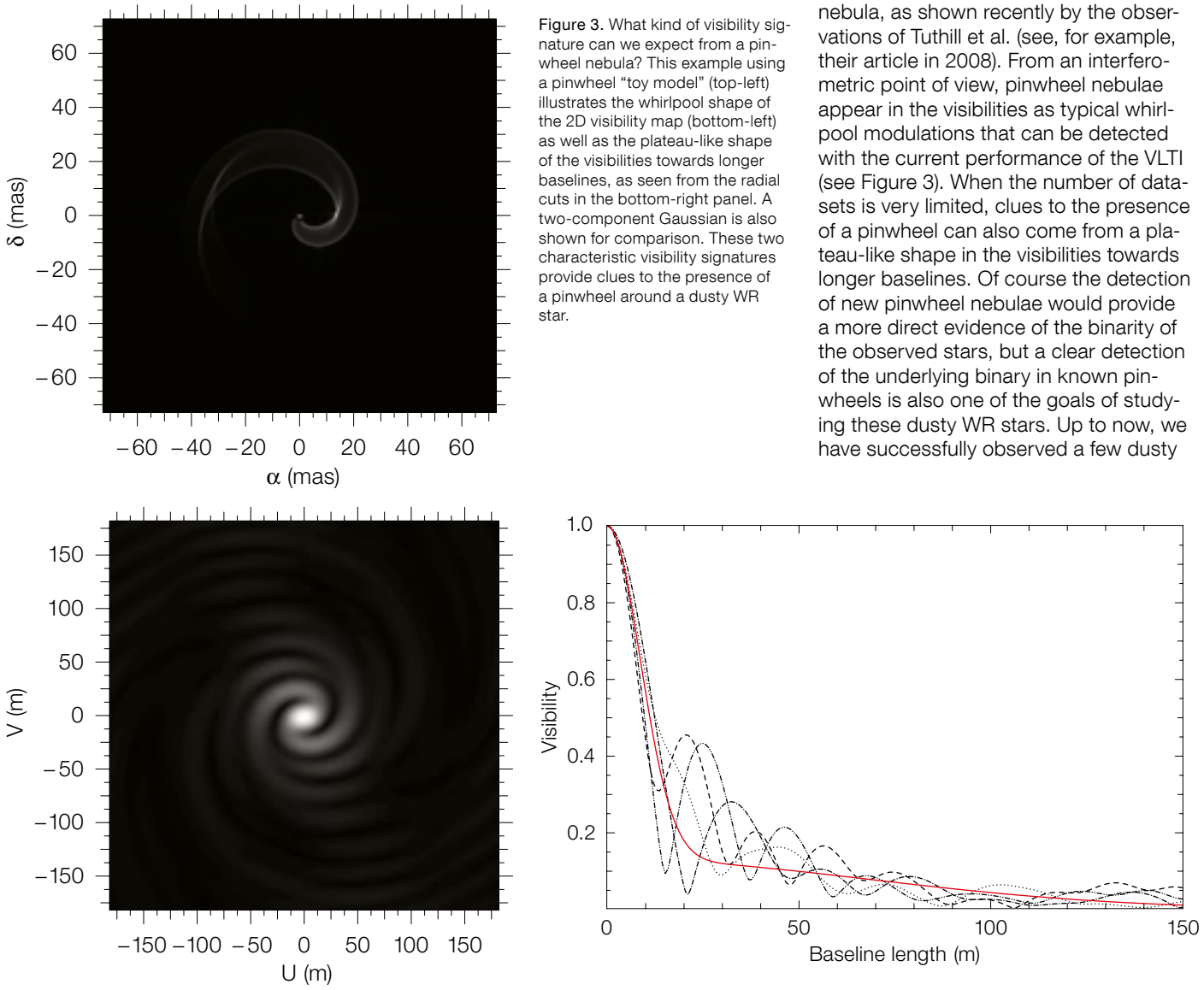

Figure 3. What kind of visibility signature can we expect from a pinwheel nebula? This example using a pinwheel "toy model" (top-left) illustrates the whirlpool shape of the 2D visibility map (bottom-left) as well as the plateau-like shape of the visibilities towards longer baselines, as seen from the radial cuts in the bottom-right panel. A two-component Gaussian is also shown for comparison. These two characteristic visibility signatures provide clues to the presence of a pinwheel around a dusty WR star.

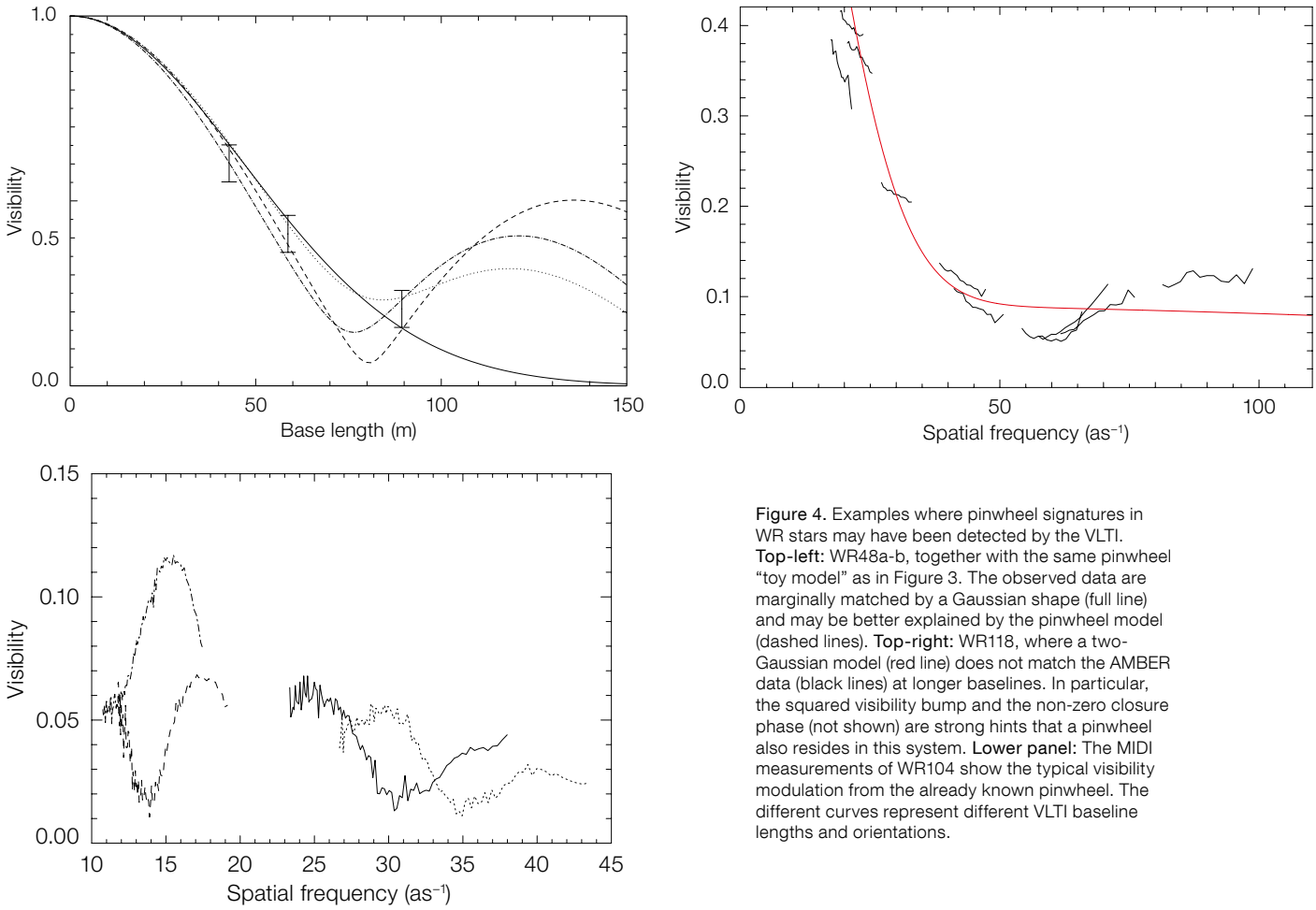

Figure 4. Examples where pinwheel signatures in WR stars may have been detected by the VLTI. **Top-left:** WR48a-b, together with the same pinwheel "toy model" as in Figure 3. The observed data are marginally matched by a Gaussian shape (full line) and may be better explained by the pinwheel model (dashed lines). **Top-right:** WR118, where a two-Gaussian model (red line) does not match the AMBER data (black lines) at longer baselines. In particular, the squared visibility bump and the non-zero closure phase (not shown) are strong hints that a pinwheel also resides in this system. **Lower panel:** The MIDI measurements of WR104 show the typical visibility modulation from the already known pinwheel. The different curves represent different VLTI baseline lengths and orientations.

Wolf-Rayet stars with the VLTI, which illustrates the potential of optical/IR interferometry to contribute to the fascinating question of the binarity of these stars.

WR 48a is a WC star producing dust in the form of eruptions, which suggests the presence of a companion. It is found to be within 1 arcsecond of the two heavily reddened, optically visible clusters Danks 1 and 2, which are themselves separated by only 2 arcseconds. Another object that also seems to be a dusty WR star (MSX6C G305.4013 + 00.0170) was found close to WR48a, which we hereafter denote as WR48a-b. No optical counterpart is reported in the literature and the JHK photometry for this source from the Two Micron All Sky Survey (2MASS) shows a spectral shape indicative of an object with high extinction (A_V ~ 10 mag). WR48a and WR 48a-b were successfully observed with the AMBER/VLTI instrument. Both objects have angular diameters of about 4–6 mas in the *K*-band and mid-IR sizes of the order of 10–15 mas. The sizes measured are quite large, compared to the expected size of single WR stars (0.1–0.5 mas), and these two objects are probably two good candidates to harbour pinwheel nebulae, even though no clear signature has been formally detected yet (Figure 4). These two targets are definitely interesting because they produce dust and, hence, are likely binary candidates, belonging to a young star-forming region whose distance is more accurately known than is usual for WR distances.

WR 118 is a highly evolved, carbon-rich Wolf-Rayet star of spectral type WC10. It is the third brightest Wolf-Rayet star in the *K*-band (*K* = 3.65), and its large IR-excess is attributed to an envelope composed of carbonaceous dust. Since no remarkable changes in the dust emission have been observed in the past two decades, WR 118 is classified as a permanent dust producer. The extended dust envelope of WR 118 was successfully resolved for the first time by Yudin et al. (2001) using bispectrum speckle interferometry with the 6-metre BTA (Large Altazimuth Telescope). Yudin et al. concluded that the apparent diameter of WR 118's inner dust shell boundary is 17 ± 1 mas. We recently measured WR 118 with AMBER in low-spectral resolution mode (see Figure 4). At first glance, the AMBER visibilities suggest that there is an unresolved component contributing approximately 15% to the total *K*-band flux. In addition, one can see that the *K*-band visibility is not spherically symmetric, and we detected non-zero closure phases. These clues illustrate that the overall shape of the measured visibility of WR 118 is in qualitative agreement with the visibility signature expected

from a spiral-like dust distribution. Currently, the interpretation of the recently obtained AMBER data is being subjected to a more detailed analysis.

The most recent dusty WR star observed with the VLTI so far was WR 104 with the MIDI instrument. WR104 is the archetype of the colliding-wind binary creating a beautiful pinwheel system, which was first detected by the technique of aperture masking with the Keck telescope (Tuthill et al., 2008). We observed it with MIDI using two of the auxiliary telescopes. The visibilities show the signature of two flux distributions on the source: a Gaussian-shaped dusty envelope surrounding the binary system and producing 80–90% of the flux in the mid-infrared, and the dust pinwheel. The characteristic pinwheel signal is seen by MIDI as a cosine modulation, evolving with time as the pinwheel rotates and the interferometer baseline length and orientation change (see Figure 4). Such a limited amount of data would be extremely difficult to interpret if the global geometry and the ephemeris of this source were not accurately known. These observations promise to evaluate precisely the size of the dust-forming region and the dust production of the system, as viewed at high spatial resolution.

Prospects

The studies described correspond to work in progress with the VLTI for observing WR stars. No imaging of these sources has been done up to now, but the AMBER instrument, with three telescopes combined, has some imaging capabilities. A first image of a pinwheel, with resolutions much higher than single pupil telescopes, would be a milestone in IR long-baseline interferometric research on dusty WR stars and would probably trigger more VLTI observing programmes in this field. On the other hand, reaching sufficient dynamic range with AMBER/VLTI in medium spectral resolution mode, would allow one to directly constrain the WR wind velocity field in the emission lines. Observing with shorter wavelengths (*H* or *J* bands, or even visible), would boost this research field, as both the interferometer resolution and the LFR extent increase towards shorter wavelengths. This would open the possibility to directly validate the competing models for WR winds or, maybe, could even lead to new and unexpected results.

References

Crowther, P. A. 2007, ARA&A, 45, 177
Castor, J. I. et al. 1975, ApJ, 195, 157
Dessart, L. et al. 2000, MNRAS, 315, 407
Gräfener, G. et al. 2002, A&A, 2002, 387, 244
Hanbury Brown, R. et al. 1970, MNRAS, 148, 103
Hillier, D. J. & Miller, D. L. 1998, ApJ, 496, 407
Millour, F. et al. 2007, A&A, 464, 107
Millour, F. et al. 2008, SPIE, 7013
North, J. R. et al. 2007, MNRAS, 377, 415
Schmutz, W. et al. 1989, A&A, 210, 236
Skinner S.L. et al. 2001, ApJL, 558, 113
Tuthill, P. G. et al. 2008, ApJ, 675, 698
van der Hucht, K. A. 2001, New Astronomy Review, 45, 135
Weigelt, G. et al. 2007, A&A, 464, 87
Yudin, B. et al. 2001, A&A, 379, 229

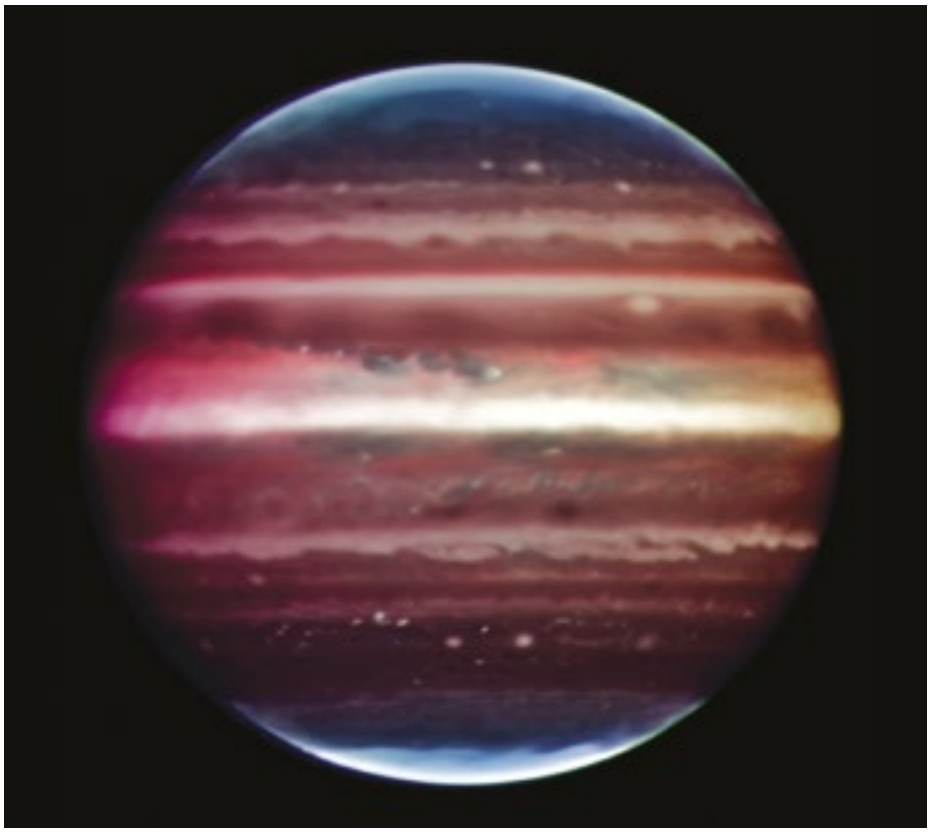

Image of Jupiter taken in near-infrared light with the VLT Multi-conjugate Adaptive optics Demonstrator (MAD) prototype instrument on 17 August 2008. This colour composite is formed from a series of images taken over a time span of about 20 minutes, through three filters at 2.2 µm (Ks-band), 2.14 µm (Brackett-γ continuum) and 2.17 µm (Brackett-γ). The filters select hydrogen and methane absorption bands. The spatial resolution is about 90 milliarcseconds across the whole disc, corresponding to 300 km on the planet surface. See ESO PR 33/08 for more details

The Beauty of Speed

Andrea Richichi[1]
Cesare Barbieri[2]
Octavi Fors[3 4]
Elena Mason[1]
Giampiero Naletto[5]

[1] ESO Garching
[2] Dipartimento di Astronomia, Università di Padova, Italy
[3] Departament d'Astronomia i Meteorologia, Universitat de Barcelona, Spain
[4] Observatori Fabra, Barcelona, Spain
[5] Dipartimento di Ingegneria dell'Informazione, Università di Padova, Italy

The burst mode of ISAAC has been used systematically to record lunar occultations with high time resolution, producing several unique new results that remain unattainable by any other technique. This is not the only possible choice of instrument for high time resolution, and fast time modes of one kind or another have been implemented on several other ESO instruments. We provide a brief overview of the present capabilities and summarise some scientific results. We speculate about the future of high temporal resolution applications, presenting the trail-blazing instrument Iqueye that recently completed its first technical run at La Silla.

The quest for high time resolution

Encoded somewhere in the human genome, there must be a love for speed. Filippo Marinetti, founder of the artistic movement known as Futurism, stated it best in his Manifesto of 1909: "We affirm that the world's magnificence has been enriched by a new beauty: the beauty of speed... Time and Space died yesterday. We already live in the absolute, because we have created eternal, omnipresent speed." Young or old, many people are infatuated with the concept of speed: in technology, in sport, or on the highway. But what about astronomers? It is generally considered that, in spite of some peculiarities, they are people too, and therefore they should not be immune to the fascination with speed. However, almost all the instruments that astronomers design and build are geared to the highest spectral resolution or the utmost sensitivity, and these demand in turn long integrations.

Yet there is a wealth of knowledge to be gained by going to the other extreme, and observing with high time resolution (see Table 1). Pulsars, stellar pulsations and oscillations, flares and bursts, transits and occultations, and more, are phenomena that are best studied by recording data at rates much faster than those usually employed by astronomers. The extragalactic community need not feel left out either: for example, the variability of active galactic nuclei (AGN) holds a crucial key to the size and structure of the central engine, and, if it is studied on timescales of minutes today, it is natural to expect that in the era of Extremely Large Telescopes (ELTs) these timescales could be down to seconds. Last but not least, if we really observe very fast, then we can also beat atmospheric turbulence, to the point that, at least for some applications, we no longer need expensive and complex correction systems.

To be sure, there are many problems in going very fast: we collect far fewer photons; we have to fight harder against detector noise and other unpleasant features; there may not be sufficient time to read the whole area of our large-format detectors for which we have paid so dearly. But first and foremost, what do we mean by "fast"? Examining Table 1, it will be noticed that the wish-list spans a range of six orders of magnitudes or more, from seconds down to microseconds or less. At ESO, most of the instruments currently in operation were originally designed without an explicit requirement for high time resolution. But as the standard modes have become more and more routine, a number of requests for fast observations are starting to be implemented on a best-effort basis. Today, several instruments at the La Silla Paranal Observatory offer high time resolution, as summarised in Table 2. We have not included here subsystems that by necessity have to include fast operation, such as adaptive optics and fringe trackers.

Modern panoramic detectors have quite large formats, and as a consequence typical readout times are, at minimum, of the order of seconds. In order to beat this limit by up to three orders of magnitudes, as required by some applications, it is generally necessary to sacrifice the number of pixels, by reading out only a small sub-window (used for example by the ESO infrared [IR] instruments ISAAC, SOFI and NACO). Other approaches are to shift the charge in CCDs, as in FORS2. Other detectors are intrinsically quite fast by design and have a relatively small format, such as the mid-IR detectors of VISIR and MIDI that have to avoid saturation by the high background signal.

In the following we will focus on recent results in two areas: the near-IR detection of lunar occultations with ISAAC in the millisecond range; and the "blazingly fast" detection enabled by a unique instrument that recently had its first technical run in La Silla.

At Paranal: the Moon in slow motion

Lunar occultations (LO) are a phenomenon in which the lunar limb acts as a straight diffracting edge. As the Moon moves over a distant background source, a fringe pattern is generated that moves over the observer. Typical speeds of this pattern are about 0.5–1 m/ms (or

Phenomenon	Timescale (current)	Timescale (ELT era)
Stellar flares and pulsations	seconds, minutes	10–100 ms
Stellar surface oscillations e.g., white dwarfs, neutron stars	1–1000 μs	1–1000 μs 0.1 μs
Tomography, eclipses, flickering e.g., close binary systems	10–100 ms	1–10 ms
Pulsars	1 μs–100 ms	1 ms–1 ns?
Variability in AGN	minutes	seconds?
Stellar occultations	1 ms	1 ms
Planetary occultations and transits	100 ms–10 s	100 ms–10 s

Table 1. Fast time applications in astronomy (partly based on an E-ELT study by Redfern & Ryan, 2006).

Instrument	Modes	Detector	Time Rate (Window)	Configuration and Mode
VISIR	Burst	DRS	12.5 ms SF	imaging, visitor
SOFI	Burst, FastPhot	Hawaii	4 ms (8 x 8), 15 ms (32 x 32)	imaging, visitor
ISAAC	Burst, FastPhot	Hawaii-1, Aladdin	3 ms (32 x 32), 6 ms (64 x 64)	imaging, visitor, service
ISAAC	Burst	Hawaii-1, Aladdin	9 ms (1024 x16)	spectro, under commisioning
NACO	Cube	Aladdin	7.2 ms (64 x 64), 350 ms (1024 x 1024)	imaging, visitor
HAWK-I	Fast	Hawaii-2RG	6.3 ms (16 x 16)	imaging
FORS2	HIT	CCD (charge shift)	up to 2.3 ms	image/spec, visitor, service
VLTI	Fast	Various	up to 1 ms	image/spec, not foreseen

Table 2. A summary of instruments available at ESO for fast time resolution with their main characteristics.

500–1000 m/s). The fringe spacing is determined by the distance to the Moon and the wavelength of observation: in the near-IR it is a few metres, so that time sampling of about one millisecond is required to measure the fringe pattern. From this measurement, a wealth of information on the background source can be recovered, including the angular diameter of stars, the projected separation and brightness ratio of binaries. It is also possible to reconstruct the brightness profiles of complex sources by a model-independent analysis. A typical concern of those who learn about LO for the first time is the effect of mountains and irregularities of the lunar limb. Luckily, this can generally be safely neglected, since we are dealing with diffraction and not with geometrical optics. A number of peculiarities characterise LO, in particular the fact that the angular resolution achieved is not dependent on the size of the telescope used for the observation. In fact, the Moon itself can be considered as our telescope in this case.

We have already reported in a previous *Messenger* article (Richichi et al., 2006) on the first successful observations of LO at the Very Large Telescope (VLT) with ISAAC at Unit Telescope 1. Using the Aladdin detector, an area of 32 x 32 pixels were read out every 3.2 ms. We announced this ground-breaking performance at the time, and this has now been confirmed by the detailed analysis carried out in two recently published papers (Richichi et al., 2008a; 2008b):

Figure 1. **Left:** Upper panel, data (dots) and best fit (solid line) for 2MASS 17453224-2833429. The lower panel shows, on a scale enlarged by four and displaced by arbitrary offsets for clarity, the residuals of three different fits. The upper two are for an unresolved and a resolved stellar disc (reduced χ^2 = 6.3), the lower one is with a model-independent analysis (reduced χ^2 = 1.6). **Right:** Brightness profile reconstructed by the model-independent analysis. The inner shell radius is estimated to be about 40 AU.

an angular resolution as good as 0.5 milliarcseconds (mas), or about 100 times better than the diffraction limit of the telescope and comparable with that of the much larger and complex VLTI; a limiting sensitivity close to K ≈ 12.5, or several magnitudes fainter than the VLTI; and a dynamic range of 8 magnitudes even within one Airy disc from the central star. All this in the blink of an eye, or, to be realistic, in a few minutes, taking into account telescope pointing and data storage: sounds too good to be true? There are indeed some major limitations to LO: they are fixed time events, and we cannot choose the targets at will.

We report a summary of the results obtained in those first two runs in Table 3. Figure 1 provides an illustration: for the AGB star 2MASS 17453224-2833429, a maser source, we could derive a clear detection of the circumstellar shell and an estimate of its angular size and distance. As a result of these first observations, the so-called burst mode of ISAAC has subsequently been offered on a regular basis since Period 80, and is now a routine technique for LO observations at the VLT. Since LO observations require a minimum amount of time, they represent an ideal filler programme: every interval of at least five minutes during which no other service mode programmes are available

Table 3. Statistics of the results obtained from the first burst-mode runs with ISAAC for lunar occultations. R and D events are reappearances and disappearances, respectively.

	March 06	August 06	Total
Total hours	4.2	8.5	12.7
Type of event	R	D	
Attempted events	51	78	129
Successful events	30	72	102
Diameters	3	1	4
Binaries/triples	2/0	6/1	9
Shells/complex	0	2	2
Planetary nebula, central stars	0	1	1
Masers	2	1	3

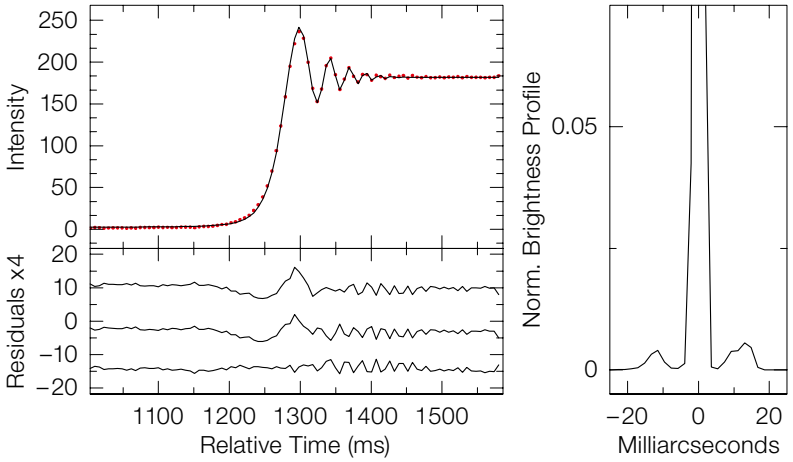

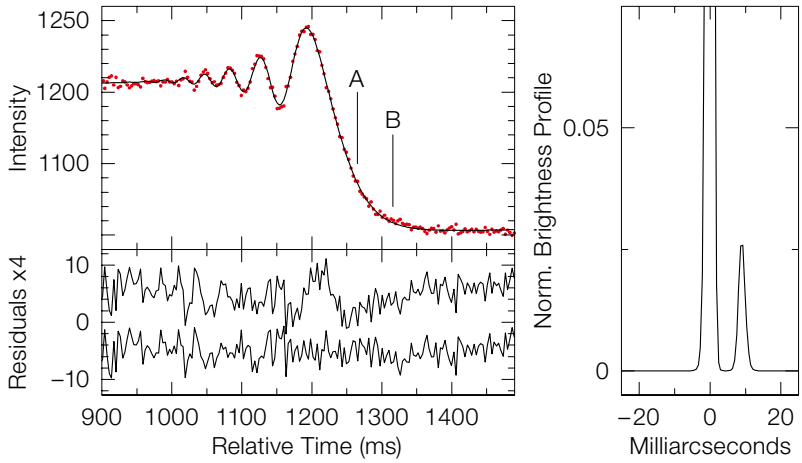

Figure 2. Same as Figure 1, for a source observed in Period 81 (K = 7.1, no known bibliographical entries). The fit residuals are for a point source (upper) and a binary source with a separation of 9.4 mas and a brightness ratio of 1:11 (lower). The right panel shows the reconstruction by a model-independent method.

or for which the atmospheric conditions are not met, an LO observation can be attempted if the Moon is above the horizon. In fact, we note that LO observations are almost insensitive to seeing and other adverse atmospheric conditions. With this strategy in mind, we submitted a filler proposal for Period 80, which unfortunately did not produce many results due to the unavailability of ISAAC during much of the period. However we submitted again for Period 81 and we waited during Period 82 so we could see the first results. These were very encouraging, and the programme was resubmitted for Period 83, and accepted. We provide here a first account of the observations carried out in Period 81.

For Period 81, we computed LO predictions to a limiting magnitude of K = 9.3 — a compromise between the number of computations and the volume of potential events. This choice resulted in 28 682 events observable within good observational constraints. Note that we discard full and waning Moon phases, the first because of the brightness and the latter because they are more challenging, and not well suited to service mode. We developed a prioritisation rule based on the K magnitude and J–K colour, preferring stars with very red colours indicative of possible circumstellar extinction. We further refined the priorities for sources with known counterparts or that had been studied previously. Then we applied a selection rule such that for every five minute interval only one star would be selected, with the highest priority among the other events close in time. As a result, 1629 Observing Blocks (OBs) were generated — a significant load for the User Support Department and our colleagues at Paranal to handle, whom we thank for their support. Equipped with this reservoir of OBs, our programmes lay dormant until summoned by an ISAAC night astronomer… an exciting wait for us in Garching! By the end of the period, a total of 125 LO events had been attempted in service mode. Of these, 116 resulted in positive detections of well-recorded light curves, a very satisfactory outcome indeed.

In order to cope with such a volume of data, we developed our own data pipeline (Fors et al., 2008), which generates extraction masks for each data cube (*viz.* sky image with time). The masks isolate the signal from the star, which, at these data rates, often has a variable and aberrated image, using twin criteria of contiguity and continuity. The background is then computed from the remaining pixels and subtracted. The pipeline processes the resulting light curve further using a multi-resolution wavelet transform analysis to produce first guesses of parameters such as the time of occultation, the intensity of the star, etc. From these parameters an initial fit is produced, and we are then presented with preliminary results and quality estimates that allow us to carry out an interactive analysis more efficiently and to focus on the interesting cases. First indications are that about six stars observed in Period 81 appear to be binary, with projected separations as small as 5 mas. One of them is illustrated in Figure 2. A few stars also appear to be resolved, although a more detailed analysis is still needed.

Most of these results, as well as those obtained previously, pertain to stars that are absent from the literature or have little information available. For some of them, not even an optical counterpart is known. Clearly, further investigations are needed in order to collect direct imaging by adaptive optics and optical and near-infrared photometry, and to provide spectral classification. We are waiting to prepare a corresponding proposal when a significant number of such stars are available. At the same time, we note that a large number of unresolved sources have been measured with upper limits on their angular diameters of order 1 mas. These limits, and the relatively faint magnitudes, make this a valuable list of calibrators for long-baseline interferometry, starting with the VLTI.

At La Silla: zooming in on pulsars

The observations presented so far may seem fast by the standards of most astronomers, but they pale in comparison with some observations recently carried out in La Silla. In January 2009, a new instrument emerged from its packing cases, and was quickly assembled at the Nasmyth B focus of the New Technology Telescope (NTT) by a team of Italian astronomers and engineers. Iqueye (Figure 3) is the NTT version of Aqueye, a prototype already previously deployed at the Asiago Observatory. The “queye” part of their names indicates the close relationship to QuantumEye, an instrument concept proposed initially for OWL, and now for the E-ELT (Dravins et al., 2005; Barbieri et al., 2008). The driver for this class of instruments is to reach ultimately the regime of time resolution in which photons are subject to quantum limits. From Figure 4, it can be seen that the Heisenberg uncertainty principle plays a dominant role in the visible range when the time resolution approaches a few picoseconds (1 ps = 10^{-12} s). But how is it possible to reach such time resolutions?

The solution selected for Iqueye is to combine astronomy with the state of the art offered by detector and nuclear physics. Iqueye and its siblings are equipped with single photon counting avalanche photodiodes (SPADs) which attain 50 ps time resolution with count rates as high as

Figure 3. Iqueye at the NTT, with some members of the team and of the supporting staff from La Silla. Two of the four SPADs are clearly seen, protruding from above and below the middle of the instrument. The rack includes the control electronics and the rubidium clock.

Figure 4. Astronomy in time and frequency. Pushing the time resolution towards the limits imposed by the Heisenberg uncertainty principle might be compared with the opening of a new window.

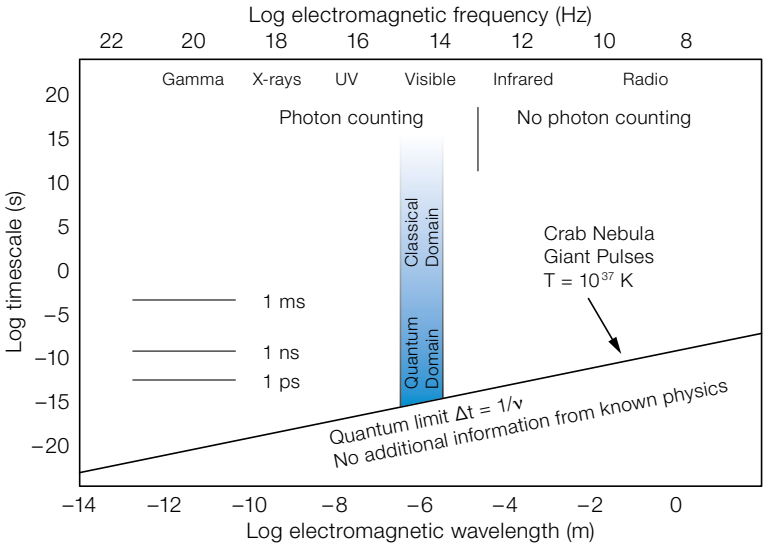

10 MHz. SPADs are very robust to high light levels, use standard voltages and do not require external cooling; their quantum efficiency reaches 60% in the visible. One shortcoming of these detectors is their deadtime, which at 70 ns limits the count rates to 14 MHz. Such devices are in a constant state of evolution, and improvements are foreseen in the near future. Both to avoid saturation in case of bright sources, and to provide independent detection statistics, Iqueye splits the telescope pupil into four, and each quadrant is observed with one SPAD. However this is only one part of the problem: the other gigantic hurdle is how to tag the arrival time of each photon. This has been achieved with two aids: an event-tagging board originally designed for CERN and a reliable and accurate time base. For this latter task, both a Global Positioning System (GPS) signal and a rubidium clock are employed. This clock has the required resolution, but it is not sufficiently stable, and so it is aligned occasionally with the GPS signal. By combining these two systems, the time-tagging achieved in Iqueye is reliable to about 30 ns over long periods of time, and to much less over shorter periods. The capabilities of Iqueye are impressive, especially if one considers that the whole is achieved in a highly compact and portable instrument, installed and successfully operated at the NTT by a small group of people, most of whom had never visited the site before!

The basic scheme of Iqueye is shown in Figure 5 and a more detailed account will be presented in the near future. For the moment, we show some impressive light curves of pulsars (Figures 6–8). The first was obtained with Aqueye at the Asiago 1.8-metre telescope in October 2008 (average signal over 30 minutes), and is compared with that taken at a much larger telescope. At the NTT, Iqueye was able to detect the Crab pulsar in a single cycle, showing its individual pulses clearly. The quality is unprecedented, and theoreticians will be able to zoom in on small details and refine their models. One can thus study pulse amplitude variations, noise in the arrival times, precession of the rotation axis, correlations with the giant radio pulses and much more. But the Crab pulsar is not the limit: at the NTT, Iqueye has been able to study another pulsar, B0540-69, with a V magnitude of only 23! This pulsar had previously been measured with good quality only by the Hubble Space Telescope (HST), and comparison of the NTT and HST data will provide an accurate deceleration rate for the pulsar. Note that these results are still preliminary, and the quantities in the figures need to be corrected for a number of effects.

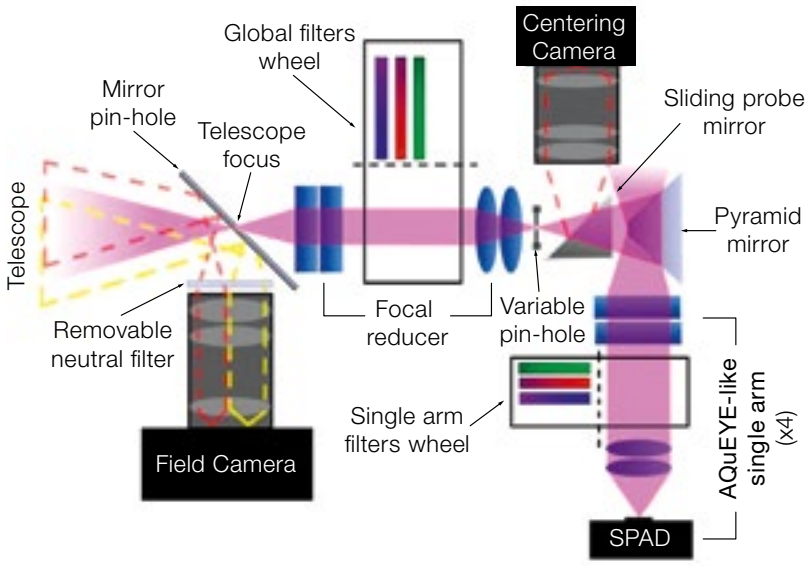

Figure 5. Schematic representation of Iqueye. Both the centering camera and the individual filters in each of the four arms are planned, but could not be included in the version for the first run at La Silla. With these additions the efficiency is increased and can provide the capability for simultaneous multi-colour observations.

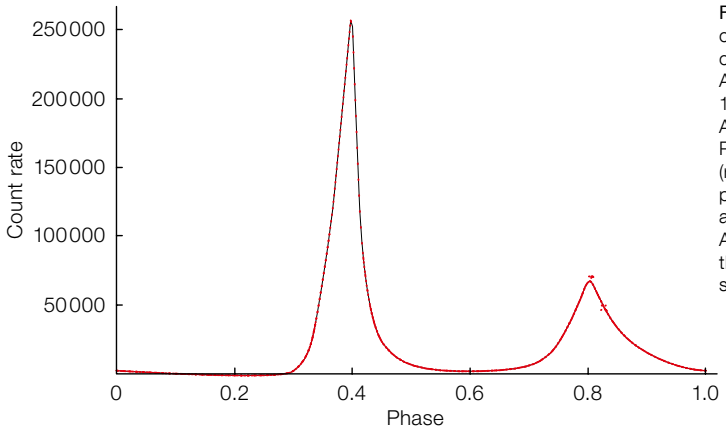

Figure 6. The light curve of the Crab pulsar (period 33 ms) observed with Aqueye in 2008 (blue, 1.8-metre telescope in Asiago) and with the Kitt Peak 4-metre telescope (red). Note the almost perfect reproducibility, and the performance of Aqueye consistent with that of a larger telescope at a better site.

The power of instruments such as Iqueye is only starting to become evident. The ability to measure events at nanosecond timescales with accurate time-tagging has already opened the door to a number of unique applications. It becomes possible not only to measure the individual light curves of fast variables such as pulsars, but also to compare, on a precise timescale, light curves taken at different times and at different locations. For pulsars, this enables the study of phase changes, derivatives, and comparison with radio observations, for example. It also offers a new approach to the technique known as intensity interferometry, originally devised and applied by Hanbury-Brown and colleagues. The method revolutionised interferometry in the 1960s through the study of the second order flux correlations between two telescopes. It was shown that this method allowed the coherence function of the emitting source to be measured, with the advantage that the required tolerances on the wavefronts were centimetres and millimetres, not microns and nanometres as in Michelson interferometers. The disadvantage with intensity interferometry is that it requires very large photon fluxes, and thus has limited sensitivity. This limitation can be significantly overcome by the better detection efficiencies and larger telescopes than were available in the 1960s; many in the community are debating the revival of intensity interferometry. In this context, plans to bring two Iqueyes to the VLT are already being proposed.

In the future, with improved hardware and the immense photon collecting power of the European ELT, it should become possible to truly attain the quantum limit, attempting detections at the picosecond level. This will open an entirely new window on the Universe, and push our knowledge into the regime where even the concept of photon and wavelength come to lose their accustomed meaning: a truly quantum eye will be born. Marinetti would have loved it!

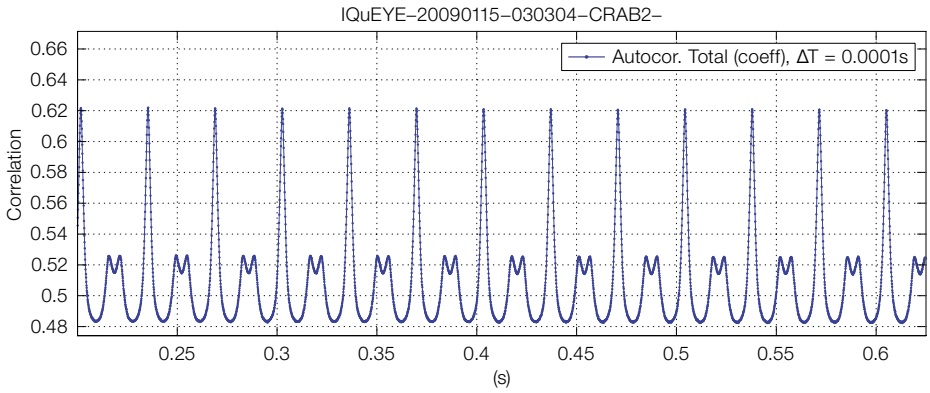

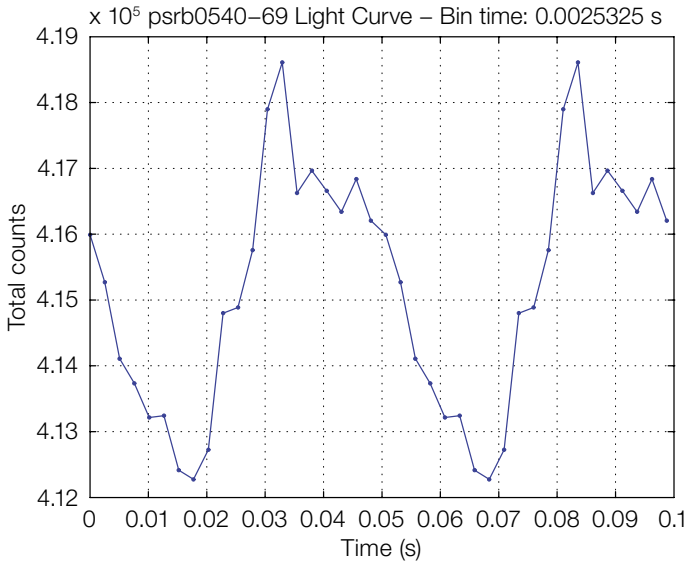

Figure 7. **(Top)** A zoom of the autocorrelation function of single pulses from the Crab pulsar, obtained by Iqueye at the NTT in January 2009. The structure in the secondary peak is due to the double-pulse shape of the light curve.

Figure 8. **(Left)** The light curve of the pulsar PSR 0540-69, with magnitude V = 23. The period can be well established from these data (preliminary value 50.7 ms), as well as features in the curve that reproduce well previous observations by HST. The data timing needs to be corrected for Earth's rotation, orbit and other effects.

References

Barbieri, C. et al. 2008, in *Instrumentation for the VLT in the ELT Era*, ed. A. Moorwood, (Berlin: Springer), 249
Dravins, D. et al. 2005, *QuantEYE. Quantum Optics Instrumentation for Astronomy*, OWL Instrument Concept Study, OWL-CSR-ESO-00000-0162
Fors O. et al. 2008, A&A, 480, 297
Redfern, M. & Ryan, O. 2006, presentation at the meeting *Towards the European ELT*, Marseille
Richichi A. et al. 2006, The Messenger, 126, 24
Richichi A. et al. 2008a, A&A, 489, 1399
Richichi A., Fors O. & Mason E. 2008b, A&A, 489, 1441

VISIR Observations of Local Seyfert Nuclei and the Mid-infrared — Hard X-ray Correlation

Hannes Horst[1]
Poshak Gandhi[2]
Alain Smette[3]
Wolfgang Duschl[1 4]

[1] Institut für Theoretische Physik und Astrophysik, Universität Kiel, Germany
[2] RIKEN Cosmic Radiation Laboratory, Wako City, Saitama, Japan
[3] ESO
[4] Steward Observatory, University of Arizona, USA

High angular resolution mid-infrared observations with the VISIR instrument at the Very Large Telescope have allowed the distribution of dust around local active galactic nuclei (AGN) to be studied. The observational results support the unified scenario for AGN and bring constraints on the properties of its key component, a dusty torus obscuring the view onto the AGN when viewed close to the equatorial plane.

Active galactic nuclei have been a prime target of extragalactic astronomy for many years. These fascinating objects comprise a supermassive black hole, a hot accretion disc feeding the black hole and an additional supply of cold gas and dust. They have many manifestations: quasars, radio galaxies, Seyfert galaxies — all of which are governed by the same physical mechanisms.

The dusty torus in AGN

The local incarnations of AGN — also known as Seyfert (Sy) galaxies — can be separated into two classes: Sy 1 galaxies with an unobscured view onto the hot, optically bright accretion disc and the surrounding broad line region (BLR); and Sy 2 galaxies that are observed through a veil of gas and dust. This has led astronomers (see, for example, Rowan-Robinson, 1977; Antonucci, 1982) to develop the unified scenario for AGN. The cornerstone of this scenario is the existence of a torus-shaped supply of molecular gas and dust that obscures the central parts of the AGN when viewed close to the equatorial plane (see Figure 1 for an illustration). Thus, Sy 1 and Sy 2 galaxies are the same beasts, just seen from different directions.

While the unified scenario has proved to be very successful and has passed many observational tests, little is known about the physical state of the torus itself. Some possible geometries for the dust distribution are shown in Figure 2:

– Panel a displays a classical smooth distribution with a constant ratio of height/radius. Such a torus has essentially the same geometry as the accretion disc in the centre of the AGN, but with much lower temperatures and a much larger extent. The border between the torus on one side and the accretion disc and broad line region on the other side is determined by the sublimation temperature of the dust. When the gas becomes too hot, the dust particles are destroyed, the gas is ionised and a hot BLR or accretion disc is observed instead of a dusty torus.

– Panel b shows the same geometry, but with the dust and gas arranged in distinct clouds. There are theoretical arguments for such clumpiness, based on the dynamical stability of the torus (Krolik & Begelman, 1988).

– Panel c illustrates the idea of the "receding" torus, first proposed by Lawrence (1991). The consequence of this model is that AGN of high luminosity will appear as obscured less frequently than AGN of low luminosity, since, when the luminosity increases, the sublimation radius and thus the inner edge of the torus move outwards. This, in turn, means that the solid angle covered by the torus as seen from the centre of the AGN decreases. There are some observational indications for this effect, but the question of the geometry of the torus in this case is far from settled.

There are many approaches to the study of the physical state of the torus. The one that seemed most promising to us was to combine mid-infrared (MIR) and hard X-ray observations. The intrinsic X-ray luminosity is a good proxy for the total luminosity of the accretion disc. The MIR emission of an AGN, on the other hand, is dominated by thermal emission of the dust within the torus. As the torus is heated by the accretion disc, one would expect a correlation between MIR and hard X-ray luminosities. Since, in Sy 1 galaxies, we can see the hot dust in the inner part of the torus, while in Sy 2 galaxies — according to the unified scenario — we can only see the cooler dust in the outer part of the torus, one would expect to find a difference in the MIR and intrinsic hard X-ray luminosities.

Two studies on the mid-infrared–hard X-ray correlation by Krabbe et al. (2001) and Lutz et al. (2004) found the expected correlation between MIR and hard X-ray

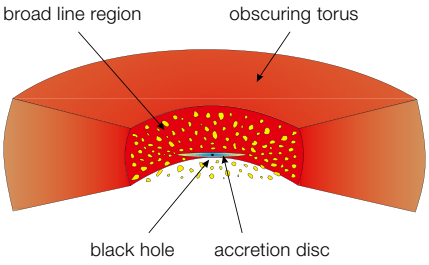

Figure 1. Sketch of the inner part of an AGN as predicted by the unified scenario. Depicted are the black hole, the accretion disc, the clumpy broad line region and the obscuring torus. The narrow line region and a possible jet are omitted for clarity.

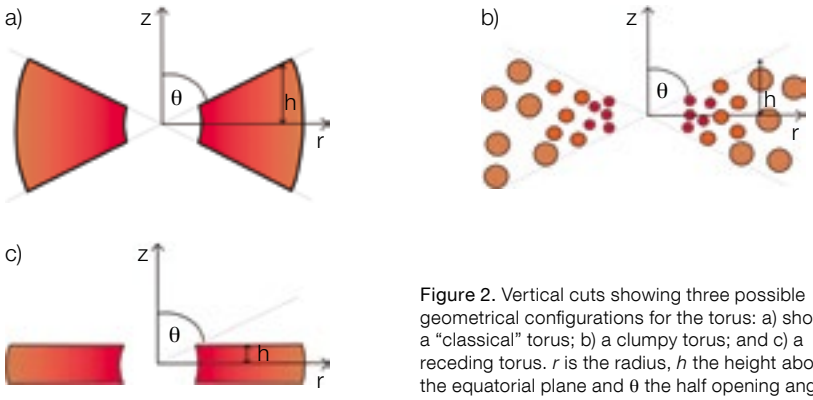

Figure 2. Vertical cuts showing three possible geometrical configurations for the torus: a) shows a "classical" torus; b) a clumpy torus; and c) a receding torus. *r* is the radius, *h* the height above the equatorial plane and θ the half opening angle.

luminosities, but not the expected difference in luminosity ratio between Sy 1 and Sy 2 galaxies.

Ramifications of assessing the MIR and X-ray properties of AGN

One limitation of earlier studies on the mid-IR–hard X-ray correlation was the low angular resolution of the MIR observations. Unfortunately, Seyfert galaxies frequently host regions of active star formation close to the AGN which also emit in the MIR regime. If it is not possible to spatially resolve these star-forming regions, a separation, e.g., by spectral decomposition methods, is very difficult. We decided to base our study on observations with the VSIR instrument (Lagage et al., 2004) at the Very Large Telescope (VLT), which offers the best combination of spatial resolution and sensitivity in the mid-infrared currently available in the world.

Besides the angular resolution of the MIR observations, another issue was the reliability of our X-ray data. As mentioned above, we need the intrinsic X-ray luminosity in order to have a proxy for the total luminosity of the accretion disc. Unfortunately, X-rays are also absorbed within the torus. However, high quality X-ray spectra allow us to correct for this effect, since absorption alters the X-ray spectral appearance of an AGN in a characteristic way. Therefore, we decided to observe a sample of Sy 1 and Sy 2 galaxies with VISIR for which high quality X-ray data were available.

In order to make the best use of VISIR's high angular resolution capabilities, we decided to only observe relatively nearby AGN. We set the limit for our sample selection at a redshift of 0.1.

VISIR observing campaigns

Between April 2005 and September 2006, we observed 29 Seyfert galaxies with VISIR and detected 25 of them. We used a standard chop/nod-procedure to remove the very bright atmospheric background in the MIR. In order to achieve the highest possible angular resolution, we chose VISIR's small field objective, which provides a pixel scale of 0.075 arcseconds and a field of view of 19 x 19 arcseconds. With this setup, we reached a typical resolution of 0.3 arcseconds, thereby significantly improving the resolution compared to previous studies. Most of the observed objects appear point-like — only in three cases did we detect extended emission around the AGN. One example of a target with extended emission — NGC 5135 — is displayed in Figure 3. In this overlay of VISIR and Hubble Space Telescope data, we see that some sources of optical and MIR emission coincide, while others do not. Where MIR sources do not have an optical counterpart, we probably see the early stages of star formation when young stars are heating their environment, but are not yet powerful enough to blow away the dusty veil that is hiding them.

Extended emission and comparison to Spitzer data

For NGC 5135 and a second object, NGC 7469, we can estimate that within the innermost 3.0 arcseconds around the AGN, at least roughly 45% of the MIR flux does not originate from the AGN. For NGC 7469, this result is in good agreement with an actual comparison of our VISIR data to archival spectra recorded with the IRS instrument aboard the Spitzer Space Telescope; the latter provides an angular resolution of ~ 3.0 arcseconds. We performed this comparison for all objects that we had observed in at least two MIR filters and for which archival IRS data were available. Interestingly, we found some cases of significant deviation of the IRS and VISIR fluxes where no extended emission was visible in the VISIR images (Horst et al., 2009). One example for this is shown in Figure 4. We interpret this discrepancy as caused by smooth, extended emission that is not observed with VISIR due to its limited sensitivity to this kind of emission. In a few cases, flux changes due to time variability between the two observing epochs, while unlikely to be the origin of this effect, cannot be completely ruled out.

The extra-nuclear emission — either directly observed with VISIR or visible through the comparison to the Spitzer data — underlines that giving priority to high angular resolution, instead of the higher sensitivity of space telescopes, was the right approach for our purpose. Of course, we cannot rule out significant contamination in our own data, but at least it will be far less than for larger aperture observations. We discuss the important point of contamination in our data in more detail in the next section.

Figure 3. The central part of NGC 5135 in an overlay of optical Hubble Space Telescope data and our VISIR observations. The optical data is shown as a false colour image and the VISIR data as a contour plot. This figure is reproduced from Horst et al. (2009).

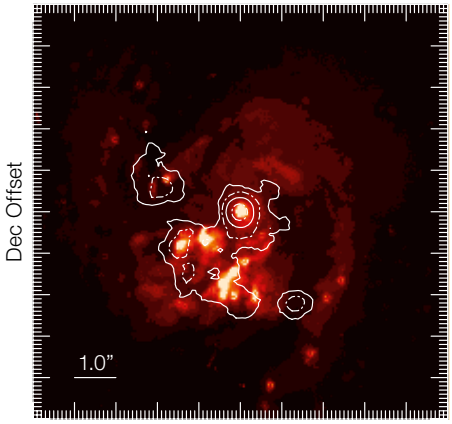

The mid-infrared–hard X-ray correlation

The primary goal of our observing campaigns was to study the mid-infrared–hard X-ray correlation. First of all, like our predecessors, we found a strong and significant correlation between these two quantities. The correlation is shown in Figure 5. In this figure, we plot hard X-ray *v.* MIR luminosity on a log–log scale. Blue squares represent Sy 1 nuclei, red diamonds are for Sy 2 nuclei and green triangles for low ionisation emission line regions (LINERS), a class of AGN with less pronounced nuclei and — relative to the AGN power — more star formation than Seyfert galaxies. Arrows mark either the upper limits of the MIR luminosity of non-detected sources or the lower limits of sources with equivocal X-ray spectra. The dotted line depicts the best-fit power-law to our first sample, observed in 2005 (see Horst et al., 2006); the dashed line then shows the best fit to the two samples combined.

The correlation has some important features. One of these is the slope, which is close to unity. On a log–log scale, a slope of one indicates a linear dependency between the two plotted quantities. Thus, we find that MIR and X-ray luminosities show a linear relationship. Secondly, Sy 1 and Sy 2 galaxies exhibit the same MIR/X-ray luminosity ratio. Again, this is in

Figure 4. Comparison of VISIR photometry (black circles) with IRS spectrophotometry (black line) for Mrk 590. The horizontal error bars depict the pass-band of the VISIR filters; dashed vertical lines indicate the wavelength position of emission lines common in AGN spectra.

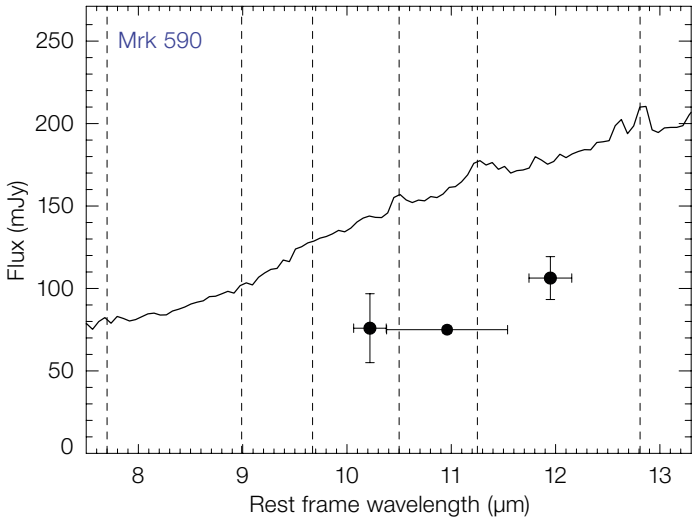

Figure 5. The mid-infrared–hard X-ray correlation as determined in this study. Blue squares are Sy 1 nuclei, red diamonds are Sy 2 nuclei and green triangles are LINERS. Arrows either depict upper limits to the MIR luminosity, in the case of MIR non-detection, or lower limits to the X-ray luminosity, in case of equivocal X-ray data. The dotted line is the best-fit power-law to our first sample, the dashed line the best-fit power-law to the combined sample. This figure is reproduced from Horst et al. (2008).

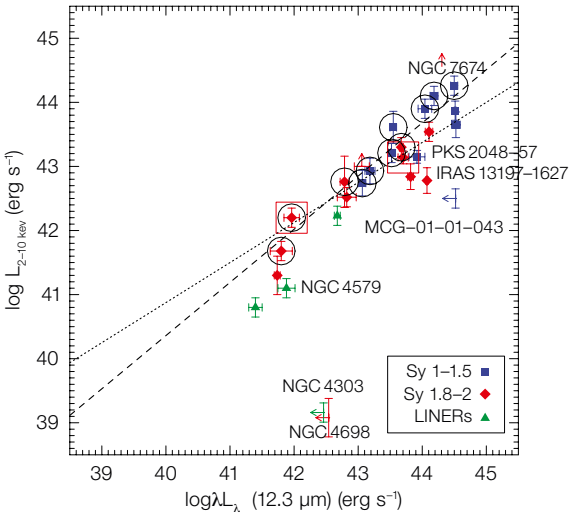

good agreement with the results of previous studies. At our high angular resolution, it is unlikely that the similarity is caused by contamination of the observed MIR luminosity with non-AGN emission. Therefore, we assume that it is intrinsic to AGN.

On account of the emphasis that we placed on the issue of angular resolution, we have to discuss the influence of contamination in our own data. In order to obtain robust results, we split our sample into two sub samples: especially well-resolved objects and less well-resolved objects. The term "well-resolved" has to be understood in terms of the dust sublimation radius that defines the inner edge of the torus. This radius can be estimated from the X-ray luminosity and is a natural scale for the dusty torus. Interestingly, we find a significant change in the MIR/X-ray luminosity ratio at an angular resolution of 560 times the dust sublimation radius (see Gandhi et al., 2009 for details). Therefore, we used this resolution as the separator for our two sub samples. The well resolved AGN are marked by black circles in Figure 5. We then checked whether the correlation would change if we used only the well-resolved objects; reassuringly, the result of this exercise showed that this is not the case. Within errors, the slopes of the two correlations are identical (the details of the statistical analysis are presented in Horst et al., 2008). Thus, we can be confident that the correlation we have determined is physically meaningful and can now discuss its implications.

Implications for the dusty torus

Our results allow us to constrain the properties of the dusty torus — at least for the AGN within the luminosity range we probed. Since we aimed for high angular resolution, we restricted ourselves to observing local AGN that are less luminous than more distant objects, e.g., quasars. Thus, it has to be kept in mind that the properties of the torus in AGN may change toward higher luminosities (and in fact there is some evidence that this is so).

Interestingly, however, we find no indication for a luminosity dependence of the appearance of the torus within our sample. Since the slope of the correlation is unity within the errors, the X-ray/MIR luminosity ratio does not change at all. Since the MIR luminosity is determined by the amount of accretion disc emission that is absorbed by the torus, it is directly proportional to the hard X-ray luminosity and the solid angle it covers when seen from the accretion disc. Thus, a constant luminosity ratio implies that the opening angle θ of the torus is constant as well. This rules out the receding torus model (panel c) in Figure 2 in its purest form. If the torus shows receding behaviour, it only does so beyond X-ray luminosities of 10^{38} W.

The fact that Sy 1 and Sy 2 nuclei follow the same correlation also has an important implication: it implies that the assumption that in Sy 1 nuclei we see hot dust, while in Sy 2 galaxies we do not, is probably incorrect. This result can only be reconciled with the existence of a torus-shaped distribution of molecular gas and dust, if the dust is arranged in distinct clouds (panel b in Figure 2). In addition, these clouds need to have a low volume filling factor within the torus. In such a configuration, we have a relatively unobstructed view through the torus onto the hot dust in its inner region.

These interesting results have motivated us to continue research along these lines. One important study was carried out by Gandhi et al. (2009) who — thanks to the arrival of the Suzaku, INTEGRAL and Swift spacecraft — managed to obtain reliable X-ray data for especially heavily obscured Sy 2 galaxies. VISIR observations of these targets showed that also they follow the correlation found in our earlier studies. The implication is that our approach has indeed allowed us to constrain the geometry and physics of the dusty torus in AGN. An interesting next step would be to widen the luminosity range covered by this study and try to assess the properties of the tori in the least, as well as the most powerful, AGN.

References

Antonucci, R. 1982, Nature, 299, 605
Gandhi, P. et al. 2009, A&A accepted
Horst, et al. 2006, A&A, 457, L17
Horst, H. et al. 2008, A&A, 479, 389
Horst, H. et al. 2009, A&A, accepted
Krabbe, A. et al. 2001, ApJ, 557, 626
Krolik, J.H. & Begelman, C. 1988, ApJ, 329, 702
Lagage, P.O. et al. 2004, The Messenger, 177, 12
Lawrence, A. 1991, MNRAS, 252, 586
Lutz, D. et al. 2004, A&A, 418, 465
Rowan-Robinson, M. 1977, ApJ, 213, 635

A VLT Large Programme to Study Galaxies at z ~ 2: GMASS — the Galaxy Mass Assembly Ultra-deep Spectroscopic Survey

Jaron Kurk[1]
Andrea Cimatti[2]
Emanuele Daddi[3]
Marco Mignoli[4]
Micol Bolzonella[4]
Lucia Pozzetti[4]
Paolo Cassata[5]
Claire Halliday[6]
Gianni Zamorani[4]
Stefano Berta[7]
Marcella Brusa[7]
Mark Dickinson[8]
Alberto Franceschini[9]
Giulia Rodighiero[9]
Piero Rosati[10]
Alvio Renzini[11]

[1] Max-Planck-Institut für Astronomie, Heidelberg, Germany
[2] Università di Bologna, Bologna, Italy
[3] CEA/Saclay, Gif-sur-Yvette cedex, France
[4] INAF/Osservatorio Astrofisico di Bologna, Italy
[5] University of Massachusetts, Amherst, USA
[6] INAF/OAA, Florence, Italy
[7] Max-Planck Institut für extraterrestrische Physik, Garching, Germany
[8] National Optical Astronomy Observatory, Tucson, USA
[9] Università di Padova, Padova, Italy
[10] ESO
[11] INAF/Osservatorio Astrofisico di Padova, Italy

We report on the motivation, sample selection and first results of our VLT FORS2 Large Programme (173.A-0687), which has obtained the longest targeted spectra of distant galaxies obtained so far with the VLT. These long exposures, up to 77 hours for objects included in three masks, were required to detect spectral features of extremely faint galaxies, such as absorption lines of passive galaxies at $z > 1.4$, a population that had previously escaped attention due to its faintness in the optical wavelength regime, but which represents a critical phase in the evolution of massive galaxies. The ultra-deep spectroscopy allowed us to estimate the stellar metallicity of star-forming galaxies at $z \sim 2$, to trace colour bimodality up to $z = 2$ and to characterise a galaxy cluster progenitor at $z = 1.6$. The approximately 200 spectra produced by GMASS constitute a lasting legacy, populating the "redshift desert" in GOODS-S.

Motivation

In 2002, the K20 survey provided the spectroscopic redshift distribution of a complete sample of 480 galaxies with $K < 20$. One of the main scientific results from this survey was the discovery of a significant population of massive K-selected galaxies at high redshift (Cimatti et al., 2002). Their spectra (Cimatti et al., 2004) showed that some of these objects were indeed very massive (10^{11} $M_{\odot}$) and already old (1–2 Gyr). Around this time, deep near-infrared (NIR) imaging surveys were also beginning to provide evidence of a new population of candidate massive galaxies at photometric redshifts $z > 2$ (Labbé et al., 2002), barely detectable even in the deepest optical images. The strong clustering of these red galaxies (Daddi et al., 2003) suggested that these were progenitors of local, massive early-type galaxies. The existence of a significant population of massive galaxies in the early Universe was not predicted by semi-analytic models of hierarchical galaxy formation, in which the most massive systems form relatively late through a slow process of merging of smaller galaxies. Together with the small and slow evolution in the K-selected galaxy population up to z of 1–1.5, it became clear that most (massive) galaxy assembly occurred at $z > 1.5$. In order to study the physical and evolutionary status of typical Milky Way mass (M^*) galaxies in this redshift range, we proposed to obtain ultra-deep spectroscopy with FORS2 at the VLT. As emission lines move out of the optical window and the redshift measurement, especially for the passive galaxies, depends on absorption features in the continuum, there are few galaxies known in the redshift range of interest, $1.3 < z < 2.5$, which has traditionally been known as the redshift desert.

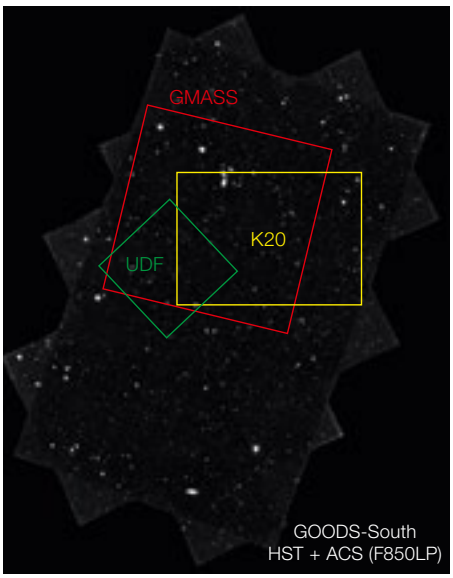

Figure 1. The location of the 6.8 x 6.8 arcminute field of GMASS (red), relative to the ACS coverage of GOODS-S (black background), the field of the K20 survey (yellow) and the Hubble Ultra Deep Field (green).

The location chosen for the survey (Figure 1) was GOODS-S in the Chandra Deep Field South, because of the available deep optical Advanced Camera for Surveys (ACS) imaging and near-infrared imaging with the Very Large Telescope (VLT) ISAAC instrument. This field would also contain the planned Hubble Space Telescope (HST) Ultra Deep Field (UDF) and contained part of the K20 survey. The proposed deep spectroscopy would be complementary to the VIMOS and FORS2 public spectroscopy surveys carried out by ESO in the GOODS-S field, which had shorter integration times and therefore targeted more luminous objects. Including overheads and pre-imaging, the total time requested for the programme was 145 hours in two semesters.

Sample selection and mask design

For the target selection, we took advantage of the very recent Spitzer/IRAC coverage of GOODS-S. The IRAC 4.5 μm photometry, which samples the 1–2 μm rest-frame for the targeted redshift range, enabled us to select on mass more reliably than possible with the K-band. We combined all available photometry from U-band to 8.0 μm to obtain photometric redshifts for the 1277 unblended sources detected at 4.5 μm (to $m_{AB} = 23.0$). These 1277 sources constitute the GMASS sample. Of this sample, we selected objects for spectroscopy according to the following constraints: $z_{phot} > 1.4$ and $B_{AB} < 26$

and $I_{AB} < 26$, excluding all objects for which spectroscopy was already available or planned. This spectroscopic sample contains 221 galaxies. Subsequently, we identified two subsamples: selecting so-called blue galaxies that were expected to have strong absorption lines below 6000 Å for the masks to be observed with the 300V grism (the blue masks); and red galaxies to be observed with the 300I grism (the red masks). For the first two pilot masks, we selected the brightest targets from both subsamples. Subsequently, we filled two blue and two red masks with fainter targets, allocating open spaces to targets already included in other masks, or otherwise to targets from the GMASS sample without spectroscopic redshifts. In total, 211 (174) objects from the GMASS (spectroscopic) sample were included in one or more masks (38 objects were included in two masks and five in three). The total exposure times for the masks were 12 h, 14 h and 15 h for the blue and 15 h, 32 h and 30 h for the red masks.

Our observational strategy for the blue masks followed the conventional optical one of having two offset positions so as to be able to correct for bad pixels, with each offset position exposed for half an hour. For the red masks, for which many variable sky emission lines make background subtraction difficult, we used four offset positions, each exposed for 15 minutes. During reduction, we computed the median value of the four positions for each pixel, which provided a reliable representation of the background. After subtraction of this background, the two-dimensional spectra were rectified and combined (taking into account the respective offsets). The remaining sky-line residuals were fitted along the columns and subtracted from the combined image. The resulting spectra have very low sky-line contamination, even above 8500 Å. We also took care to interpolate only once during the entire reduction process, to minimise any noise introduced by this process.

Redshifts obtained

After extracting the one-dimensional spectra and fitting the absorption and emission line features, 130 new redshifts at $z > 1.4$ were obtained. In addition, 37 new redshifts at $z < 1.4$ were obtained and more than twenty formerly known redshifts were confirmed and, in most cases, determined with higher accuracy. The fraction of redshifts successfully determined for the targets observed is about 85%. The same number applies to the fraction of targets with photometric redshifts $z > 1.4$ that were confirmed by spectroscopy to have $z > 1.4$ (a few of the galaxies from the spectroscopic sample were included erroneously and are not considered in this fraction). Figure 2 shows a histogram of the photometric and known spectroscopic redshifts in the GMASS field. Also shown is the fraction of known spectroscopic redshifts provided by GMASS, which increases from 30% to 85% between redshifts 1.4 and 1.8, and is 100% for most bins in the range $1.8 < z < 2.9$.

Superdense passive galaxies at $z > 1.4$

One of the main purposes of GMASS was to discover (spectroscopically) and study passive galaxies in the redshift desert. Although this desert is no longer as empty as before, the galaxies known in this redshift range are mostly UV-selected (Steidel et al., 2000) and therefore actively star-forming galaxies. Using IRAC selection, we were able, instead, to uncover 13 passive galaxies in the range $1.39 < z < 1.99$. Their spectra (see Figure 3) are similar to those of other old passive galaxies at $z > 1$, such as that of 53w091 at $z = 1.55$ (Dunlop et al., 1996).

We obtained a high signal-to-noise stacked spectrum (shown in Figure 4) by averaging all 13 individual spectra, assigning the same weight to each spectrum

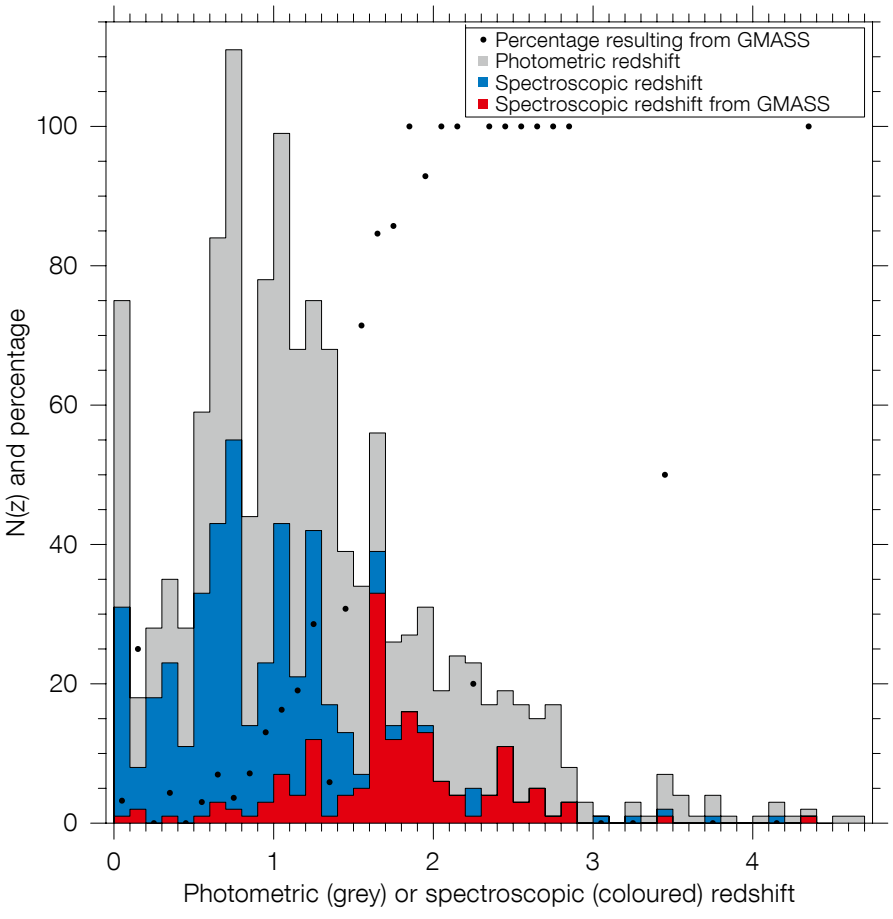

Figure 2. Histogram of photometric (grey), previously known spectroscopic redhsifts (blue) and spectroscopic redshifts resulting from GMASS (red) in the GMASS field. Also shown is the percentage of known spectroscopic redshifts determined by GMASS (black dots).

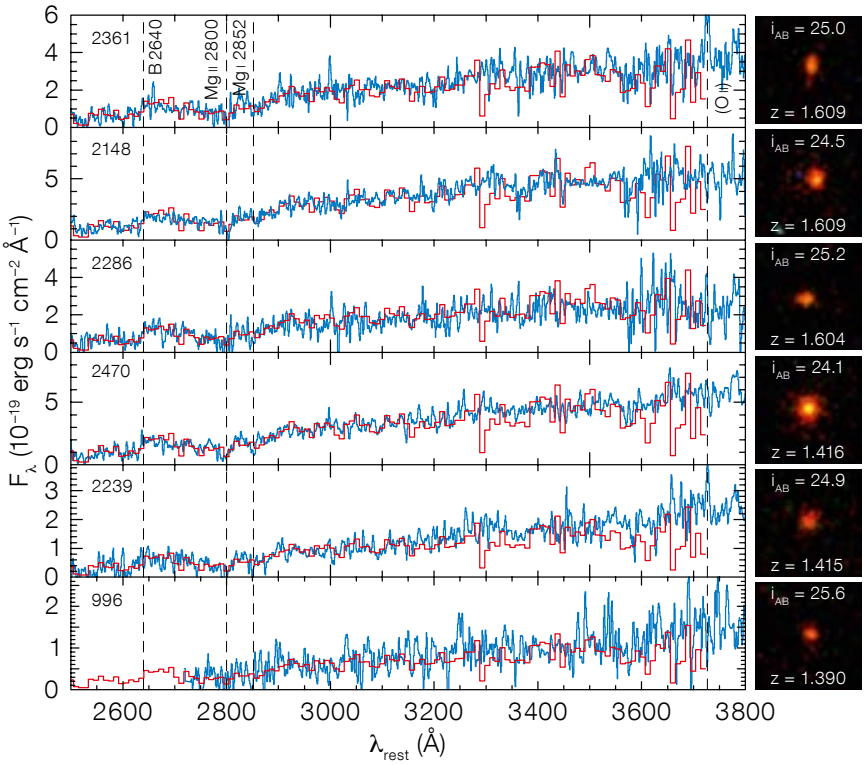

Figure 3. Individual spectra of six of the thirteen passive galaxies with GMASS spectra (blue). The spectra are very similar to the overlayed spectrum (red) of the old galaxy LBDS 53w091 at z = 1.55 (Dunlop et al., 1996). Shown on the right are 3.7 x 3.7 arcsecond *BVI* stamp images, constructed from HST/ACS images.

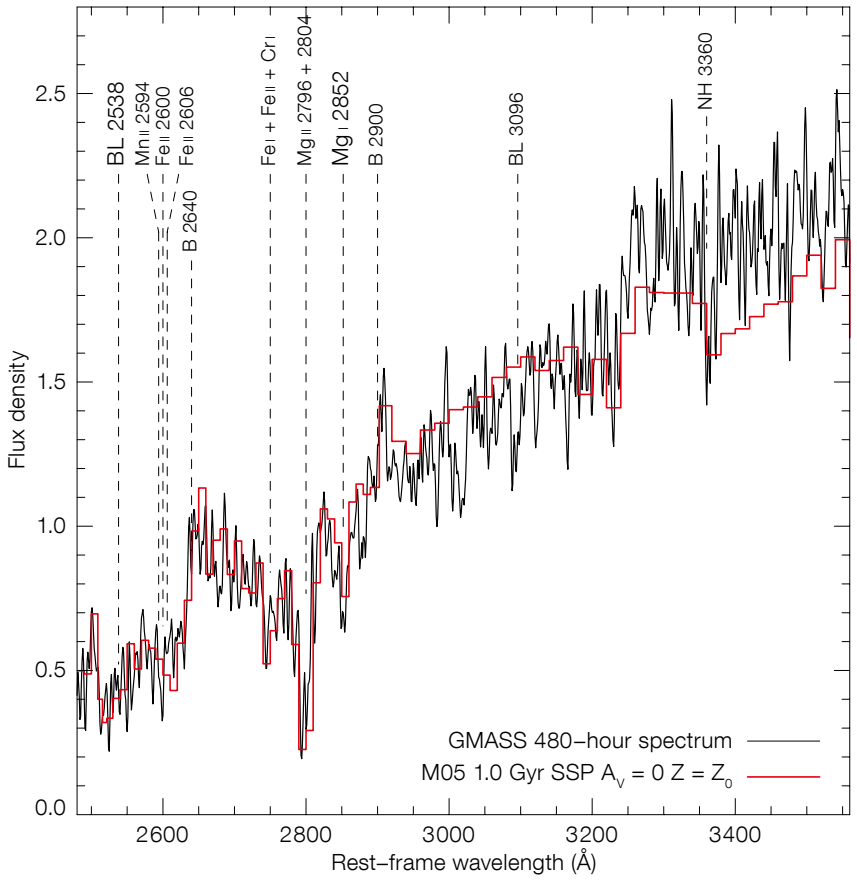

Figure 4. The stacked average spectrum of the thirteen passive GMASS galaxies (black) overlayed with the best-fit synthetic spectrum (red) from the models of Maraston (2005).

after normalisation in the 2600–3100 Å wavelength range. The stacked spectrum was compared with various libraries of synthetic spectra to estimate the age of the stellar population. In practice, using the observed rest-frame UV spectrum only, provides an estimate of the time elapsed since the last major episode of star formation. Since a degeneracy exists between the effects of age and metallicity, we calculated ages for a range of metallicities, finding best-fit ages between 0.7 and 2.8 Gyr for metallicities Z = 1.5 to 0.2 $Z_\odot$. We also fitted synthetic spectra to the available photometry (11 bands, including HST/ACS BVIz, VLT/ISAAC JHK$_s$, and Spitzer/IRAC 3.6, 4.5, 5.8, 8 μm) and derived a mean age, mass, and upper limit to the star formation rate (SFR) of 1.1 Gyr, 5 x 10^{10} $M_\odot$, and 0.2 $M_\odot$/yr respectively. Owing to the depth of the spectroscopy, it was possible to study galaxies that span a wide range in stellar mass: from very massive 10^{11} $M_\odot$ galaxies to systems of only 10^{10} $M_\odot$. Our analysis of the ages indicate that the bulk of the stars in these passively evolving galaxies must have formed at $2 < z < 3$, which is in excellent agreement with the evidence found for early-types observed at $0 < z < 1$, as well as for recent observations of early-types at $z > 1.4$.

A visual classification by eye of the ACS images shows that the majority of passive galaxies have a spheroidal morphology typical of early-type galaxies (Figure 3). For data acquired with the reddest available ACS filter, we modelled the surface brightness distribution by fitting a Sersíc profile, after the point spread function (PSF) was determined from ten stars in the field. Most of the passive galaxies have a Sersíc index n > 2, indicating that the bulk of the light from the galaxy comes from a bulge component. The galaxy radii are in the range 0.6–3.2 kpc with a mean

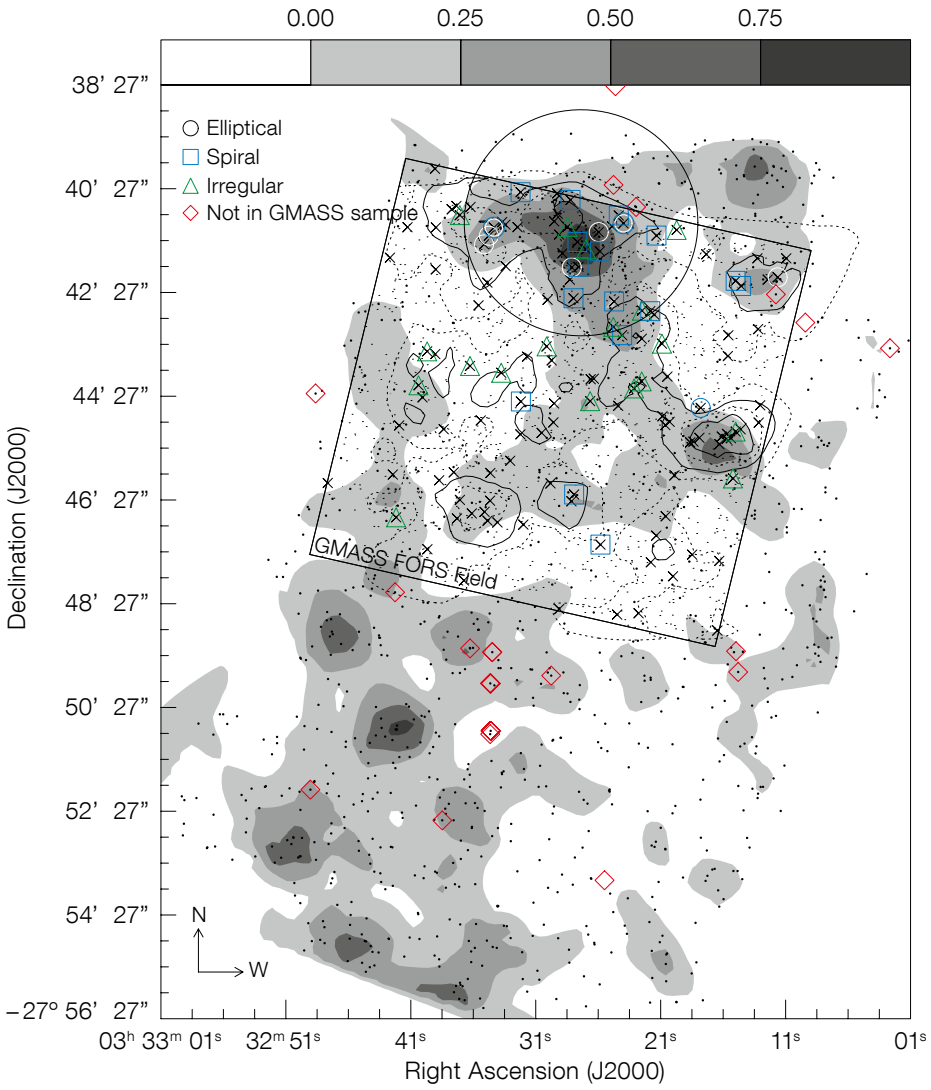

Figure 5. Density maps of galaxies at z = 1.6 in the GOODS-S field. Filled contours are based on GOODS/MUSIC (Grazian et al., 2006) photometric redshifts (indicated by filled circles) and solid and dashed contours are based on spectroscopic redshifts from GMASS and ESO/GOODS (indicated by crosses). Small dots indicate galaxies in the GMASS catalogue outside the redshift spike. Additional symbols are plotted according to morphology: elliptical galaxies (circles), spiral galaxies (squares) or irregulars (triangles). Diamonds indicate those galaxies in the overdensity at z = 1.6 not in the GMASS sample.

of 1.4 kpc. These values are much smaller than those observed in early-type galaxies of the same stellar mass in the local Universe. The small sizes that we measure are neither due to an unresolved central source, nor due to our imaging being in the rest-frame mid-UV (several authors have demonstrated that the sizes of spheroidal galaxies do not vary substantially as a function of wavelength). The measured galaxy sizes are smaller by a factor of two to three compared with $z \sim 0$ galaxies, implying that the stellar mass surface density of passive galaxies at $< z > \sim 1.6$ is five to ten times higher. Such superdense early-type galaxies with radii > 1 kpc are extremely rare in the local Universe (Shen et al., 2003).

This significant difference in size raises two questions: firstly, how did these small systems form, and what mechanisms can explain their growth in size in the past 10 Gyr? The derived constraints on the age, star formation history, and stellar masses indicate that intense star formation (SFR > 100 $M_{\odot}$/yr) must have taken place at $z > 2$. Among the possible precursor candidates, only sub-mm/mm-selected galaxies (SMGs) have sizes and mass surface densities comparable to those of the passive galaxies at $1.4 < z < 2$. In addition, the correlation lengths and estimated masses of these two populations are similar. SMGs are, however, an order of magnitude rarer than these passive descendants, which leads to an estimated sub-mm/mm galaxy duty cycle of ~ 0.15 Gyr. SMGs may therefore represent rapid and highly dissipative major mergers at $z > 2$, which become compact, superdense remnants that evolve almost passively at $z < 2$.

The other question is how superdense galaxies at $z \sim 2$ migrated to the size-mass relation at $z \sim 0$. One possibility is dissipationless (or dry) merging: according to some models, this process can increase the size and mass of a system without altering the stellar population content. The increase in size is expected to depend on the orbital properties and the mass of the merging system, with the most massive galaxies increasing their size more strongly than their less massive counterparts. If the mass-dependent size evolution is applicable, most GMASS passive galaxies would be the progenitors of early-types that today have stellar masses $10^{11}\ M_{\odot} < M < 10^{12}\ M_{\odot}$, i.e. the most massive E/S0 systems at $z = 0$.

An overdensity of galaxies at z = 1.6

Several spikes in the histogram of galaxy redshifts in the GOODS-S field are known. The overdensity of one of the highest redshift spikes, at z = 1.6, was described in Castellano et al. (2007). Within the large-scale overdensity, a peak was discerned that would evolve into a cluster of galaxies, although from the evidence at z = 1.6 the structure is unlikely to be virialised. Since the peak is located in our field, GMASS added 32 galaxies with confirmed z = 1.6 redshifts to the ten previously known (from ESO/GOODS spectroscopy). We confirm that there is a significant, narrow spike in the distribution of spectroscopic redshifts at z = 1.610, which forms an overdensity in redshift space by a factor of six. The velocity

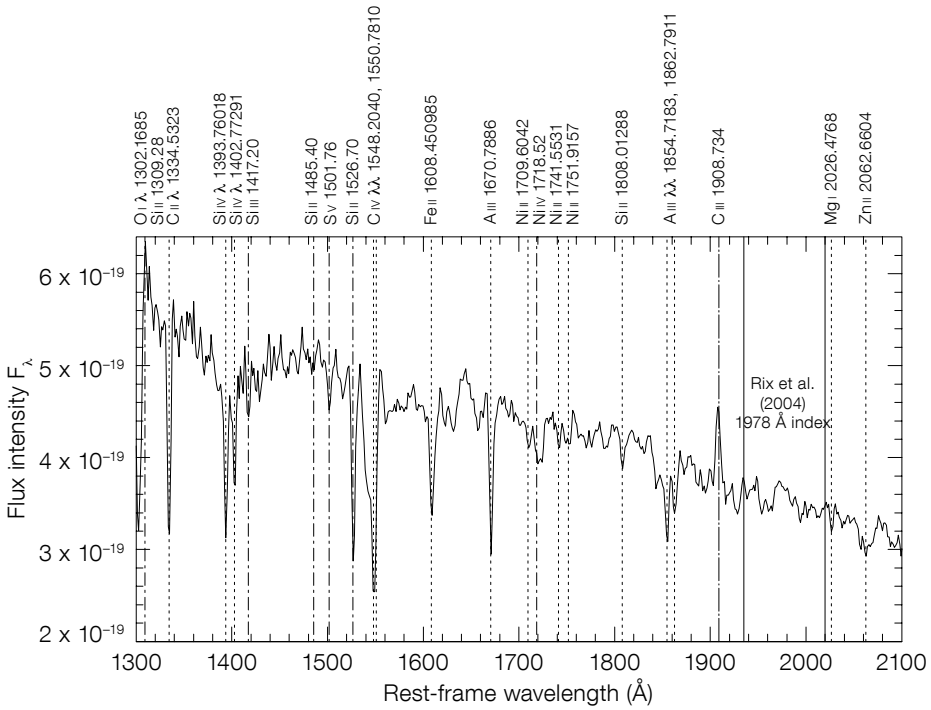

Figure 6. The average combined spectrum of 75 star-forming GMASS galaxy spectra. Lines indicate interstellar rest-frame mid-UV absorption features (dotted), photospheric absorption features (dot–short dash), and C III 1909 Å emission (dot–long dash).

dispersion of these 42 galaxies is 450 km/s, which should increase with redshift to become comparable with that of a cluster of galaxies. The redshift distribution is not Gaussian, but rather bimodal with a primary peak at z = 1.610 and a secondary at z = 1.602. Although we do not detect significant spatial separation between the primary and secondary peaks, this may be additional evidence that the structure is not yet virialised. Towards the northern part of the GMASS field, the surface density of spike galaxies is five times higher than in the remainder of the field. The properties of spike galaxies in this high density region are different from those outside: the mean age and mass are higher, while the mean star formation rate (SFR) and specific SFR (SFR per unit mass) are lower. Six out of the eight passive galaxies in the spike are in this region, three of which appear to form a sub-group of size smaller than 90 kpc. This group of passive galaxies is not located at the peak of the surface density of spike galaxies (Figure 5), but about 800 kpc away. The available NIR imaging allows a colour-magnitude diagram of the galaxies with confirmed redshifts to be compiled using the J-K colour, which brackets the 4000 Å break at this redshift. We detect a red sequence, which is consistent with a theoretical sequence of galaxies that formed their stars in a short burst at z = 3.

This is the first and only structure of this nature known: its redshift is higher than that of any known galaxy cluster and the structure contains spectroscopically confirmed, red, early-type galaxies. Its irregularity in angular and redshift space, including at least two localised higher density peaks, suggests that the structure is still relaxing, which is consistent with its low X-ray emission. Since this structure exhibits some of the properties typical of clusters, it may be the progenitor of a cluster of galaxies, observed at its assembly.

Other results from GMASS

Apart from the two projects described above, published in Cimatti et al. (2008) and Kurk et al. (submitted), two other papers based on GMASS spectra are published. In Halliday et al. (2008), we study the stellar metallicity of galaxies at z ~ 2, using a stacked spectrum of 75 star-forming galaxies (see Figure 6), corresponding to a total integration time of 1653 hours. With this spectrum, it was possible for the first time to measure the iron abundance and thus the stellar metallicity at a median redshift of z = 1.88. We constrain the metallicity to $\log(Z/Z_\odot) = -0.57 \pm 0.16$. Cassata et al. (2008) describe the colour bimodality in the galaxy population up to very high redshifts. We find that the red sequence of passive galaxies is recognisable up to z ~ 2, but then disappears. In addition, Daddi et al. (2007a,b) used GMASS spectra, in combination with other spectra of distant galaxies, to study star formation and obscured active galactic nuclei (AGN). Several more papers are in preparation, describing the survey strategy and resulting redshifts (Kurk et al.), the morphological analysis (Cassata et al.) and dust properties of galaxies up to z ~ 2.5. The published GMASS spectra will be publicly available through the ESO GOODS website, forming a lasting legacy for studies of high redshift galaxies.

References

Cassata, P. et al. 2008, A&A, 483, L39
Castellano, M. et al. 2007, ApJ, 671, 1497
Cimatti, A. et al. 2002, A&A, 391, L1
Cimatti, A. et al. 2004, Messenger, 118, 51
Cimatti, A. et al. 2008, A&A, 482, 21
Daddi, E. et al. 2003, ApJ, 588, 50
Daddi, E. et al. 2007a, ApJ, 670, 156
Daddi, E. et al. 2007b, ApJ, 670, 173
Dunlop, J. et al. 1996, Nature, 381, 581
Grazian, A. et al. 2006, A&A, 449, 951
Halliday, C. et al. 2008, A&A, 479, 417
Labbé, I. et al. 2002, The Messenger, 110, 38
Maraston, C. 2005, MNRAS, 362, 799
Shen, S. et al. 2003, MNRAS, 343, 978
Steidel, C. C. et al. 2000, ApJ, 604, 534

Credit: IAU/Jose Francisco Salgado

Credit: IAU/Lee Pullen

Two views of the official opening of the International Year of Astronomy 2009 held at the UNESCO headquarters in Paris. Upper: Jean-Michel Jarre, master of ceremonies, is seen with the distinguished panel of speakers. Lower: the Kronos Quartet playing to delegates.

VirGO: A Visual Browser for the ESO Science Archive Facility

Evanthia Hatziminaoglou[1]
Fabien Chéreau[1]

[1] ESO

VirGO is the next generation Visual Browser for the ESO Science Archive Facility (SAF) developed in the Virtual Observatory Project Office. VirGO enables astronomers to discover and select data easily from millions of observations in a visual and intuitive way. It allows real-time access and the graphical display of a large number of observations by showing instrumental footprints and image previews, as well as their selection and filtering for subsequent download from the ESO SAF web interface. It also permits the loading of external FITS files or VOTables, as well as the superposition of Digitized Sky Survey images to be used as background. All data interfaces are based on Virtual Observatory (VO) standards that allow access to images and spectra from external data centres, and interaction with the ESO SAF web interface or any other VO applications.

VirGO as an alternative to the traditional ESO archive query

The main ESO archive query form[1], a web interface, allows the user to search the ESO archive based on Target Name or Coordinates, Observing Date or Programme ID, request the type of observations (Imaging, Spectroscopy, Interferometry etc.) and the Category (Science or Calibration frames). The query may take anything from a few seconds to several tens of minutes, depending on the volume of the requested data required by the user. The information is returned in the form of a table, listing the frames, as well as the position, programme ID, exposure time, filter and other quantities and is followed by two tables summarising the total number of frames and exposure times, broken down by the various instruments or exposure time/instrument/filter.

VirGO[2] offers an alternative to this "traditional" querying form, by providing a visual impression of the available data, their overlaps and the instrument footprints, while allowing the resulting frames to be filtered in real-time, before launching the query to the ESO archive. This solution presents many challenges in the field of user interface design, such as displaying and navigating through many observations simultaneously without confusing the observer, or filtering out and selecting relevant observations in an intuitive way. An important aspect of VirGO is its capacity to access and handle large data collections on both the client and server sides, as well as to exchange data with other VO tools. These two features are achieved thanks to VO standards: the Simple Image Access/Simple Spectral Access (SIA/SSA) protocols for retrieving images and spectra, respectively, from a variety of astronomical repositories through a uniform interface; and the PLASTIC (Platform for Astronomy Tool InterConnection) protocol for communication with other VO tools.

Overview of main features

VirGO is a plug-in for the open source (GPL) software Stellarium (Chéreau et al., 2007, 2008), whose target audience is the general public, and it therefore benefits from many standard features such as the display of star and planet positions, landscape rendering, intuitive real-time navigation, a variety of projection modes, etc. To this set of standard features, VirGO adds the necessary tools for browsing through the ESO data archive. Figure 1 gives an overview of the general look-and-feel of VirGO. The main features of VirGO are:

1) The main Graphical Window contains the dynamical view of the observations in the current field of view. Images with footprints and previews (Rite et al., 2008) as well as superimposed spectra can be visualised simultaneously, all on a multi-resolution Digitized Sky Survey (DSS) background, if the user so desires (see below).

2) The List Browser displays a single summary line for each frame selected in the Graphical Window. The displayed information includes observation date, exposure time, filter and instrument. The existence of a preview is also indicated by the presence of a tick-box.

3) The Info Window contains detailed information about the observation

Figure 1. Overview of the main Virgo window. For an explanation of the numbered items, see text.

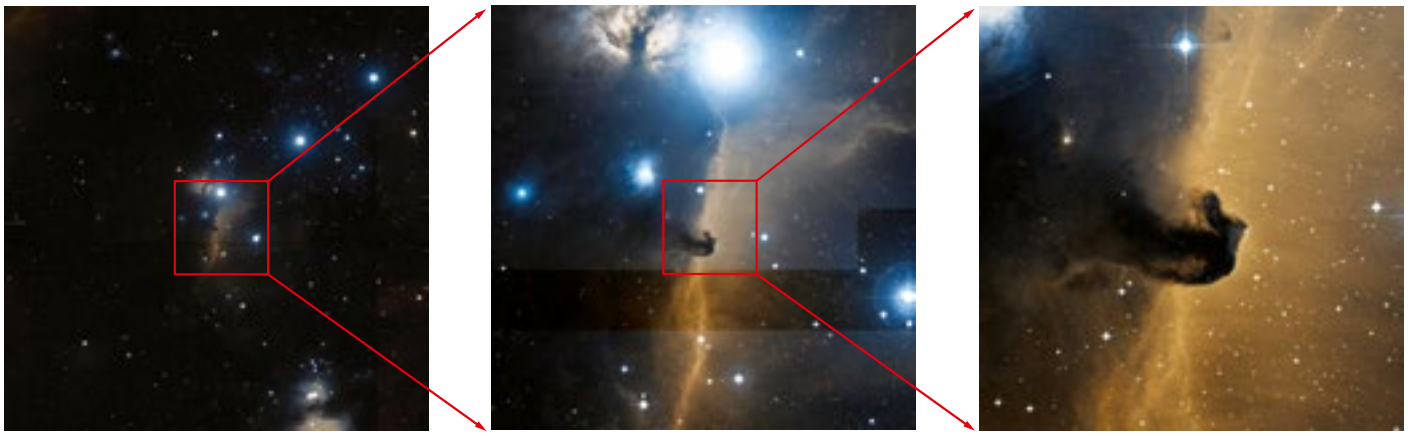

Figure 2. An example of the multi-resolution DSS background implemented in VirGO.

currently selected in the List Browser. It also provides a direct link to access the datasets, the preview images or transmission curves if available.

4) The View Selector allows the user to choose which observations to show/hide by defining a set of constraints such as observation type (images or spectra), processing type (raw data, highly processed data etc.), date or exposure time. The second part of this window is the Tree Browser, which contains a telescope/instrument/filter tree reflecting which observations are currently loaded in VirGO. It gives refined control over what to show/hide from the Graphical Window.

5) The Target Selection uses either the Simbad name resolver or the exact coordinates.

6) Additional functionalities in form of Tabs allow the user to see the servers being queried, select grouping options (e.g., footprint blending) and frame blending (depending on the number of superposed frames), or to send a direct query for the selected frames to the ESO Archive.

7) Finally, the Menu Bar gives quick access to functionalities such as the download of observations from the ESO SIA/SSA servers; the activation of the DSS background, grid display, etc.

In the current release of VirGO (1.4), observational data are accessed from ESO Science Archive Facility servers using VO SIA/SSA services. The VOTables provided by these services are loaded by VirGO in streaming mode to allow a fluid interaction even when downloading large datasets. The background is a multi-resolution false-colour JPEG version of the DSS originally created at STScI[3] by processing and combining the original blue, red and near-IR DSS images, allowing for more flexibility, e.g., at the time of defining an archive query. The special version hosted at ESO was post-processed and indexed for use in VirGO (see Figure 2 for an example).

Interaction with VO tools and services

VirGO is able to communicate through the PLASTIC protocol with a variety of other VO-compliant tools and services, such as Aladin[4] (a sky atlas allowing for visualisation of images, superimposition of catalogues, or access of related data and information from e.g., Simbad or VizieR), SPLAT-VO[5] (a spectral analysis tool) or TOPCAT[6] (an interactive graphical viewer and editor for tabular data). For example, FITS images can be sent to Aladin for quick visualisation before being requested from the archive. Similarly, all reduced spectra available as Advanced Data Products (comprising most UVES and HARPS spectra as well as FORS2 and VIMOS GOODS spectra) can be visualised using SPLAT-VO. VirGO's communication with the VO world is a two-way communication. For instance, it can receive and display catalogues retrieved using Aladin or TOPCAT.

Use cases

We illustrate two examples of where using VirGO has advantages over the archive query form.

– A user preparing an observing proposal in the Chandra Deep Field South (CDF-S)

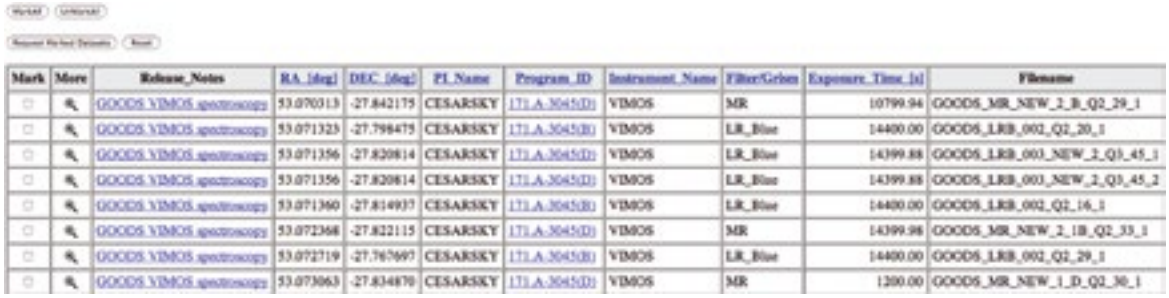

Mark	More	Release_Notes	RA [deg]	DEC [deg]	PI_Name	Program_ID	Instrument_Name	Filter/Grism	Exposure_Time [s]	Filename
		GOODS VIMOS spectroscopy	53.070313	-27.842175	CESARSKY	171.A-3045(D)	VIMOS	MR	10799.94	GOODS_MR_NEW_2_B_Q2_29_1
		GOODS VIMOS spectroscopy	53.071323	-27.798475	CESARSKY	171.A-3045(B)	VIMOS	LR_Blue	14400.00	GOODS_LRB_002_Q2_20_1
		GOODS VIMOS spectroscopy	53.071356	-27.820814	CESARSKY	171.A-3045(D)	VIMOS	LR_Blue	14399.88	GOODS_LRB_003_NEW_2_Q3_45_1
		GOODS VIMOS spectroscopy	53.071356	-27.820814	CESARSKY	171.A-3045(D)	VIMOS	LR_Blue	14399.88	GOODS_LRB_003_NEW_2_Q3_45_2
		GOODS VIMOS spectroscopy	53.071360	-27.814937	CESARSKY	171.A-3045(B)	VIMOS	LR_Blue	14400.00	GOODS_LRB_002_Q2_16_1
		GOODS VIMOS spectroscopy	53.072368	-27.822115	CESARSKY	171.A-3045(D)	VIMOS	MR	14399.98	GOODS_MR_NEW_2_1B_Q2_33_1
		GOODS VIMOS spectroscopy	53.072719	-27.767697	CESARSKY	171.A-3045(B)	VIMOS	LR_Blue	14400.00	GOODS_LRB_002_Q2_29_1
		GOODS VIMOS spectroscopy	53.073063	-27.834870	CESARSKY	171.A-3045(D)	VIMOS	MR	1200.00	GOODS_MR_NEW_1_D_Q2_30_1

Figure 3. Example output of the Advanced Data Products query form for ESO spectroscopy in the Chandra Deep Field – South (CDF–S).

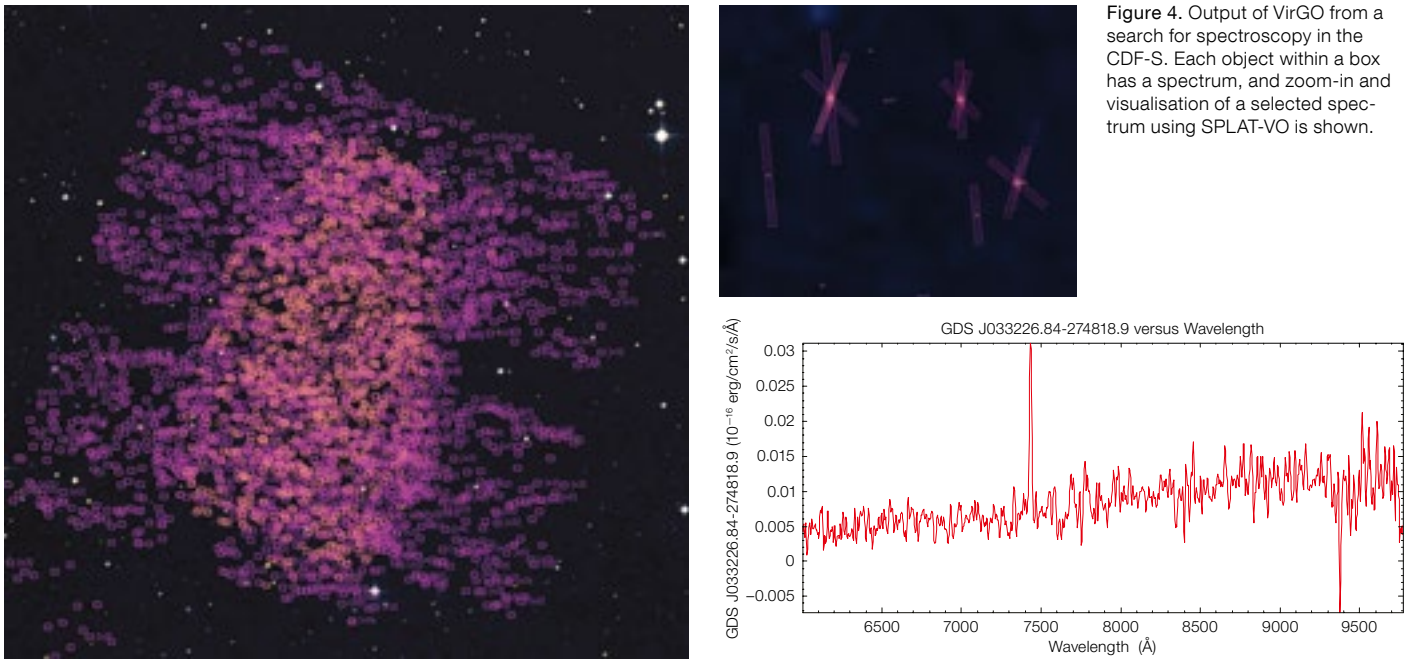

Figure 4. Output of VirGO from a search for spectroscopy in the CDF-S. Each object within a box has a spectrum, and zoom-in and visualisation of a selected spectrum using SPLAT-VO is shown.

wants to know about all the available ESO observations within one square degree in this field. Using the main ESO archive query form, the user will have to wait about 28 minutes for all the frames (more than 31 000) to be returned in the form of an HTML table. The same query using VirGO will require only four minutes and will return the list in a visual form, like that shown in Figure 1, allowing the user to see the overlaps between observations immediately, to get a feeling for the depth of the exposures (using the footprint blending option) or to look selectively at the reduced data.

– A user wants to know which targets have been followed up spectroscopically by ESO/GOODS in the CDF-S. The Advanced Data Products query form[7] will again return an HTML list of files with the relevant information, like that shown in Figure 3. The same query using VirGO will return a visualisation of the available reduced spectra, shown in Figure 4. The user can then select an image to use as a background to identify the sources or, by zooming in, see the orientation of the slit (whenever available) or the number of spectra composing the final product per object, or even visualising individual spectra using other VO tools (here SPLAT-VO) before requesting them from the archive.

Future developments

Although fully functional, VirGO is a recent application, and several major capabilities as well as technical features still have to be implemented. The next objectives are the following:

– add access to more ESO data, especially science-ready data such as Large Programmes and Surveys, large sets of pipeline-processed data, and Press Release images;

– dissemination: some features of VirGO will be included in the standard version of Stellarium, e.g., the display of Press Release images (Kapadia et al., 2007). VirGO/Stellarium, along with other VO tools, is also brought to schools in organised practical sessions in classrooms with teachers and students, as part of a dedicated outreach effort within AIDA[8] (Astronomical Infrastructure for Data Access) and this effort will continue in the future;

– on the technical side, the immediate objectives include the improvement of server scalability, the optimisation of image and catalogue access and the use of improved caching, as well as a deeper integration with the ESO website.

References

Chéreau et al. 2007, Stellarium 0.10.0, www.stellarium.org
Chéreau F. 2008, in ASP Conf. Series, Vol. 394, ADASS XVII, ed. Argyle R. W., Bunclark P. S. & Lewis J. R., 221
Kapadia et al. 2007, in Christensen, L.L. & Zoulias, M. (eds.) Communicating Astronomy with the Public, 2007
Rité, C. et al. 2008, in ASP Conf. Series, Vol.394, ADASS XVII, ed. Argyle R. W., Bunclark P. S. & Lewis J. R., 605

Notes

[1] http://archive.eso.org/eso/eso_archive_main.html
[2] http://archive.eso.org/cms/virgo
[3] http://www-gsss.stsci.edu/Acknowledgements/DataCopyrights.htm
[4] http://aladin.u-strasbg.fr/
[5] http://astro.dur.ac.uk/~pdraper/splat/splat-vo/splat-vo.html
[6] http://www.star.bris.ac.uk/~mbt/topcat/
[7] http://archive.eso.org/eso/eso_archive_adp.html
[8] http://cds.u-strasbg.fr/twikiAIDA/bin/view/EuroVOAIDA/WebHome

News from the ESO Science Archive Facility

Nausicaa Delmotte[1]
(for the ESO archive team)

[1] ESO

The latest developments from the ESO archive are presented. Information is provided to the astronomical community on new data releases and services.

Blu-ray discs for data distribution

The new Blu-ray disc technology will be introduced mid-2009 in the Science Archive Facility. Besides FTP transfer for small volumes of data, the archive is currently offering its users the following media for data distribution: CD, DVD-R, and USB discs for data requests larger than 60 GB. The reasons for the change are the adoption of the most economical technologies and the adaption to larger data volumes. A Blu-ray disc has about ten times the capacity of a single-layer DVD. With the introduction of the Blu-ray discs, the archive will stop offering CDs as an archive data distribution medium. Therefore, archive users anticipating large data requests and Principal Investigators (PIs) expecting significant data deliveries from their observing programmes are advised to make sure that they have Blu-ray disc readers available.

New query forms

Besides the general archive query form that gives unified access to the complete ESO collection of raw data, the Science Archive Facility also offers several instrument specific and technically oriented access points for astronomers who are already familiar with ESO instrument set-ups and observing strategies. Two new instrument specific query forms[1] have been released: one for AMBER (near-infrared instrument of the VLT Interferometer) raw data and one for HAWK-I (near-infrared wide field imager) raw data.

The database of ambient conditions for the Paranal and La Silla observatory sites has been extended to include weather information from the APEX observatory site. The APEX weather station is located on a free-standing 6-metre high tower located about 50 m west of the APEX telescope and data are recorded every minute. APEX weather data, beginning 1 January 2007, are available from the archive[2] and can be searched by date interval, or any meteorological parameter such as temperature, humidity, wind speed/direction or precipitable water vapour.

Figure 1. A view of part of the ESO Data Centre where the ESO Science Archive is stored and accessed.

New data releases

Several major scientific data releases have taken place through the ESO archive over the last months and are summarised here. The 30 Doradus raw data taken during the HAWK-I commissioning phase were released in December 2008 and the raw data from the AMBER/FINITO/UTs science verification were released in October 2008. The second release (DR2) of advanced data products from the zCOSMOS redshift survey (Lilly et al., 2008) took place in October 2008. It contains the results of the zCOSMOS-bright spectroscopic observations that were carried out with VIMOS in service mode during the period April 2005 to June 2006.

Faster access to raw proprietary data

The modification of the archive systems and interfaces to allow PIs to request their own raw proprietary data and the introduction of the automatic data transfer through the network from Paranal to Garching (Zampieri et al., 2008) has led to significantly improved data delivery services. PIs, can now access their own raw data, in most cases only a few hours after the observations have completed.

Contact

For more information about the ESO archive, or to subscribe to the archive RSS feed to be informed about the latest archive developments, see the archive web page[3].

For any questions or comments on the ESO archive, contact us at archive@eso.org.

References

Lilly, S. et al. 2008, The Messenger, 134, 35
Zampieri, S. et al. 2008, to appear in ASP Conf. Proc. ADASS XVIII

Notes

[1] http://archive.eso.org/cms/eso-data/instrument-specific-query-forms
[2] http://archive.eso.org/wdb/wdb/eso/meteo_apex/form
[3] http://archive.eso.org/

New Infrastructures Require New Training: The Example of the Very Large Telescope Interferometer Schools

Paulo Garcia[1]
(on behalf of the European Interferometry Initiative)

[1] Universidade do Porto, Portugal

The discovery space for astronomy is dramatically widening with the operation, construction and planning of ambitious new infrastructures. A key aspect of the scientific return from these facilities is the training of its users. We report on a series of summer schools designed to train a new generation of young astronomers in optical interferometry with the Very Large Telescope Interferometer.

Eleven years have passed since first light on the Very Large Telescope (VLT). The last decade has been a vibrant one for astronomy. Common key words in contemporary astronomy such as "dark energy" or "exoplanets" appeared for the first time in the title of a refereed journal article only about ten years ago. The thrust of astronomical discovery is driven by carefully planned new facilities and infrastructure. The last decade has witnessed the deployment of the VLT and the VLT Interferometer (VLTI), the planning and initial construction of the Atacama Large Millimeter/submillimeter Array (ALMA) and the planning of the European Extremely Large Telescope (E-ELT). These new facilities will come online in the next decade. The E-ELT will enable tremendous gains in sensitivity, making it possible, for example, to probe the acceleration of the Universe. The profound gain of the ALMA interferometer in both resolving power and sensitivity is driven by three key science goals, one of them being the study of the physics and chemistry of planet-forming discs around young stars.

New opportunities come with new challenges and these were clearly identified by the *ASTRONET Infrastructure Roadmap* (Bode et al., 2008): "Recruiting and training the future generation of Europeans with advanced scientific and technological skills is therefore a key aspect of any realistic Roadmap for the future." Training new generations of astronomers on new observational techniques is of the utmost importance as new facilities come online. This article shares the very successful experiences of the VLTI training schools project ONTHEFRINGE that took place between January 2006 and December 2008.

The birth of the project

At the start of the training schools project, the VLTI was operational, but had yet to ramp up and become the top optical interferometric facility in the world. Expertise in optical interferometry was concentrated in a few institutes involved in instrument building and was not widespread across Europe and the ESO user community. If this uneven distribution of expertise continued it would clearly inhibit the scientific maximisation of the investment in the new interferometric infrastructure.

A few schools had been organised previously with FP5 funding (for example, the Les Houches school in 2002) and institute funding (for example, the Leiden schools in 2000 and 2004), but any wider coordination was lacking. In contrast, a very successful annual programme of optical interferometry summer schools (the Michelson/Sagan Summer Schools) has been running in the US since 1999. The creation of the European Interferometry Initiative (EII) network signalled the beginning of a European-wide cooperation between countries with and without expertise in optical interferometry. Under the auspices of EII, the ONTHEFRINGE project was submitted to the European Commission for FP6 and awarded funding. The project was coordinated by Universidade do Porto/CAUP, with ESO, Observatoire de Paris/LESIA, Max-Planck-Institute for Astronomy, Heidelberg and INAF/ Osservatorio Astrofisico di Arcetri as partners and, as third parties, the Laboratoire d'Astrophysique de Grenoble, the Nicolaus Copernicus University in Torun, Poland and the Konkoly Observatory of the Hungarian Academy of Sciences.

The goals of the schools

The ONTHEFRINGE project aimed to overcome the training gap by providing an integrated and structured approach to European training in optical interferometry. One goal of the schools was to educate a new generation of young astronomers, equipping them with the ability to carry out scientific programmes at the VLTI (from preparation to data reduction and analysis). Another important goal was to place optical interferometry in context with other techniques in key astronomical areas of European leadership such as adaptive optics and radio/sub-mm interferometry. In contrast with the NEON observing schools that took place at observatories, the VLTI schools were held in relatively geographically isolated locations, but with sufficient computing capacity for hands-on training. The very nature of the VLTI made it unreasonable to carry out the training at the La Silla Paranal observatory. Since VLTI observations are normally carried out in service mode, its location in Chile and the full-time science use of the facility meant that the schools obviously could not take place on-site.

The project consisted of four schools:

– Observation and Data Reduction with the Very Large Telescope Interferometer, Les Houches, June 2006

– Circumstellar Disks and Planets at Very High Angular Resolution, Porto, May–June 2007

– Active Galactic Nuclei at the Highest Angular Resolution: Theory and Observations, Torún, August – September 2007

– Astrometry and Imaging with the Very Large Telescope Interferometer, Keszthely, June 2008.

The first and fourth schools were data reduction schools, aimed at hands-on observation preparation and data reduction, the first focusing on AMBER/MIDI and the fourth on PRIMA and image reconstruction. The second and third schools were science schools aimed at placing optical interferometry in a wider context, in two fields where it has a major impact.

Although the schools were open to all researchers, EU requirements only allowed funding to particular categories

of participants, essentially PhD students and young postdocs.

The design of the schools

Previous experience with the one week school at Les Houches in 2002 showed that it was difficult to combine both the teaching of new information and the necessary contact-building time among participants successfully, in such a short time. Although, in theory, optical interferometry is not very difficult to understand (the practice, however, requiring a significantly steeper learning curve), most of the students had not been in contact with the discipline before, in contrast with optical/infrared spectroscopy or photometry, for example. Therefore they had to be immersed in a Fourier space environment for some time to become acquainted with optical interferometry methods. The schools lasted for two weeks, a couple of days more than the ideal. We found that including a free afternoon as early as the second day of the school greatly improved the contact-building among participants. The right balance of fun and work was found important to keep productivity high in the unfamiliar environment of optical interferometry. It should be stressed that during fun time, students were building contacts among themselves and the senior lecturers that not only were the basis for group work at the school, but could, in the future, be important for collaborations or the sharing of information about relevant institutes and supervisors for a future postdoctoral position.

The school's time was essentially divided between lectures/seminars and practical sessions. The lectures addressed the basic aspects of interferometry and the seminars the typical astronomical results obtained. In the astrophysical schools a set of review lectures focused on the astrophysics of the target objects and complementary techniques, such as adaptive optics or radio/sub-mm interferometry. In the practical sessions the students went through the observation preparation software, in groups of two sharing a computer. This experience was found to be very useful in learning the basics of interferometry. Exercises focused initially on the observables measured by the interferometer and how they could be used to constrain models of the astronomical object(s) to be observed. Then, more complex and realistic aspects of the observations were included, such as UV coverage, closure phases, noise in the observables and model-fitting. In the data reduction schools, the participants went through the steps in the reduction pipelines. At the end of the schools, groups of students worked on a VLTI observation proposal and presented it to their colleagues, facing scrutiny and advice from seasoned observers. These sessions helped to mature a student's understanding of the technique and certainly helped to make them more able to design scientific programmes at the VLTI – the main goal of the schools.

As a requirement of an EU funded training programme, we designed a series of lectures on complementary skills — from presentation skills, to paper and telescope proposal writing, career development and ethics. We were surprised at the interest of the students. Many were not aware of what an impact factor was, or what the refereeing process was all about, or even that job hunting should start well in advance of the end of a PhD. Many of them were discussing ethical aspects in the practice of astronomy research for the first time, or learning that a PhD is not enough (c.f. Feibelman, 1993) for a successful career in science.

The number of students attending each school was around 55, with PhD students accounting for well over two thirds of the total. Such a number was a compromise between a school environment and reaching a larger audience. The logistics required to keep 30 computers up and running (including updating and installing software and data) with internet access in isolated regions of Europe was not trivial. Even with so many participants, many more had applied and could not be selected to attend. The selection of participants was based on a motivation letter, institute and national balance, with preference given to PhD students. In order to reach a wider audience, all the materials at the schools (presentations, software, data, lecture notes) were made available on the project website[1]. In retrospect some of the lectures should have been videotaped and streamed through the site.

Highlights and results of the schools

The total number of participants in the four schools, including lecturers, was around 280. A lecturer attending four schools counted as four participants. The number of participants who did not lecture was around 200, composed essentially of PhD students and young postdocs. The selection procedure kept multiple attendance to below 10%. During the three years of the project there were about 1500 PhD students in astronomy, about half of whom were in Europe (Gibson, 2002). The total number of ESO member country participants was around 105. If we assume that half of the total PhDs are awarded in ESO member countries, then this project reached around 14% of the total PhD student population in Europe. This number would increase by a small factor if specific areas were considered, such as ground-based observational astrophysics. The gender balance of the non-lecturing participants was around 60% male: 40% female and increasing to 70% male: 30% female if we included the lecturing participants. Figure 1 presents the distribution of non-lecturing students by country. Interestingly, countries that have recently become members of ESO or intend to join soon had a high attendance at these schools.

These schools were very important for software developers (at ESO and the Jean-Marie Mariotti Center) and they provided a unique opportunity for immediate and massive feedback from a pool of interested new users.

The ambiance of the schools was uniformly excellent, providing a perfect balance between hard-working and brain-cooling moments. The best experts and seasoned lecturers taught not only all about optical interferometry, adaptive optics, radio/sub-mm interferometry, but also the physics of young stellar discs or active galactic nuclei. The participants, from all around the globe, had a taste of the best of Europe! Sampling red wine and French cuisine at the Chateau de Goutelas, or enjoying the sun and the beach at the Portuguese seaside (and of course a glass of Port), visiting the stunning town where Copernicus was born and becoming an expert in *wódka*, or finally watching the views from the hills

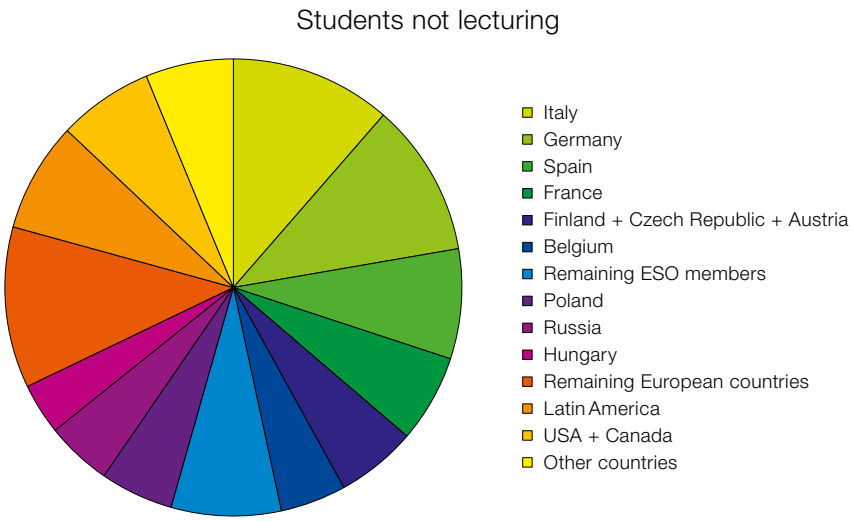

Figure 1. Pie chart showing the distribution of students (non-lecturing participants) by host country attending the four VLTI Summer Schools.

near Lake Balaton while discovering the bouquet of an old Tokay. I will not forget the awed face of lecturers as, when arriving late, they witnessed the computer room full of students working hard on their telescope proposals. At the end of the telescope proposal presentations, the students would rush to Françoise Delplanke and proudly collect ESO stickers, posters, hats or calendars. This new generation of young astronomers surely deserves the great new infrastructure we are now planning and building.

Acknowledgements

This project was supported by EC contract No. MSCF-CT-2005-029954. We warmly thank the consortium institutions and staff (Universidade do Porto/CAUP, ESO, Observatoire de Paris, MPIA, INAF-Arcetri, Jean-Marie Mariotti Center, Torun University and Hungarian Academy of Sciences) for their full support. Special thanks go to the lecturers and students; kudos too to Júlio Carreira, Gilles Duvert, Manuel Monteiro and Elsa Silva.

References

Bode, M. F., Cruz, M. J., Molster, F. J. (eds) 2008, *The ASTRONET Infrastructure Roadmap*, ISBN: 978-3-923524-63-1

Feibelman, P.J. 1993, *A PhD Is Not Enough: A Guide To Survival In Science*, (Basic Books: New York), ISBN: 978-0201626636

Gibson, B.K. 2002, Astr. Soc. of Australia Newsletter, 26, 4

Notes

[1] http://www.vlti.org

Figure 2. A selection of group photographs from the four VLTI summer schools at (clockwise): Les Houches, France, 2006; Porto, Portugal, 2007; Torun, Poland, 2007; and Keszthaly, Hungary, 2008.

Report on the ESO Workshop

Large Programmes

held at ESO Headquarters, Garching, Germany, 13–15 October 2008

Gautier Mathys[1]
Bruno Leibundgut[1]

[1] ESO

A report is presented of the workshop on the progress of ESO Large Programmes completed between the last workshop in May 2003 and September 2007.

Five years after the first workshop on ESO Large Programmes (see the summary by Wagner & Leibundgut, 2004), about 50 participants, including the PIs of the second round of Large Programmes (LPs), as well as several members of the Observing Programmes Committee (OPC) and the Science and Technical Committee (STC) together with some Council members, gathered in Garching from 13–15 October 2008. The VLT has been in operation for nearly ten years and a large fraction (15%) of the observing time has been devoted to the execution of Large Programmes. At the request of the OPC, ESO organised this second workshop to obtain a new overview of the scientific results achieved through the Large Programmes conducted at the La Silla Paranal Observatory. The workshop featured scientific presentations of all LPs that were completed between the May 2003 LP workshop and end of ESO Period 79 (30 September 2007). The teams of investigators leading these LPs were invited to present their scientific results and the impact of their project on its field. The presentations were followed by a discussion session on the general scientific impact of ESO facilities.

One of the outcomes of the May 2003 workshop was a suggestion that ESO should archive the legacy data products of Large Programmes. This suggestion was implemented with the requirement that Large Programmes that started after 1 April 2005 deliver Advanced Data Products (ADPs) to the ESO science archive by the time of publication of their results in a refereed journal. The workshop featured a presentation of the ADP submission process and a discussion of its value for the ESO scientific community.

The first two days were devoted to the presentation of 20 LPs with topics ranging from the distant Universe and the determination of cosmological parameters to the characterisation of the population of nearby galaxies and the search for habitable exoplanets. Most fields in astrophysics were represented by an LP. The morning of the third day was dedicated to a discussion of the special scheduling constraints and challenges presented by LPs, a bibliometric assessment of the scientific impact of LPs and a presentation on how to submit the reduced data products to the ESO archive. After a brilliant summary by Willy Benz on the scientific value of LPs and how they can succeed (or fail), a discussion, led by the STC chair, Linda Tacconi, on the various aspects of LPs took place. The workshop programme and the presentations can be found online[1].

A number of the projects presented actually encompassed more than one LP, among them the public surveys (the ESO Imaging Survey [EIS] and the Great Observatory Origins Deep Survey [GOODS]). There were projects requiring large data samples or deep searches for extremely rare objects and, in some cases, a long time span was essential for the observations to record a light curve or to measure proper motions or radial velocities. Several LPs complemented other large efforts by space- or ground-based consortia. Very few LPs could be considered failures: most of these cases had to cope with instrumental problems, with the result that the final data quality was not sufficiently high to achieve their goals.

It was stated several times that LPs have changed some of the culture of astronomical observations. The need for large data samples and complex data analyses requires teams with a wide range of expertise. This leads to large collaborations. Consequently, most LPs were granted to large collaborations. Nevertheless, there are specific experiments, which can be run by a dedicated small team concentrating on a specific problem. In most cases the scientific returns of the LPs have been very good, some even spectacular. The chance to obtain enough observing time to approach a major astrophysical problem over four semesters was generally appreciated.

The bibliometric analysis of LPs compared to other programmes shows a good publication record. While 15% of the observing time was devoted to LPs they returned 18% of the refereed publications. This may be partly due to the fact that LPs do receive a high priority for observations. Papers based on LPs appear to have a slightly higher impact — as measured by the number of citations per paper — than all other types of programmes (Normal, Target of Opportunity, Guaranteed Time Observations and Director Discretionary Time). The effect is significant, but not dramatic. It is remarkable that LPs have requested time on all instruments, with ISAAC, FORS2, VIMOS and WFI being the most used. The distribution over the different scientific categories further reveals a predominance of cosmological projects (OPC category A), requesting and being allocated about half the time. The other three categories share the remaining fraction equally. With the extension of LPs on La Silla to four years (compared to the two years so far on all ESO telescopes) a marked increase in the time requests for HARPS for Period 83 can be noted. The demand for LPs remains high and the OPC has seen a significant increase in the number of LP proposals in the past two semesters.

According to the summary by Willy Benz, LPs need to be bottom-up, i.e., tailored to the user's needs. This is guaranteed first through the selection by the OPC, and then by the regular status reports provided to the OPC, that enable a judgement whether the continued investment in telescope resources is still warranted. Also, LPs should not be regarded in isolation, but should be seen as a complement to other types of observing programmes. They should enable projects, which otherwise would not be possible at a public observatory. The results from this workshop as well as the first workshop in 2003 show that LPs have enabled European astronomers to compete on a par with some of the private large facilities in the US. At the same time, it has to be realised

that LPs make use of an expensive resource and that they have to provide additional benefits for the community. This has led to the requirement that reduced data from LPs, once published, should be returned to the ESO Archive so that they can be used by other astronomers, possibly for different purposes. The large investment by the community into LPs should justify this modest return. There was a lively discussion on how this return should be achieved and whether it would put astronomers using ESO facilities at a disadvantage compared to users of private observatories.

The workshop overall was very successful and clarified the need for, and the competitive edge of, Large Programmes at ESO facilities. The increased demand for the 3.6-metre telescope after the time limit for LPs was raised to four years speaks for itself. There are some very substantial programmes in progress, which will keep this telescope busy for years to come.

Beyond the Large Programmes, the Public Surveys with VISTA and VST will start during this year and next year. These will be truly massive projects, which complement the current arsenal of programme types undertaken with ESO facilities at the upper end. It is planned to monitor their success in another workshop in a few years time.

References

Wagner, S. & Leibundgut, B. 2004, The Messenger, 115, 41

Notes

[1] http://www.eso.org/sci/meetings/LP2008/program.html

ESO and the International Year of Astronomy 2009 Opening Ceremony

Pedro Russo[1 2]
Lars Lindberg Christensen[1]
Douglas Pierce-Price[1]

[1] ESO
[2] International Astronomical Union

The ESO contributions to the International Year of Astronomy 2009 and the Opening Ceremony, held in Paris in January 2009, are summarised.

"The International Year of Astronomy 2009 is an important step in furthering the interest of the public in what is arguably the oldest of all sciences: astronomy." ESO Director General, Tim de Zeeuw, on the United Nations proclaiming 2009 as the International Year of Astronomy.

Few areas of science touch on as many topics of interest for the general public as astronomy. For countless thousands of years, eyes have gazed up at the heavens and wondered; it could be argued that everyone is born an astronomer. Modern astronomy is a highly professional field, but is not exclusively the domain of specialised scientists. The sky is a shared resource and intense public interest means that many organisations, such as ESO, invest in outreach initiatives.

Credit: IAU/Jose Francisco Salgado

Figure 1. Catherine Cesarky, IAU President, addressing the audience during the IYA2009 Opening Ceremony

The year 2009 has been launched by the International Astronomical Union (IAU) and the United Nations Educational, Scientific and Cultural Organization (UNESCO) as the International Year of Astronomy 2009 (IYA2009) under the theme "The Universe, Yours to Discover". The IYA2009 marks the 400th anniversary of the first astronomical observation through a telescope by Galileo Galilei. Proclaimed by the United Nations (UN) and endorsed by the International Council for Science, the IYA2009 has already captured the imagination of countless individuals. The aim of the IYA2009 is to stimulate worldwide interest, especially among young people, in astronomy and science. Events and activities will promote a greater appreciation of the inspirational aspects of astronomy that ESO is keen to foster.

The opening ceremony of IYA2009 was held in Paris, on 15–16 January, 2009, under the aegis of the UN, UNESCO and the IAU. The ceremony itself featured keynote speeches, research findings, an exhibition and also social aspects. About 900 people attended, among them eminent scientists, including Nobel Laureates, and also around 100 young students from individual countries. The ceremony was very well received, and the quality of talks highly praised. The enthusiasm of all involved shone through, and proved that

Credit: IAU/Lee Pullen

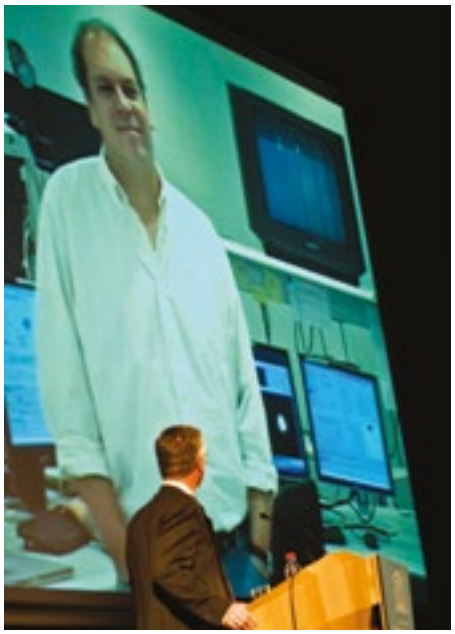

Figure 2. A video link with Paranal made a big impression on the audience. Here, ESO Director General Tim de Zeeuw is seen talking to Christophe Dumas on the big screen, live from the VLT Control Room.

the IYA2009 has already gained plenty of momentum to help popularise astronomy throughout 2009, and beyond.

ESO's contribution to the ceremony

ESO held an exhibition at the UNESCO headquarters in Paris as part of the opening ceremony. The exhibition presented information about ESO's role in astronomy and the Very Large Telescope (VLT), the European Extremely Large Telescope (E-ELT) and the Atacama Large Millimeter/submillimeter Array (ALMA) projects. A scale model of the E-ELT complemented the exhibition. The official IYA2009 brochure, an E-ELT brochure, and "Eyes on the Skies" DVDs were available for visitors.

The afternoon session on Thursday, 15 January, was chaired by the ESO Director General Tim de Zeeuw. The session saw two fascinating talks: "The New Frontier: The Exploration of the Solar System" by André Brahic; and "Echoes of Creation: Discovery of the Big Bang Fossil Radiation", by Nobel Laureate Robert Wilson. A highlight on Friday, 16 January, was Tim de Zeeuw's overview of ESO activities and the live video conference from the auditorium in Paris to ESO's VLT on Cerro

Credit: ESO/D. Pierce-Price

Figure 3. The ESO exhibition took prominent position in the display room.

Paranal in Chile. This was a rare opportunity for the audience to join astronomers at work in the VLT control room, towards the end of the Chilean night. Christophe Dumas, head of the Science Operations Department at the VLT, discussed the night's observations and shared a recent image from the telescope. You can watch this on the IYA2009 Opening Ceremony video archive[1]. IYA2009 science writer, Lee Pullen, kept a "Cosmic Diary Live-Blog" during the ceremony. This diary of events was regularly updated, and followed by people in over 130 countries.

ESO's commitment to public outreach and to IYA2009

Since plans for IYA2009 were first laid in 2003, ESO has played a major role in the project. ESO is hosting the IYA2009 Secretariat for the International Astronomical Union, which coordinates the activities globally. ESO is one of the Organisational Associates of IYA2009, and was also closely involved in the resolution submitted to the UN by Italy, which led to the 62nd General Assembly of the UN proclaiming 2009 as the International Year of Astronomy.

In addition to a wide array of activities planned both at the local and international level, ESO is leading three of the eleven global Cornerstone projects. These are 100 Hours of Astronomy, a worldwide observing marathon during which ESO will coordinate a 24-hour webcast from research observatories; the Cosmic Diary, a blog that gives the public insight into the lives of professional astronomers; and the Portal to the Universe, a global one-stop website for online astronomy content.

Figure 4. The International Year of Astronomy 2009 logo.

The IYA2009 Secretariat at ESO HQ is the central hub of the IAU's implementation of the IYA2009, and was established to coordinate activities during the planning, execution and evaluation of IYA2009. The secretariat liaises continuously with the — currently 137 — national nodes, task groups, partners and organisational associates, the media and the general public to ensure the progress of IYA2009 at all levels. The secretariat is staffed by Pedro Russo, the IYA2009 coordinator, IYA2009 assistant Mariana Barrosa and is managed by Lars Lindberg Christensen, head of ESO's education and Public Outreach Department. ESO's own organisational IYA2009 contact is Douglas Pierce-Price.

Astronomy is one of the oldest fundamental sciences, yet continues to make a profound impact on our culture and is a powerful expression of the human intellect. 2009 is the year in which individuals and organisations can make a difference by popularising astronomy as never before and really "bring the Universe down to Earth". ESO's presence at the opening ceremony shows our commitment to this grand aim.

Notes

[1] http://www.astronomy2009.org/webcast

Announcement of the ESO Workshop

MAD and Beyond: Science with Multi-Conjugate Adaptive Optics Instruments

8–10 June 2009, ESO Headquarters, Garching, Germany

ESO has pioneered the use of adaptive optics assisted instruments for research in astronomy. Come-On+ and its heir, Adonis, were the first common-user adaptive optics instruments. Nowadays adaptive optics (AO) instruments are standard at all major observatories. AO adapters are routinely used to feed spectrographs that require very small entrance windows to achieve very high spectral resolution, such as CRIRES, or to increase the spatial resolution of spectro-imagers, such as SINFONI on the Very Large Telescope (VLT). In addition AO adapters are indispensable for the Very Large Telescope Interferometer (VLTI). The biggest shortcoming of AO instruments is their small corrected field of view, which is limited by the size of the isoplanatic patch that even in the infrared and at the best sites rarely exceeds 15 arcseconds. The ESO Workshop on AO in Venice in 2001 paved the way, on the basis of theory and simulations by researchers in Europe and the USA, to overcoming the isoplanatic barrier and thus atmospheric tomography was born.

The study phase for the European Extremely Large Telescope (E-ELT) provided the opportunity to actually demonstrate that atmospheric tomography, as implemented in its best known version of Multi-Conjugate Adaptive Optics (MCAO), can provide AO performance over fields of view significantly larger than the isoplanatic patch. This led to the construction of the Multi-conjugate Adaptive-optics Demonstrator, MAD, for the VLT. Thus, about 20 years after the deployment of the AO demonstrator Come-On at the 3.6-metre telescope at La Silla, ESO is again pioneering the field by commissioning MAD on Unit Telescope 3 at the VLT. The commissioning was so successful, that strong demand from the community led MAD to be offered for scientific observations, initially for 14 nights in the Chilean summer of 2007/2008 and then, again at the request of the community, for an additional nine nights in August 2008 to cover the winter period. One year after the first science demonstration run, close to ten papers based on MAD data have been published and many others are in preparation, showing that the community is keen to apply MCAO techniques to ambitious astronomical problems.

The success of MAD also demonstrated that the technology is mature, and the community prepared for the next generation of MCAO instruments. The aims of the workshop, therefore, will be twofold: to celebrate the achievements of MAD through a dedicated discussion of its design constraints and scientific achievements, and, with the strong foundation provided by the scientific results, to outline the high level requirements for the next generation of MCAO instruments. Thus, the spirit of the conference will be both festive, because we are celebrating MAD, and visionary, because we are dreaming about the future.

Further details can be found at www.eso.org/sci/meetings/mad2009/index.html. The deadline for registration is 10 May 2009.

Announcement of the IAU Special Session 1

IR and Sub-mm Spectroscopy: A New Tool for Studying Stellar Evolution

3–6 August 2009, IAU General Assembly, Rio de Janeiro, Brazil

This IAU Special Session aims at fostering collaboration between various fields and will bring together experts from theoretical and observational astrophysics, instrumentation and laboratory spectroscopy. In combination, these fields hold the key for the scientific success of current and planned facilities. New observations will foster new approaches to old problems and will no doubt lead to transformational thinking on stellar evolution.

The conference occurs at a particularly advantageous time for the transfer of knowledge in IR and sub-millimetre spectroscopy from mission to mission. Certain space missions have produced a wealth of data — Spitzer will have completed its cryogenic mission and entered the "warm" phase, while AKARI has ended operations after completing an all-sky survey. Others will either be presenting early results (Herschel) or making advanced preparations for launch (SOFIA, JWST). New ground-based facilities (VLT, Gemini, Keck) have matured to the point of presenting results of unprecedented quality. In the near future ALMA will open up the study of sub-millimetre sources to unprecedented sensitivity. The next generation of extremely large telescopes (ELTs) will allow the study of individual stars in other galaxies. In this field, IR spectroscopy will be particularly important, as only the combination of ELTs with active optics will allow individual stars to be singled out in crowded regions.

For details please visit the website at: www.eso.org/sci/meetings/iau2009-sps1/index.html

Announcement of the ESO Workshop

Detectors for Astronomy 2009

12–16 October 2009, ESO Headquarters, Garching, Germany

Astronomical observations are critically dependent on focal-plane array technology, and detectors continue to play a key role in continuing to extend the scope of astronomical observations. Higher sensitivity, reduced noise, larger formats, better cosmetic quality, higher quantum efficiency, smaller point-spread functions, lower dark current, higher bandwidth, and many more, constantly set new milestones on the roadmap towards the goal of artefact-free photon shot noise limited images of reality. One of the fastest growing applications is signal sensing, especially wavefront sensing for adaptive optics and fringe tracking for interferometry, which have become vital enabling technologies for both interferometry and extremely large telescopes. Topics of active research are large format Complementary Metal Oxide Semiconductor (CMOS) and Charge Coupled Devices (CDD) array mosaics, orthogonal transfer CCDs, electron multiplication CCDs, electron avalanche photodiode arrays, quantum-well infrared photon detectors, Application Specific Integrated Circuits (ASICs), blocked-impurity band arrays, novel readout technologies, to name a few. In a field with such rapid and complex developments, it is essential that designers, manufacturers and users gather regularly in order to exchange information about requirements, technical possibilities and achievements on a worldwide scale.

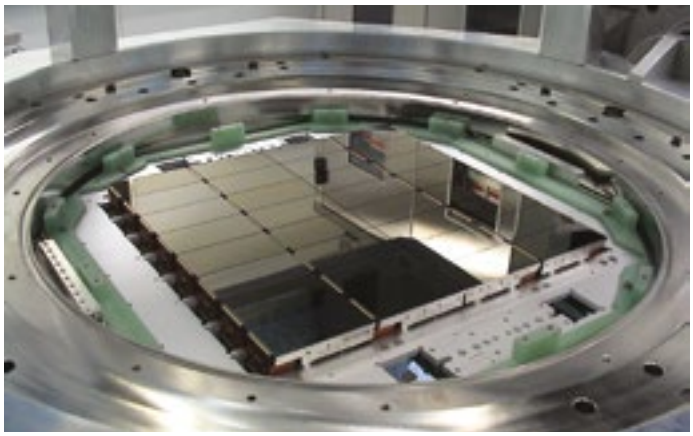

Figure 1. The 8 x 4 mosaic of e2v CCD82-44 2K x 4K CCDs (16K x 16K pixels in total) for OmegaCAM, which will capture the full 1 degree x 1 degree field of view of the VLT Survey Telescope (VST).

The 2009 Workshop Detectors for Astronomy aims at providing an up-to-date platform for such exchanges and continues a series of similar meetings in 1991, 1993, 1996, 1999 (all at ESO-Garching), 2002 (Waimea), and 2005 (Taormina). The 2009 meeting will specifically address the following topics:

– Detector technologies and design
– Detector manufacturing
– Detector evaluation and calibration
– Control electronics
– ASICs
– Control software
– Detector systems
– Mosaic focal-plane arrays
– Cryo-vacuum technologies
– Instruments with very demanding and/or novel requirements on detectors
– Scientific applications and results that depend on high performance detectors
– Test methodology and quality control
– Calibration of performance

Contributions are invited irrespective of wavelength and deployment on the ground or in space. The main focus will be on the optical and infrared domains. Depending on interest, splinter meetings dealing with topics of special interest can be organised. Contributions with demonstrations of hard- or software are welcome (subject to technical feasibility).

For registration and more information please visit www.eso.org/sci/meetings/dfa2009/.

ESO's Studentship Programmes: Training Tomorrow's Astronomers Today

Michael West[1]
Marina Rejkuba[1]
Bruno Leibundgut[1]
Eric Emsellem[1]

[1] ESO

Students are the lifeblood of astronomy, the next generation of astronomers. While other scientific disciplines are facing declining student enrollments, the ASTRONET strategic plan for European Astronomy notes "young students have continued to enter the field at a steady level". Indeed, with Very Large Telescope (VLT), Atacama Large Millimeter/submillimeter Array (ALMA) the European Extremely Large Telescope (E-ELT) and other exciting new facilities on the horizon, it is hard to imagine a better time to be an astronomy student.

ESO is a leader in shaping the future of astronomy, and one important way to achieve this goal is by offering short-term and long-term studentships that provide excellent opportunities for students to pursue research under the supervision of ESO staff astronomers. Since its inception two decades ago, hundreds of young astronomers have spent some time during their PhD programme at ESO in Garching or Santiago. Many have gone on to leading positions

Figure 1. **(Left)** Group portrait of students at ESO Garching.

Figure 2. **(Right)** Students at ESO Chile enjoy an excursion to Paranal.

at universities, observatories and other organisations in Europe and beyond.

PhD Studentships

Through its PhD studentship programme, ESO offers training to future users of its state-of-the-art observational facilities. Students that come to ESO through the PhD studentship programme are already enrolled in doctoral programmes in astronomy, physics or related fields at universities in ESO member states or non-member state institutes.

ESO PhD students typically spend one or two years pursuing their doctoral research under the co-supervision of an ESO faculty astronomer, in close contact with activities and people at one of the world's foremost observatories. After returning to their home universities, these students are often expert users of ESO observing facilities. Upon the completion of their PhD a large majority of these students pursue a career as a professional astronomer, and some have become postdoctoral fellows or staff astronomers at ESO.

Short-term studentships

Opportunities also exist for a limited number of students to come to ESO for periods of one to three months to work on research projects with ESO astronomers. Such positions are usually funded by the Director General Discretionary Fund, which supports a broad range of needs related to scientific projects by ESO staff astronomers.

There is no formal application procedure for short-term studentships at ESO. Students interested in the possibility of working on a short-term research project at ESO should explore the science staff web pages to identify one or more ESO staff astronomers with whom they might wish to work and then contact those astronomers directly, or contact the Head of the Office for Science in Garching or Santiago for more information.

Students in Garching

Currently 22 students from 15 countries are working on their PhD research at ESO Garching (see Figure 1). Fifteen of them are enrolled in the ESO studentship programme and will spend one or two years at ESO during their PhD and will receive the degree from their home university. One student is participating in an exchange programme with Chinese universities, and six students are enrolled in the International Max-Planck Research School (IMPRS) on Astrophysics.

ESO's Garching Headquarters forms part of one of the world's largest centres for astronomy and physics, with other leading institutes such as the Max-Planck Institute for Astrophysics, the Max-Planck Institute for Extraterrestrial physics, MPE, the Institute for Plasma Physics, the Max-Planck Institute for Quantum Optics and the campus of the Munich Technical University nearby. The strength of this concentration of scientific expertise was recently recognised by the German authorities, and led to the creation of the Excellence Cluster on the "Origin and Structure of the Universe". In such a vibrant environment students have an abundance of choice for seminars and lectures with unique opportunities to learn about the hottest topics and most important open questions in physics and astronomy.

Students in Santiago

Surrounded by the splendour of the Andes Mountains, seven students are currently pursuing their PhD research at ESO offices in Santiago, together with a constant stream of short-term students (Figure 2). During the past year alone, students from universities in Belgium, Chile, Denmark, England, France, Germany, Iceland, Italy, Portugal and the United States have participated in ESO Chile's short-term and long-term studentship programmes. ESO offices in Chile provide a stimulating scientific environment for students, with a science team of nearly 80 staff astronomers, fellows, students and visitors, plus close connections with ALMA and the astronomy departments at top Chilean universities in Santiago and beyond.

In addition to engaging in scientific research under the supervision of an ESO staff astronomer, students at ESO Chile have a unique opportunity to get hands-on experience with the technical aspects of observatory operations at Paranal, La Silla, ALMA or the Atacama Pathfinder Experiment (APEX), a millimetre/submillimetre telescope. This month, for example, ESO Chile PhD student Pedro Almeida will travel to La Silla to spend two weeks working on polarimetry data from EFOSC2 and participating in observations using HARPS, all under the guidance of ESO astronomers.

ESO

European Organisation
for Astronomical
Research in the
Southern Hemisphere

ESO Studentship Programme

The European Southern Observatory research student programme aims to provide opportunities to enhance the PhD programmes of ESO member-state universities. Its goal is to bring young scientists into close contact with the activities and people at one of the world's foremost observatories. For more information about ESO's astronomical research activities please consult www.eso.org/science/.

The ESO studentship programme is shared between the ESO Headquarters in Garching (Germany) and the ESO offices in Santiago (Chile). These positions are open to students enrolled in a PhD programme in astronomy or related fields. In addition, ESO will provide up to two studentship positions per year in Santiago for students enrolled in South American universities.

Students in the programme work on their doctoral project under the formal supervision of their home university. They come to either Garching or Santiago for a stay of normally between one and two years to conduct part of their studies under the co-supervision of an ESO staff astronomer. Candidates and their supervisors at the home institute should agree on a research project together with the ESO local supervisor. A list of potential ESO supervisors and their research interests can be found at www.eso.org/sci/activities/personnel.html. A list of current PhD projects offered by ESO staff is available at www.eso.org/sci/activities/thesis-topics/. It is highly recommended that the applicants start their PhD studies at their home institute before continuing their PhD work and developing observational expertise at ESO.

ESO Chile students will have an opportunity to visit the observatories and get involved in small projects aimed at providing an insight into operations at the observatory. Such visits and projects, which are voluntary, will be scheduled to ensure that they do not interfere with the research project of the student in Santiago.

In Garching, students can benefit from the series of lectures given to the PhD students enrolled in the IMPRS (International Max-Planck Research School on Astrophysics) PhD programme; attendance is voluntary. Students who are already enrolled in a PhD programme in the Munich area (e.g., the IMPRS or at a Munich University) and wish to apply for an ESO studentship in Garching, should provide compelling justification for their application.

The Outline of the Terms of Service for Students (www.eso.org/public/employment/student.html) provides some more details on employment conditions and benefits.

The closing date for applications is 15 June 2009.
Late applications will be accepted until all the positions are filled.

Please attach to your application the following documents:

– a Curriculum Vitae (including a list of publications, if any), with a copy of the transcript of university certificate(s)/diploma(s);

– a summary of the Masters thesis project (if applicable) and ongoing projects, indicating the title and the supervisor (maximum half a page), as well as an outline of the PhD project, highlighting the advantages of coming to ESO (recommended 1 page, max. 2);

– two letters of reference, one from the supervisor/advisor at the home institute and one from the ESO local supervisor;

– a letter from the home institution that: i) guarantees financial support for the remaining PhD period after the completion of the ESO studentship; and ii) indicates whether the requirements to obtain the PhD degree at the home institute have already been fulfilled.

All documents should be submitted in English (but no translation is required for the certificates and diplomas).

Review of the received material, including the recommendation letters, will start on June 15. Applications arriving after this deadline will be considered until all the positions are filled. Incomplete applications will not be considered. All reference letters should be sent electronically to vacancy@eso.org.

Candidates will be notified of the results of the selection process in July 2009. Studentships typically begin between August and December of the year in which they are awarded. In well-justified cases, starting dates in the year following the application can be negotiated.

For further information please contact Christina Stoffer (cstoffer@eso.org).

The post is open equally to suitably qualified male and female applicants.

New Staff at ESO

Jonathan Smoker

Jonathan Smoker

Although born in Chicago, I was brought up on a smallholding in rural England. Amongst the chickens, sheep, goats, windmill and methane digester could be found a 6-inch Newtonian telescope that my Dad had made out of a plastic tube and a mirror that someone had given us. So, that's how I became an astronomer! Although I can't quite remember the Moon landings, one thing that I do recall clearly came later, in the 1970s, when Viking touched down on Mars and "discovered" life there, and later on the first shuttle launch.

I went to university in Manchester for my undergraduate degree, then did my PhD in radio astronomy at Jodrell Bank, studying the neutral hydrogen content of low surface brightness and blue compact galaxies, but also doing a bit of imaging and spectroscopy. After a six-month spell living in a tent at Jodrell, I switched to system administration at the Institute of Astronomy in Cambridge, before moving to Queen's University, Belfast, working on the Magellanic Bridge and high velocity clouds. I went on 22 observing trips in four years, giving me enough experience to be able to apply for a staff position at ESO in 2002. After a year or so I was lucky enough to be involved in the science verification of FLAMES, for which I later became instrument scientist. It still amazes me how the robot can place so many fibres with an accuracy of a fraction of an arcsecond! After a spell back in Belfast and travelling in South America whilst working on my laptop, I returned to ESO in 2008, again initially working on FLAMES-UVES, but who knows what the future will hold? One of the great things about ESO is that there are always opportunities to work on new projects, although balancing observatory work, science and the odd trip to the Andes is always a challenge!

My research is concerned with probing the tiny-scale (astronomical unit) structure of the interstellar medium, using UVES to observe early type stars at high resolution and twin epochs. I have also dabbled as a collaborator in high latitude stars and typing the precursors of supernovae.

Although working on Paranal can be tiring, it is balanced by the satisfaction of being part of a team that has contributed so much to astronomy over the last 10-plus years. There is nearly always something new happening on the mountain (APE is testing on Melipal and a GRB Target of Opportunity has arrived as I write these words)... may that stay the same for years to come!

Wolfgang Wild

In November 2008 I took up the position of Head of the ALMA Division and European ALProject Manager. Having worked in the field of sub-/millimetre and far-infrared instrumentation and astronomy for quite some years, I am enjoying the new challenges presented by the Atacama Large Millimeter/submillimeter Array (ALMA) project and this large international collaboration.

Working and living in the Munich area again is a pleasure after 18 years of "venturing" through the world at different institutes and observatories. After studying physics in Munich and obtaining a PhD on submillimetre instrumentation and astronomy in 1990, I moved to Chile to work at SEST (Swedish–ESO Submillimetre Telescope) as an ESO fellow on La Silla. These were interesting times both at the telescope and in Chile — the country had just made the transition to a democracy. I much enjoyed the variety of tasks

Wolfgang Wild

in the small SEST team, ranging from helping visiting astronomers and doing my own astronomical research to improving the system and solving technical problems (I remember once crawling inside the antenna structure at night trying to find a short circuit). The good working atmosphere at La Silla and the friendly people and natural beauty of Chile also contributed to memorable years.

When the ESO fellowship came to an end I had the opportunity to become Site Manager of the Pico Veleta Observatory near Granada in southern Spain. The observatory belongs to the French–German–Spanish Institute IRAM (Institut de Radioastronomie Millimetrique) with its headquarters in Grenoble (France). During my years at the IRAM 30-metre telescope, I was responsible for the operations and improvements of the observatory together with a group of scientific and technical experts — an interesting job that taught me a lot. I also enjoyed life in Granada and married a "Granadina".

However, after nine years of working at telescopes, by around 1999 it was time for a change and I wanted to go back to instrumentation development. At that time, ALMA was just about to become a joint project between Europe and the US. It was still called "MMA–LSA" (Millimeter Array/Large Southern Array), which was a merger between two similar, but different, interferometer projects in the US and Europe. Following various meetings and discussions, the MMA–LSA evolved into the ALMA project, and with the participation of East Asia (Japan and Taiwan) and Canada, ALMA developed into what it is today — a large international collaboration to build a new interferometer at a high site in Chile. Wanting to contribute to ALMA on the instrumentation side, I heard of a new group being built up in the Netherlands for the development of the ALMA Band 9 receivers, one of the challenging high frequency bands. I applied for the position of Project Manager and group leader and was hired as the first person in this new undertaking between NOVA, the SRON Netherlands Institute for Space Research and the University of Groningen.

Those early ALMA days were quite exciting — I started by hiring another person, so we began with two people, many ideas, an empty lab, a budget (never enough of course) and a lot of enthusiasm. Today, almost ten years later, the group in Groningen comprises twelve people and has built nine state-of-the-art receivers for ALMA with another 60+ to be built over the next few years. During these early ALMA days, from 1999 to 2002, I was also the European Receiver Team Leader working closely with colleagues from North America and Japan on the design of the ALMA receivers. It looked like I would stay with ALMA for quite a while, but then in 2002 there was the opportunity to contribute to a space instrument in the same institute, and I worked on HIFI (Heterodyne Instrument for the Far-Infrared), one of the three instruments onboard ESA's Herschel Space Observatory, foreseen for launch on an Ariane 5 rocket in April this year. In 2004 I was appointed Head of SRON's Low Energy Astrophysics Division (with HIFI being the major project), and from 2007 onward I became responsible for SRON's infrared and submillimetre programme as Programme Scientist. During my time at SRON I also held a position at the Kapteyn Astronomical Institute of the University of Groningen, and in 2005 I was appointed Professor for Techniques of Far-Infrared and (Sub-)Millimetre Astronomy.

I am very happy to be part of ESO again, and with such exciting projects like ALMA and the European Extremely Large Telescope I am looking forward to these great new observatories and the science they will enable.

Credit: ESO/L. Testi

Sunset over the ALMA Test Facility (ATF) in Socorro, New Mexico. The prototype US and European antennas, shown here, were used for testing and development of hardware and software and were interferometrically linked (see ESO PR 10/07). The ATF closed in December 2008, having successfully fulfilled its purpose.

Fellows at ESO

Jean-Baptiste Le Bouquin

Jean-Baptiste Le Bouquin

I started astronomy in quite an unusual way. I first studied heat engines and other sorts of machinery using thermal energy. Having been lured into an increasing passion for physics, I continued studying fundamental physics for several more years.

There came a time when I had to choose between particle physics and astrophysics. My wife found the best strategy to make this dramatic choice: look at the potential colleagues in both areas and assess how they were set up in life (properly dressed or not, with family or not, etc.). The "vote" definitely went to astrophysics!

I completed my PhD thesis in the city of Grenoble, in the French Alps, conveniently located near numerous ski resorts. I visited Paranal once during my graduate studies, where I worked on the VLTI and was definitely impressed by this huge machine. Press a button and you have two giant telescopes pointing together and unveiling the mysteries of some unknown stars. I decided to be part of this adventure.

I arrived at ESO in April 2006. I devoted a significant part of my duties and research time to improving the abilities of the VLTI. I greatly appreciated sharing the work with engineers, technicians and astronomers. I am proud of what has been achieved within these last three years. As well as managing technical challenges, we have succeeded in getting unprecedented astrophysical results. I am now in the fourth year of my ESO fellowship and thinking about future projects and the next generation of VLTI instrumentation that will use the four giant telescopes together.

My wife and I have enjoyed Chile immensely — the people, nature, food, and all the new friends we now have. Moreover, we will leave Chile with two everlasting souvenirs: our son Tobie and our daughter Anaelle.

Hugues Sana

11 961 km... That's the distance between Liège and Santiago. 11 961 km... it is difficult to get further away. It is further than the US West coast, Hong Kong or Beijing, and even further than Tokyo. The only way to go further would be to head for Australia, to some small Pacific island or to Antarctica.

11 961 km... it is not the other side of the world, but it is getting close and that is the adventure I had the chance to take up about three years ago when I was offered a fellowship position at ESO. It was on a Wednesday morning, two days before Christmas, 1145 days ago and 11 961 km away from where I am sitting right now.

Since then, I have enjoyed 54 Lan Chile snack boxes, delighted in 233 wonderful sunsets in Paranal and survived 671 rides from my house in Santiago to the Vitacura office. In Paranal, I had the opportunity to be trained on two UTs, Antu and Kueyen, performing over 1500 OBs for a cumulative open shutter time of 587 hours. Given the ratio of the instrument aperture sizes, it would have taken 17 290 years for Galileo to collect as many photons as I did.

But the most impressive part is not about numbers, sizes or advanced technology (although they are very impressive), it is about the people, working around the clock, away from family, often tired because of the workload, stress and lack of sleep. It is about their problem-solving attitude, their constant mood and their incredible motivation. My ESO fellowship has certainly been a wonderful challenge and one of the most intense life experiences. If I had to summarise what I learned in a single word, it would be "balance". Balance between observatory duties, science time, private life and personal development, and what it takes, as a juggler, to keep that many balls flying in the air.

About me — I obtained my PhD at Liège University in 2005, working on optical and X-ray spectroscopy of massive stars. After an additional year in Liège, I moved to ESO/Chile in May 2006. In Paranal, I first joined the CRIRES instrument team before taking over the enjoyable task of UVES instrument scientist, where I am learning what it takes to have an instrument working to the best of its performance. In Santiago, I pursue my own research projects on massive stars, taking advantage of the active collaboration of a dozen colleagues working in the nearby field of stellar clusters.

Hugues Sana

Personnel Movements

Arrivals (1 January–31 March 2009)

Europe	
Zinsmeyer, William (US)	Software Engineer
Micol, Alberto (IT)	VO and Astronomical Data Specialist
Chasiotis, Stella-Maria (DE)	Secretary
Vraux, Jean Pierre (FR)	Contract Office
Verzichelli, Gianluca (IT)	System Engineer
Baginksi, Isabelle (DE)	Administrative Assistant
Fourie, Petrus Gerhardus (ZA)	System Engineer
Sharkey, Colleen (US)	Hubble Outreach Coordinator
Hekman, Peter (NL)	Electronic Engineer
Paolo Ghiretti (IT)	Civil Engineer
Emsellem, Eric (FR)	Head of the Office for Science - Garching
Ferguson, Neil (GB)	Software Engineer
Singh, Paul (IT)	Junior Optical Engineer
Argomedo, Javier (CL)	Software Engineer
Ruiz Velasco, Alma (MX)	Student
Guidetti, Daria (IT)	Student
Lopez Silva, Joao (CL)	Student
Hoffstadt Urrutia, Arturo (CL)	Student
McNeil, Emily Kate (US)	Student
Mueller, Eric (DE)	Student
Daemgen, Sebastian (DE)	Student
Zheng, Zheng (CN)	Student
Müller, André (DE)	Student

Chile	
Kneissl, Ruediger (DE)	Operations Astronomer
Vila Vilaro, Baltasar (ES)	Systems Astronomer
Poupar, Sébastien (FR)	Mechanical Engineer
Rawlings, Mark (GB)	Operations Astronomer
Rengaswamy, Sridharan (IN)	VLTI Astronomer
Evatt, Matthew (US)	Mechanical Engineer
Oestreich, Martin (DE)	Electrical Engineer
Ramírez, Christian (CL)	Mechanical Engineer
Díaz, Alvaro (CL)	Instrument Technician
Montagnier, Guillaume (FR)	Fellow
Alvarez Candal, Alvaro (AR)	Fellow
Asmus, Daniel (DE)	Student

Departures (1 January–31 March 2009)

Europe	
Puech, Florence (FR)	VLTI System Engineer
da Rocha, Cristiano (BR)	Fellow
Mazzoleni, Ruben (IT)	Paid Associate
Lorch, Henning (DE)	Software Engineer
Stöckl, Josef (AT)	Student
Lopez Silva, Joao (CL)	Student

Chile	
Hubrig, Swetlana (DE)	Operations Astronomer
Mirabel, Igor-Feliz (FR)	Representative of ESO - Chile
Gallardo, Javier (CL)	Software Engineer
Sanzana, Lilian	Software Engineer
Naef, Dominique (CH)	Fellow
Sahlman, Johannes (DE)	Student

Credit: ESO/FOTOAG

The Garching science campus, home to the Munich Technical University, four Max Planck Institutes, computing and research institutes, and ESO, shown in an aerial photograph taken in July 2007. The tracks of the U-Bahn (underground city railway) are seen to the bottom left (west) and the River Isar to the upper right (east). The dome just above image centre is the old research reactor, with the new reactor housed in the large grey building to its right. The ESO Headquarters building is towards the lower left of the photograph with the storage hall to the east. The ESO extension building will occupy parts of the field to the south (see Figure 3 of Fischer & Walsh, p. 4).

Annual Index 2008 (Nos. 131–134)

Subject Index

The Organisation

The Perfect Machine; de Zeeuw, T.; 132, 2
10th Anniversary of First Light of the VLT; 132, 4
Austria Declares Intent to Join ESO; 132, 5
The ASTRONET Infrastructure Roadmap: A Twenty Year Strategy for European Astronomy; Bode, M.; Monnet, G.; ASTRONET Roadmap Working Group; 134, 2

Telescopes and Instrumentation

Advanced Calibration Techniques for Astronomical Spectrographs; Bristow, P.; Kerber, F.; Rosa, M. R.; 131, 2
Laser Guide Star Adaptive Optics without Tip-tilt; Davies, R.; Rabien, S.; Lidman, C.; Le Louarn, M.; Kasper, M.; Schreiber, N. M. F.; Roccatagliata, V.; Ageorges, N.; Amico, P.; Dumas, C.; Mannucci, F.; 131, 7
DAZLE on the VLT; McMahon, R.; Parry, I.; Venemans, B.; King, D.; Ryan-Weber, E.; Bland-Hawthorn, J.; Horton, A.; 131, 11
Phase Correction for ALMA: Adaptive Optics in the Submillimetre; Nikolic, B.; Richer, J.; Hills, R.; Stirling, A.; 131, 14
Hawk-I – First Results from Science Verification; Doherty, M.; Wehner, E.; Willis, J.; Seifahrt, A.; Preibisch, T.; McCaughrean, M.; Mora Fernandes, A.; Gieles, M.; Norris, M.; Larsen, S.; Kuntschner, H.; Kneib, J.; Venemans, B.; Lidman, C.; Kissler-Patig, M.; Fontana, A.; 132, 7
Seeing is Believing: New Facts about the Evolution of Seeing on Paranal; Lombardi, G.; Sarazin, M.; Melnick, J.; Navarrete, J.; 132, 11
EFOSC2 Episode IV: A New Hope; Snodgrass, C.; Saviane, I.; Monaco, L.; Sinclaire, P.; 132, 18
Two Volume-phased Holographic Grisms Now Available for EFOSC2; Monaco, L.; Saviane, I.; 132, 20
The ALMA Antenna Transporter; Kraus, M.; Stanghellini, S.; Martinez, P.; Koch, F.; Dimmler, M.; Moresmau, J. M.; Rykaczewski, H.; 132, 23
Recent Progress at the ALMA Test Facility; Laing, R.; 132, 28
Cute-SCIDAR at Paranal for E-ELT Site Characterisation; Ramió, H. V.; Reyes, M.; Delgado, J. M.; Hernández, E.; Cagigal, M. N.; Fuensalida, J. J.; Lombardi, G.; Derie, F.; Navarrete, J.; Sarazin, M.; 132, 29
Progress on the European Extremely Large Telescope; Comerón, F.; D'Odorico, S.; Kissler-Patig, M.; Gilmozzi, R.; Spyromilio, J.; 133, 2
E-ELT and the Cosmic Expansion History – A Far Stretch?; D'Odorico, V.; Levshakov, S.; Bonifacio, P.; Bouchy, F.; Wiklind, T.; Queloz, D.; Udry, S.; Moscardini, L.; Molaro, P.; Murphy, M.; Lovis, C.; D'Odorico, S.; Zucker, S.; Mayor, M.; Pepe, F.; Cristiani, S.; Viel, M.; Haehnelt, M.; Pasquini, L.; Dessauges, M.; Vanzella, E.; Liske, J.; Grazian, A.; 133, 10
The Quest for Near-infrared Calibration Sources for E-ELT Instruments; J. Sansonetti, C.; Ralchenko, Y.; Kerber, F.; Nave, G.; Bristow, P.; Aldenius, M.; 133, 14
Detector Upgrade for FLAMES: GIRAFFE Gets Red Eyes; Gieles, M.; Palsa, R.; Bendek, E.; Peña, E.; Castillo, R.; Hanuschik, R.; Naef, D.; Deiries, S.; Melo, C.; Pasquini, L.; Downing, M.; 133, 17
The VLTI PRIMA Facility; van Belle, G. T.; Sahlmann, J.; Abuter, R.; Accardo, M.; Andolfato, L.; Brillant, S.; de Jong, J.; Derie, F.; Delplancke, F.; Duc, T. P.; Dupuy, C.; Gilli, B.; Gitton, P.; Haguenauer, P.; Jocou, L.; Jost, A.; Di Lieto, N.; Frahm, R.; Ménardi, S.; Morel, S.; Moresmau, J.; Palsa, R.; Popovic, D.; Pozna, E.; Puech, F.; Lévêque, S.; Ramirez, A.; Schuhler, N.; Somboli, F.; Wehner, S.; ESPRI Consortium, T.; 134, 6
News on the Commissioning of X-shooter; D'Odorico, S.; 134, 12
Report on the JENAM 2008 Meeting Symposium Science with the E-ELT; Monnet, G.; 134, 14

Astronomical Science

A Multi-Wavelength Study of the 2003–2006 Outburst of V1647 Orionis; van den Ancker, M.; Fedele, D.; Petr-Gotzens, M.; Rafanelli, P.; 131, 20
The VLT-FLAMES Survey of Massive Stars; Evans, C.; Hunter, I.; Smartt, S.; Lennon, D.; de Koter, A.; Mokiem, R.; Trundle, C.; Dufton, P.; Ryans, R.; Puls, J.; Vink, J.; Herrero, A.; Simón-Díaz, S.; Langer, N.; Brott, I.; 131, 25
Seeking for the Progenitors of Type Ia Supernovae; Patat, F.; Chandra, P.; Chevalier, R.; Justham, S.; Podsiadlowski, P.; Wolf, C.; Gal-Yam, A.; Pasquini, L.; Crawford, I.; Mazzali, P.; Pauldrach, A.; Nomoto, K.; Benetti, S.; Cappellaro, E.; Elias-Rosa, N.; Hillebrandt, W.; Leonard, D.; Pastorello, A.; Renzini, A.; Sabbadin, F.; Simon, J.; Turatto, M.; 131, 30
The Antares Emission Nebula and Mass Loss of alpha Sco A; Reimers, D.; Hagen, H.; Baade, R.; Braun, K.; 132, 33
SINFONI Observations of Comet-shaped Knots in the Planetary Nebula NGC 7293 (the Helix Nebula); Matsuura, M.; Speck, A.; Smith, M.; Zijlstra, A.; Lowe, K.; Viti, S.; Redman, M.; Wareing, C.; Lagadec, E.; 132, 37
Hunting for the Building Blocks of Galaxies like our own Milky Way with FORS; Haehnelt, M. G.; Rauch, M.; Bunker, A.; Becker, G.; Marleau, F.; Graham, J.; Cristiani, S.; Jarvis, M. J.; Lacey, C.; Morris, S.; Peroux, C.; Röttgering, H.; Theuns, T.; 132, 41
Behind the Scenes of the Discovery of Two Extrasolar Planets: ESO Large Programme 666; Wyrzykowski, L.; Soszynski, I.; Szewczyk, O.; Szymanski, M.; Ulaczyk, K.; Kubiak, M.; Shporer, A.; Tamuz, O.; Diaz, R.; Zoccali, M.; Ruiz, M. T.; Gieren, W.; Pietrzynski, G.; Ramirez, S.; Hoyer, S.; Udry, S.; Mayor, M.; Mazeh, T.; Gillon, M.; Queloz, D.; Santos, N.; Moutou, C.; Naef, D.; Udalski, A.; Minniti, D.; Pont, F.; Melo, C.; 133, 21
Probing Sagittarius A* and its Environment at the Galactic Centre: VLT and APEX Working in Synergy; Wiesemeyer, H.; Zamaninasab, M.; Zensus, A.; Vogel, S.; Thum, C.; Straubmeier, C.; Sjouwerman, L.; Schuster, K.; Moultaka, J.; Mužić, K.; Najarro, F.; Pott, J.; Meyer, L.; Mauerhan, J.; Markoff, S.; Lu, R.; Kunneriath, D.; Krips, M.; König, S.; Krichbaum, T.; Karas, V.; Duschl, W.; Downes, D.; Dovčiak, M.; Morris, M. R.; Weiss, A.; Baganoff, F.; Witzel, G.; Bertram, T.; García-Marín, M.; Schödel, R.; Eckart, A.; 133, 26
Stellar Populations of Bulges of Disc Galaxies in Clusters; Bertola, F.; Sarzi, M.; Pizzella, A.; Méndez-Abreu, J.; Maria Corsini, E.; Coccato, L.; Morelli, L.; Saglia, R.; Pompei, E.; 133, 31
Mid-infrared Interferometry of Active Galactic Nuclei: an Outstanding Scientific Success of the VLTI; Jaffe, W.; Röttgering, H.; Burtscher, L.; Tristram, K.; Schartmann, M.; Raban, D.; Meisenheimer, K.; 133, 36
The Supernova Legacy Survey; Balland, C.; Sullivan, M.; 133, 42
From the Dynamics of Cepheids to the Milky Way Rotation and the Calibration of the Distance Scale; Nardetto, N.; Kervella, P.; Barnes, T.; Bersier, D.; Fokin, A.; Fouqué, P.; Gillet, D.; Groh, J.; Kraus, S.; Mathias, P.; Mérand, A.; Millour, F.; Mourard, D.; Stoekl, A.; 134, 20
STRESS Counting Supernovae; Botticella, M. T.; Cappellaro, E.; Riello, M.; Greggio, L.; Benetti, S.; Patat, F.; Turatto, M.; Altavilla, G.; Pastorello, A.; Valenti, S.; Zampieri, L.; Harutyunyan, A.; Pignata, G.; Taubenberger, S.; 134, 25
Swift, VLT and Gamma-Ray Bursts: The Richness and Beauty of the Global View; Chincarini, G.; Margutti, R.; Covino, S.; D'Avanzo, P.; Fugazza, D.; Guidorzi, C.; Mao, J.; Moretti, A.; Capalbi, M.; Cusumano, G.; D'Elia, V.; Della Valle, M.; Fiore, F.; Mangano, V.; Molinari, E.; Perri, M.; Romano, P.; Salvaterra, R.; Zerbi, F.; Campana, S.; Giommi, P.; Guarneri, A.; Stella, L.; Tagliaferri, G.; Pian, E.; Palazzi, E.; Piranomonte, S.; Antonelli, A.; Salotti, L.; Soto, A. F.; 134, 30
The zCOSMOS Data Release 2: the "zCOSMOS-bright 10k-sample" and structure in the Universe out to redshifts of order unity; Lilly, S.; The zCOSMOS team; 134, 35

Astronomical News

The 2007 Users Feedback Campaign; Primas, F.; Marteau, S.; Hainaut, O.; Mathys, G.; Romaniello, M.; Sterzik, M.; 131, 36

ESO Reflex: A Graphical Workflow Engine for Astro nomical Data Reduction; Hook, R.; Romaniello, M.; Ullgrén, M.; Maisala, S.; Solin, O.; Oittinen, T.; Savolainen, V.; Järveläinen, P.; Tyynelä, J.; Péron, M.; Izzo, C.; Ballester, P.; Gabasch, A.; 131, 42

News from the ESO Science Archive Facility; Delmotte, N.; 131, 45

ALMA Science: the ESO–Garching Astronomer's View; Testi, L.; 131, 46

News from the ALMA Test Facility; Hunter, T.; Laing, R.; 131, 47

Report on the 2007 ESO Fellowship Symposium held at ESO, Vitacura, Chile, 12–14 November 2007; West, M.; Leibundgut, B.; 131, 48

Report on the ESO Chile Science Days held at ESO, Vitacura, Chile, 20 November and 5 December 2007; West, M.; 131, 48

Astronomical Observatories and the Republic of Chile Pave the Way for Future Projects; Argandoña, G.; Mirabel, F.; 131, 49

Report on the ELSA School on the Science of Gaia held at the Lorentz Center, Leiden, the Netherlands, 19–28 November 2007; Brown, A.; Lindegren, L.; Kontizas, M.; Turon, C.; Muinonen, K.; 131, 50

Fellows at ESO; 131, 51

New Staff at ESO; 131, 52

Announcement of ESO Large Programmes on the Gran Telescopio Canarias; 131, 53

Announcement of the ASTRONET Infrastructure Roadmap Symposium: An Opportunity to Contribute to the European Astrophysical Strategy for the Next 20 Years, 16–19 June 2008, Liverpool, United Kingdom; 131, 53

Announcement of the MPA/ESO/MPE/USM 2008 Joint Astronomy Conference on Chemical Evolution of Dwarf Galaxies and Stellar Clusters; 131, 54

Announcement of the Joint ESO/INAF-Arcetri Workshop on Future Ground-based Solar System Research: Synergies with Space Probes and Space Telescopes; 131, 55

Personnel Movements; 131, 55

News from the ESO Science Archive Facility; Delmotte, N.; 132, 47

FP7 E-ELT Preparation – Grant Agreement Funded by the European Commission is Underway; Monnet, G.; Gilmozzi, R.; Robinson, M.; 132, 48

Report on the International Workshop on Star Formation Across the Milky Way Galaxy; Melo, C.; Melnick, J.; Sterzik, M.; 132, 49

Announcement of the ESO Workshop on Large Programmes, 13–15 October 2008, Garching, Germany; 132, 50

Announcement of the Topical Symposium "Science with the E-ELT" at JENAM 2008, 8–12 September 2008, Vienna, Austria; 132, 51

Fellows at ESO; 132, 51

ESO Fellowship Programme 2008/2009; 132, 52

New Staff at ESO; 132, 53

Exploring the Cold Universe – A Planetarium Show for the IYA 2009; Boffin, H.; Acker, A.; 132, 54

Personnel Movements; 132, 55

Scientific Approach for Optimising Performance, Health and Safety in High-Altitude Observatories; Vogt, J.; Nolle-Gösser, T.; Böcker, M.; 133, 49

Report on the ESO and Radionet Workshop on Gas and Stars in Galaxies – A Multi-Wavelength 3D Perspective; De Breuck, C.; Kuntschner, H.; Zwaan, M.; Lehnert, M.; 133, 52

ESO at SPIE – Astronomical Telescopes and Instruments in Marseille; Moorwood, A.; 133, 57

In Memoriam Bengt Westerlund; Breysacher, J.; Danziger, J.; 133, 58

Do you know your Solar System? Children in Garching do!; Kerber, F.; Kuntschner, H.; Hanuschik, R.; 133, 58

Lights, Camera, Astronomers! Media training at ESO Chile; Argandoña, G.; West, M.; 133, 60

Social Engagement at ESO; Böcker, M.; 133, 61

New Staff at ESO; 133, 61

Fellows at ESO; 133, 63

Announcement of the Joint ESO, CTIO, ALMA/NRAO and Universidad Valparaíso Workshop The Interferometric View on Hot Stars; 133, 64

Announcement of the ESO Workshop on ALMA and ELTs: A Deeper, Finer View of the Universe; 133, 65

Announcement of the Report by the ESA–ESO Working Group on Galactic Populations, Chemistry and Dynamics; 133, 66

Personnel Movements; 133, 66

Preparing for the ESO Public Surveys with VISTA and VST: New Tools for Phase 2 and a Workshop with the Survey PIs; Arnaboldi, M.; Dietrich, J.; Hatziminaoglou, E.; Hummel, W.; Hussain, G.; Neeser, M.; Rejkuba, M.; Bierwirth, T.; Comeron, F.; Dorigo, D.; Emerson, J.; Nunes, P.; Primas, F.; 134, 42

Announcement of the Workshop The E-ELT Design Reference Mission and Science Plan; 134, 45

The ESA–ESO Working Group on Galactic Populations, Chemistry and Dynamics; Turon, C.; Primas, F.; Binney, J.; Chiappini, C.; Drew, J.; Helmi, A.; Robin, A.; G. Ryan, S.; 134, 46

Report on the Workshop Interstellar Medium and Star Formation with ALMA: Looking to the Future. A Workshop to Honour Tom Wilson; Martin-Pintado, J.; 134, 50

Award of the Ioannes Marcus Marci Medal to Tom Wilson, Associate Director for ALMA; Wilson, T.; 134, 52

Report on the Conference Optical Turbulence — Astronomy meets Meteorology; Masciadri, E.; 134, 53

Report on the Conference Future Ground-based Solar System Research: Synergies with Space Probes and Space Telescopes; Käufl, H. U.; Tozzi, G. P.; 134, 56

Report on the ALMA Workshop Simulations for ALMA; Nikolic, B.; Richer, J.; Gueth, F.; Laing, R.; 134, 57

Report on the Conference 400 Years of Astronomical Telescopes; Brandl, B.; Stuik, R.; 134, 59

Announcement of the ESO–Porto Conference Towards Other Earths: Perspectives and Limitations in the ELT Era; 134, 61

Announcement of the ElROforum School of Instrumentation (ESI); 134, 61

ESO ALMA Fellowship Programme; 134, 62

Daniel Enard 1939–2008; Cullum, M.; 134, 63

New Staff at ESO; 134, 64

Fellows at ESO; 134, 65

ESO at the European City of Science; Boffin, H.; Heyer, H.; Janssen, E.; 134, 66

ESO and the International Year of Astronomy 2009; Pierce-Price, D.; Russo and Lars Lindberg Christensen, P.; Lindberg Christensen, L.; 134, 66

Personnel Movements; 134, 67

Conference Supplement

Special Report on the MPA/ESO/MPE/USM 2008 Joint Astronomy Conference Chemical Evolution of Dwarf Galaxies and Stellar Clusters; Primas, F.; Weiss, A.; 134supp, 2

The Complex Evolution of Simple Systems; Mateo, M.; 134supp, 3

Abundances in Globular Cluster Stars: What is the Relation with Dwarf Galaxies?; Gratton, R.; 134supp, 9

Evidence for Sub-Populations in Globular Clusters: Their Properties and Relationship with Cluster Properties; Renzini, A.; Milone, A.; Gratton, R.; Cassisi, S.; Bragaglia, A.; Piotto, G.; 134supp, 13

Linking Chemical Signatures of Globular Clusters to Chemical Evolution; D'Antona, F.; Ventura, P.; 134supp, 18

Chemical Signatures in Dwarf Galaxies; Hill, V. M.; Venn, K. A.; 134supp, 23

Chemical Evolution of Dwarf Galaxies and Stellar Clusters: Conference Summary; Freeman, K. C.; 134supp, 28

Author Index

A

Aldenius, M.; Kerber, F.; Bristow, P.; Nave, G.; Ralchenko, Y.; J. Sansonetti, C.; The Quest for Near-infrared Calibration Sources for E-ELT Instruments; 133, 14

Argandoña, G.; Mirabel, F.; Astronomical Observatories and the Republic of Chile Pave the Way for Future Projects; 131, 49

Argandoña, G.; West, M.; Lights, Camera, Astronomers! Media training at ESO Chile; 133, 60

Arnaboldi, M.; Dietrich, J.; Hatziminaoglou, E.; Hummel, W.; Hussain, G.; Neeser, M.; Rejkuba, M.; Bierwirth, T.; Comeron, F.; Dorigo, D.; Emerson, J.; Nunes, P.; Primas, F.; Preparing for the ESO Public Surveys with VISTA and VST: New Tools for Phase 2 and a Workshop with the Survey PIs; 134, 42

B

Böcker, M.; Vogt, J.; Nolle-Gösser, T.; Scientific Approach for Optimising Performance, Health and Safety in High-Altitude Observatories; 133, 49

Böcker, M.; Social Engagement at ESO; 133, 61

Bode, M.; Monnet, G.; ASTRONET Roadmap Working Group; The ASTRONET Infrastructure Roadmap: A Twenty Year Strategy for European Astronomy; 134, 2

Boffin, H.; Acker, A.; Exploring the Cold Universe – A Planetarium Show for the IYA 2009; 132, 54

Boffin, H.; Janssen, E.; Heyer, H.; ESO at the European City of Science; 134, 66

Botticella, M. T.; Cappellaro, E.; Riello, M.; Greggio, L.; Benetti, S.; Patat, F.; Turatto, M.; Altavilla, G.; Pastorello, A.; Valenti, S.; Zampieri, L.; Harutyunyan, A.; Pignata, G.; Taubenberger, S.; STRESS Counting Supernovae; 134, 25

Brandl, B.; Stuik, R.; Report on the Conference 400 Years of Astronomical Telescopes; 134, 59

Bristow, P.; Kerber, F.; Rosa, M. R.; Advanced Calibration Techniques for Astronomical Spectrographs; 131, 2

Brown, A.; Lindegren, L.; Kontizas, M.; Turon, C.; Muinonen, K.; Report on the ELSA School on the Science of Gaia held at the Lorentz Center, Leiden, the Netherlands, 19-28 November 2007; 131, 50

C

Cassisi, S.; Bragaglia, A.; Gratton, R.; Milone, A.; Piotto, G.; Renzini, A.; Evidence for Sub-Populations in Globular Clusters: Their Properties and Relationship with Cluster Properties; 134supp, 13

Chincarini, G.; Margutti, R.; Covino, S.; D'Avanzo, P.; Fugazza, D.; Guidorzi, C.; Mao, J.; Moretti, A.; Capalbi, M.; Cusumano, G.; D'Elia, V.; Della Valle, M.; Fiore, F.; Mangano, V.; Molinari, E.; Perri, M.; Romano, P.; Salvaterra, R.; Zerbi, F.; Campana, S.; Giommi, P.; Guarneri, A.; Stella, L.; Tagliaferri, G.; Pian, E.; Palazzi, E.; Piranomonte, S.; Antonelli, A.; Salotti, L.; Soto, A. F.; Swift, VLT and Gamma–Ray Bursts: The Richness and Beauty of the Global View; 134, 30

Cullum, M.; Daniel Enard 1939–2008; 134, 63

D

D'Antona, F.; Ventura, P.; Linking Chemical Signatures of Globular Clusters to Chemical Evolution; 134supp, 18

D'Odorico, S.; News on the Commissioning of X-shooter; 134, 12

Danziger, J.; Breysacher, J.; In Memoriam Bengt Westerlund; 133, 58

Davies, R.; Rabien, S.; Lidman, C.; Le Louarn, M.; Kasper, M.; Schreiber, N. M. F.; Roccatagliata, V.; Ageorges, N.; Amico, P.; Dumas, C.; Mannucci, F.; Laser Guide Star Adaptive Optics without Tip-tilt; 131, 7

de Zeeuw, T.; The Perfect Machine; 132, 2

Delmotte, N.; News from the ESO Science Archive Facility; 131, 45

Delmotte, N.; News from the ESO Science Archive Facility; 132, 47

E

Eckart, A.; Schödel, R.; García-Marín, M.; Witzel, G.; Weiss, A.; Baganoff, F.; Morris, M. R.; Bertram, T.; Dovčiak, M.; Downes, D.; Duschl, W.; Karas, V.; König, S.; Krichbaum, T.; Krips, M.; Kunneriath, D.; Lu, R.; Markoff, S.; Mauerhan, J.; Meyer, L.; Moultaka, J.; Mužić, K.; Najarro, F.; Pott, J.; Schuster, K.; Sjouwerman, L.; Straubmeier, C.; Thum, C.; Vogel, S.; Wiesemeyer, H.; Zamaninasab, M.; Zensus, A.; Probing Sagittarius A* and its Environment at the Galactic Centre: VLT and APEX Working in Synergy; 133, 26

Evans, C.; Hunter, I.; Smartt, S.; Lennon, D.; de Koter, A.; Mokiem, R.; Trundle, C.; Dufton, P.; Ryans, R.; Puls, J.; Vink, J.; Herrero, A.; Simón-Díaz, S.; Langer, N.; Brott, I.; The VLT-FLAMES Survey of Massive Stars; 131, 25

F

Freeman, K. C.; Chemical Evolution of Dwarf Galaxies and Stellar Clusters: Conference Summary; 134supp, 28

G

Gilmozzi, R.; Monnet, G.; Robinson, M.; FP7 E-ELT Preparation – Grant Agreement Funded by the European Commission is Underway; 132, 48

Gratton, R.; Abundances in Globular Cluster Stars: What is the Relation with Dwarf Galaxies?; 134supp, 9

H

Haehnelt, M. G.; Rauch, M.; Bunker, A.; Becker, G.; Marleau, F.; Graham, J.; Cristiani, S.; Jarvis, M. J.; Lacey, C.; Morris, S.; Peroux, C.; Röttgering, H.; Theuns, T.; Hunting for the Building Blocks of Galaxies like our own Milky Way with FORS; 132, 41

Hook, R.; Romaniello, M.; Ullgrén, M.; Maisala, S.; Solin, O.; Oittinen, T.; Savolainen, V.; Järveläinen, P.; Tyynelä, J.; Péron, M.; Izzo, C.; Ballester, P.; Gabasch, A.; ESO Reflex: A Graphical Workflow Engine for Astronomical Data Reduction; 131, 42

Hunter, T.; Laing, R.; News from the ALMA Test Facility; 131, 47

K

Kerber, F.; Hanuschik, R.; Kuntschner, H.; Do you know your Solar System? Children in Garching do!; 133, 58

Kissler-Patig, M.; Fontana, A.; Venemans, B.; Kneib, J.; Doherty, M.; Lidman, C.; Kuntschner, H.; Norris, M.; Larsen, S.; Gieles, M.; Mora Fernandes, A.; McCaughrean, M.; Preibisch, T.; Seifahrt, A.; Willis, J.; Wehner, E.; Hawk-I – First Results from Science Verification; 132, 7

Kraus, M.; Stanghellini, S.; Martinez, P.; Koch, F.; Dimmler, M.; Moresmau, J. M.; Rykaczewski, H.; The ALMA Antenna Transporter; 132, 23

L

Laing, R.; Recent Progress at the ALMA Test Facility; 132, 28

Lehnert, M.; De Breuck, C.; Kuntschner, H.; Zwaan, M.; Report on the ESO and Radionet Workshop on Gas and Stars in Galaxies – A Multi-Wavelength 3D Perspective; 133, 52

Lilly, S.; The zCOSMOS team; The zCOSMOS Data Release 2: the "zCOSMOS-bright 10k-sample" and structure in the Universe out to redshifts of order unity; 134, 35

Liske, J.; Grazian, A.; Vanzella, E.; Dessauges, M.; Viel, M.; Pasquini, L.; Haehnelt, M.; Cristiani, S.; Pepe, F.; Bonifacio, P.; Bouchy, F.; D'Odorico, S.; D'Odorico, V.; Levshakov, S.; Lovis, C.; Mayor, M.; Molaro, P.; Moscardini, L.; Murphy, M.; Queloz, D.; Udry, S.; Wiklind, T.; Zucker, S.; E-ELT and the Cosmic Expansion History – A Far Stretch?; 133, 10

M

Martin-Pintado, J.; Report on the Workshop Interstellar Medium and Star Formation with ALMA: Looking to the Future A Workshop to Honour Tom Wilson; 134, 50

Masciadri, E.; Report on the Conference Optical Turbulence — Astronomy meets Meteorology; 134, 53

Mateo, M.; The Complex Evolution of Simple Systems; 134supp, 3

Matsuura, M.; Speck, A.; Smith, M.; Zijlstra, A.; Lowe, K.; Viti, S.; Redman, M.; Wareing, C.; Lagadec, E.; SINFONI Observations of Comet-shaped Knots in the Planetary Nebula NGC 7293 (the Helix Nebula); 132, 37

McMahon, R.; Parry, I.; Venemans, B.; King, D.; Ryan-Weber, E.; Bland-Hawthorn, J.; Horton, A.; DAZLE on the VLT; 131, 11

Meisenheimer, K.; Raban, D.; Tristram, K.; Schartmann, M.; Jaffe, W.; Röttgering, H.; Burtscher, L.; Mid-infrared Interferometry of Active Galactic Nuclei: an Outstanding Scientific Success of the VLTI; 133, 36

Melo, C.; Pasquini, L.; Downing, M.; Deiries, S.; Naef, D.; Hanuschik, R.; Palsa, R.; Castillo, R.; Peña, E.; Bendek, E.; Gieles, M.; Detector Upgrade for FLAMES: GIRAFFE Gets Red Eyes; 133, 17

Minniti, D.; Melo, C.; Naef, D.; Udalski, A.; Pont, F.; Moutou, C.; Santos, N.; Queloz, D.; Mazeh, T.; Gillon, M.; Mayor, M.; Udry, S.; Diaz, R.; Hoyer, S.; Ramirez, S.; Pietrzynski, G.; Gieren, W.; Ruiz, M. T.; Zoccali, M.; Tamuz, O.; Shporer, A.; Kubiak, M.; Soszynski, I.; Szewczyk, O.; Szymanski, M.; Ulaczyk, K.; Wyrzykowski, L.; Behind the Scenes of the Discovery of Two Extrasolar Planets: ESO Large Programme 666; 133, 21

Monnet, G.; Report on the JENAM 2008 Meeting Symposium Science with the E-ELT; 134, 14

Moorwood, A.; ESO at SPIE – Astronomical Telescopes and Instruments in Marseille; 133, 57

Morelli, L.; Pompei, E.; Pizzella, A.; Méndez-Abreu, J.; Maria Corsini, E.; Coccato, L.; Saglia, R.; Sarzi, M.; Bertola, F.; Stellar Populations of Bulges of Disc Galaxies in Clusters; 133, 31

N

Nardetto, N.; Kervella, P.; Barnes, T.; Bersier, D.; Fokin, A.; Fouqué, P.; Gillet, D.; Groh, J.; Kraus, S.; Mathias, P.; Mérand, A.; Millour, F.; Mourard, D.; Stoekl, A.; From the Dynamics of Cepheids to the Milky Way Rotation and the Calibration of the Distance Scale; 134, 20

Nikolic, B.; Richer, J.; Hills, R.; Stirling, A.; Phase Correction for ALMA: Adaptive Optics in the Submillimetre; 131, 14

Nikolic, B.; Richer, J.; Gueth, F.; Laing, R.; Report on the ALMA Workshop Simulations for ALMA; 134, 57

P

Patat, F.; Chandra, P.; Chevalier, R.; Justham, S.; Podsiadlowski, P.; Wolf, C.; Gal-Yam, A.; Pasquini, L.; Crawford, I.; Mazzali, P.; Pauldrach, A.; Nomoto, K.; Benetti, S.; Cappellaro, E.; Elias-Rosa, N.; Hillebrandt, W.; Leonard, D.; Pastorello, A.; Renzini, A.; Sabbadin, F.; Simon, J.; Turatto, M.; Seeking for the Progenitors of Type Ia Supernovae; 131, 30

Pierce-Price, D.; Russo and Lars Lindberg Christensen, P.; Lindberg Christensen, L.; ESO and the International Year of Astronomy 2009; 134, 66

Primas, F.; Marteau, S.; Hainaut, O.; Mathys, G.; Romaniello, M.; Sterzik, M.; The 2007 Users Feedback Campaign; 131, 36

Primas, F.; Weiss, A.; Special Report on the MPA/ESO/MPE/USM 2008 Joint Astronomy Conference Chemical Evolution of Dwarf Galaxies and Stellar Clusters; 134supp, 2

R

Ramió, H. V.; Reyes, M.; Delgado, J. M.; Hernández, E.; Cagigal, M. N.; Fuensalida, J. J.; Lombardi, G.; Derie, F.; Navarrete, J.; Sarazin, M.; Cute-SCIDAR at Paranal for E-ELT Site Characterisation; 132, 29

Reimers, D.; Hagen, H.; Baade, R.; Braun, K.; The Antares Emission Nebula and Mass Loss of alpha Sco A; 132, 33

S

Sarazin, M.; Melnick, J.; Navarrete, J.; Lombardi, G.; Seeing is Believing: New Facts about the Evolution of Seeing on Paranal; 132, 11

Saviane, I.; Monaco, L.; Two Volume-phased Holographic Grisms Now Available for EFOSC2; 132, 20

Snodgrass, C.; Saviane, I.; Monaco, L.; Sinclaire, P.; EFOSC2 Episode IV: A New Hope; 132, 18

Spyromilio, J.; Comerón, F.; D'Odorico, S.; Kissler-Patig, M.; Gilmozzi, R.; Progress on the European Extremely Large Telescope; 133, 2

Sterzik, M.; Melnick, J.; Melo, C.; Report on the International Workshop on Star Formation Across the Milky Way Galaxy; 132, 49

Sullivan, M.; Balland, C.; The Supernova Legacy Survey; 133, 42

T

Testi, L.; ALMA Science: the ESO–Garching Astronomers View; 131, 46

Turon, C.; Primas, F.; Binney, J.; Chiappini, C.; Drew, J.; Helmi, A.; Robin, A.; G. Ryan, S.; The ESA–ESO Working Group on Galactic Populations, Chemistry and Dynamics; 134, 46

U

Käufl, H. U.; Tozzi, G. P.; Report on the Conference Future Ground-based Solar System Research: Synergies with Space Probes and Space Telescopes; 134, 56

V

van Belle, G. T.; Sahlmann, J.; Abuter, R.; Accardo, M.; Andolfato, L.; Brillant, S.; de Jong, J.; Derie, F.; Delplancke, F.; Duc, T. P.; Dupuy, C.; Gilli, B.; Gitton, P.; Haguenauer, P.; Jocou, L.; Jost, A.; Di Lieto, N.; Frahm, R.; Ménardi, S.; Morel, S.; Moresmau, J.; Palsa, R.; Popovic, D.; Pozna, E.; Puech, F.; Lévêque, S.; Ramirez, A.; Schuhler, N.; Somboli, F.; Wehner, S.; ESPRI Consortium, T.; The VLTI PRIMA Facility; 134, 6

van den Ancker, M.; Fedele, D.; Petr-Gotzens, M.; Rafanelli, P.; A Multi-Wavelength Study of the 2003–2006 Outburst of V1647 Orionis; 131, 20

Venn, K. A.; Hill, V. M.; Chemical Signatures in Dwarf Galaxies; 134supp, 23

W

West, M.; Leibundgut, B.; Report on the 2007 ESO Fellowship Symposium held at ESO, Vitacura, Chile, 12–14 November 2007; 131, 48

West, M.; Report on the ESO Chile Science Days held at ESO, Vitacura, Chile, 20 November and 5 December 2007; 131, 48

ESO is the European Organisation for Astronomical Research in the Southern Hemisphere. Whilst the Headquarters (comprising the scientific, technical and administrative centre of the organisation) are located in Garching near Munich, Germany, ESO operates three observational sites in the Chilean Atacama desert. The Very Large Telescope (VLT), is located on Paranal, a 2 600 m high mountain south of Antofagasta. At La Silla, 600 km north of Santiago de Chile at 2 400 m altitude, ESO operates several medium-sized optical telescopes. The third site is the 5 000 m high Llano de Chajnantor, near San Pedro de Atacama. Here a new submillimetre telescope (APEX) is in operation, and a giant array of submillimetre antennas (ALMA) is under development. Over 2 000 proposals are made each year for the use of the ESO telescopes.

The ESO Messenger is published four times a year: normally in March, June, September and December. ESO also publishes Conference Proceedings and other material connected to its activities. Press Releases inform the media about particular events. For further information, contact the ESO Education and Public Outreach Department at the following address:

ESO Headquarters
Karl-Schwarzschild-Straße 2
85748 Garching bei München
Germany
Phone +49 89 320 06-0
Fax +49 89 320 23 62
information@eso.org
www.eso.org

The ESO Messenger:
Editor: Jeremy R. Walsh
Layout/typesetting: Mafalda Martins
Design: Jutta Boxheimer
www.eso.org/messenger/

Printed by
Peschke Druck
Schatzbogen 35
81805 München
Germany

ISSN 0722-6691

Contents

The Organisation
R. Fischer, J. Walsh — An Extension for ESO Headquarters 2

Telescopes and Instrumentation
A. Baudry — The ALMA Correlator: Performance and Science Impact in the Millimetre/Submillimetre 6
M. Scodeggio et al. — Improving the Multiplexing of VIMOS MOS Observations for Future Spectroscopic Surveys 13
C. Melo et al. — Six Years of FLAMES Operations 17

Astronomical Science
S. Hubrig et al. — Studying the Magnetic Properties of Upper Main-sequence Stars with FORS1 21
F. Millour et al. — Wolf-Rayet Stars at the Highest Angular Resolution 26
A. Richichi et al. — The Beauty of Speed 32
H. Horst et al. — VISIR Observations of Local Seyfert Nuclei and the Mid-infrared — Hard X-ray Correlation 37
J. Kurk et al. — A VLT Large Programme to Study Galaxies at z ~ 2: GMASS — the Galaxy Mass Assembly Ultra-deep Spectroscopic Survey 40

Astronomical News
E. Hatziminaoglou, F. Chéreau — VirGO: A Visual Browser for the ESO Science Archive Facility 46
N. Delmotte — News from the ESO Science Archive Facility 49
P. Garcia — New Infrastructures Require New Training: The Example of the Very Large Telescope Interferometer Schools 50
G. Mathys, B. Leibundgut — Large Programmes 53
P. Russo et al. — ESO and the International Year of Astronomy 2009 Opening Ceremony 54
MAD and Beyond: Science with Multi-Conjugate Adaptive Optics Instruments 56
IR and Sub-mm Spectroscopy: A New Tool for Studying Stellar Evolution 56
Detectors for Astronomy 2009 57
M. West et al. — ESO's Studentship Programmes: Training Tomorrow's Astronomers Today 57
ESO Studentship Programme 59
New Staff at ESO 60
Fellows at ESO 62
Personnel Movements 63
Annual Index 2008 (Nos. 131–134) 64

Front Cover: Colour composite of the centre of NGC 5128 containing the radio source Centaurus A. Three separate image sets are combined: APEX LABOCA 870 µm image in orange; Chandra X-ray Observatory combined 0.5–2 keV image in blue; visible light (*B*, *V* and *I* band) WFI images from the MPG/ESO 2.2 m telescope. See ESO 03/09 for details.